Reprint of Structures and Materials Research Bulletin
Series 100, Issue 5
Division of Structural Engineering and Structural Mechanics
Department of Civil Engineering

BEHAVIOR OF A CONTINUOUS CONCRETE SLAB PRESTRESSED IN TWO DIRECTIONS

A Report of an Investigation by

T. Y. LIN
Professor of Civil Engineering

A. C. SCORDELIS
Associate Professor of Civil Engineering

R. ITAYA
Assistant Engineer

INSTITUTE OF ENGINEERING RESEARCH
UNIVERSITY OF CALIFORNIA
Berkeley, California

AUGUST 1958

to the

DIVISION OF ARCHITECTURE
DEPARTMENT OF PUBLIC WORKS
STATE OF CALIFORNIA

FOREWORD

The Research Program of the Division of Architecture, of which this project is a part, is intended to develop information in those fields of materials, designs and construction which would be in the best interest of the State of California in connection with the economy and safety of design and construction of public school buildings and which is of such general nature as to be overlooked by industry research and other research organizations.

It should be recognized that the information presented in this report is not regulatory but may aid in the development of new standards or the modification of existing standards, all leading towards more economical, safe school building construction. The findings of this project should contribute to economy and safety not only in public schools but in the building industry in general.

State Architect

March 3, 1959

Structures and Materials Research
Division of Civil Engineering

BEHAVIOR OF A CONTINUOUS CONCRETE SLAB PRESTRESSED IN TWO DIRECTIONS

A Report of an Investigation

by

T. Y. Lin, Professor of Civil Engineering

A. C. Scordelis, Associate Professor of Civil Engineering

R. Itaya, Assistant Engineer

to the

DIVISION OF ARCHITECTURE
DEPARTMENT OF PUBLIC WORKS
STATE OF CALIFORNIA

Institute of Engineering Research
University of California
Berkeley 8

August, 1958

TABLE OF CONTENTS

LIST OF TABLES

LIST OF FIGURES

LIST OF FIGURES (CONT'D)

LIST OF FIGURES (CONT'D)

I. INTRODUCTION

1. Object and Scope

In the past few years a large number of structures, utilizing flat slabs prestressed in two directions, have been erected using the lift slab method of construction. These slabs have performed well in service. An essentially crack free slab having deflections under working load which have been minimized or practically nullified can be obtained by proper prestressing. As yet very little experimental data is available regarding the behavior of such slabs through the elastic and plastic ranges and finally under ultimate load. In an earlier study[1] the case of a square slab prestressed in two directions and supported at four points was considered. The investigation reported herein considers the case of a square slab simply supported at nine points, these support points simulating column supports.

Present design of prestressed concrete lift slabs is based on approximate procedures.[2] The procedure normally used is to divide the structure into a series of bents, each consisting of a row of columns or supports and strips of supported slabs, each strip bounded laterally by the centerline of the panel on either side of the centerline of columns or supports. A series of such bents is first taken longitudinally and then transversely through the building. Each bent is analyzed for the various loading conditions which may come upon the slab. The slab moments obtained, which are for a full panel width, are then apportioned to the column strips and middle strips. The

---

1. Superscripts refer to references listed on page 45.

percentage going to each is dependent on edge and support conditions, but has usually been taken as 45 and 55 percent going to the middle and column strips respectively. From these analyses an envelope of maximum and minimum slab moments in the longitudinal and transverse directions is plotted. Using these moment envelopes the magnitude and location of the prestress force required at each section to keep the stresses within certain allowable limits can be determined. In cases where the slab to column connection is not rigid or where the column stiffness relative to the slab stiffness is small the problem described above reduces to the analysis of a continuous beam in each direction rather than a bent. The continuous beam in each case having a width equal to the panel width. This method of analysis, often called the "beam method", is an approximate one, since it reduces the two-way action involved in the actual slab to the one way action of a beam in each direction.

A more precise determination of the slab moments and deflections can be found by using the elastic plate theory, which does take into account the two-way action of the slab. For the case of continuous slabs this requires a considerable amount of mathematical effort and for this reason it is not generally used directly in design.

The purpose of this investigation was to determine the behavior, through and above the elastic range, of a continuous concrete slab prestressed in two directions. Some of the questions which the investigation endeavored to answer for this type of slab were: 1. Is the elastic plate theory valid up to the appearance of cracks? 2. Can the cracking

load be predicted by the elastic plate theory using the flexural tensile strength as determined by plain concrete specimens? 3. What is the physical behavior of the slab through the plastic range and finally under ultimate load? Does it deflect excessively? Is the failure sudden or gradual? 4. Can the ultimate strength be predicted by available theories for ultimate strength of slabs? 5. Are the present methods of design, which are approximate, sufficiently accurate for predicting the behavior of such a slab? If not how should they be changed or modified? 6. What is the distribution of moments in the slab in the elastic and plastic ranges, under various loading conditions and under prestress alone?

In order to answer the questions posed above as well as to study other practical design problems involved in this type of slab, a 15 x 15 ft. slab 3 in. thick and supported at 9 points was first prestressed and then subjected to a series of loading tests under laboratory controlled conditions to insure accuracy. In the final test the slab was loaded to failure so that information on its behavior at ultimate load was obtained.

2. Acknowledgments

The program reported herein was conducted in the Structural Engineering Laboratory, Division of Civil Engineering, University of California. The program was sponsored by the Division of Architecture, Department of Public Works, State of California through a research grant administered by the Institute of Engineering Research, University of California. The program was carried on between July 1957 and

August 1958.

The Division of Architecture is under the direction of Anson Boyd, State Architect. Special appreciation for their help and suggestions is due to C. M. Herd, Chief Construction Engineer; Charles Peterson, M. W. Sahlberg, Principal Structural Engineers; and A. H. Brownfield, J. F. Meehan, Supervising Structural Engineers; all of the Division of Architecture.

3. Notation

The letter symbols used in this report are generally defined when they are introduced. The most frequently used symbols are listed below for convenient reference:

A_s = Area of prestressing steel

a = Side dimension of a single panel

D = Flexural rigidity of slab = $\frac{Eh^3}{12(1-\mu^2)}$

E_c = Modulus of elasticity of concrete

E_s = Modulus of elasticity of steel

F = Effective prestress force per cable

F_1 = Effective prestress per foot of width

f'_c = Compressive strength of 6 x 12 in. cylinders

f'_t = Modulus of rupture of concrete

h = Slab thickness

M_x, M_y = Bending moments per unit length acting on sections normal to the x- and y-axes, respectively

M_{xy}, M_{yx} = Torsional moments per unit length acting on sections normal to the x- and y-axes, respectively

$M = \frac{M_x + M_y}{1 + \mu}$

n = Number of subdivisions of the span "a" for finite difference elements

Q_x, Q_y = Vertical shearing forces acting on sections normal to the x- and y-axes, respectively

q = Load per unit area on slab

R = Reaction at supports

V_x, V_y = Total equivalent shearing forces acting on sections normal to the x- and y-axes, respectively at free boundaries

w = Deflection

x, y = Cartesian coordinates with the center of the slab as origin

ε = Strain

λ = Length of finite difference elements = $\frac{a}{n}$

μ = Poisson's ratio

σ = Stress

$U = \frac{M}{q \lambda^2}$, dimensionless quantity used in finite difference solution.

$Z = \frac{wD}{q \lambda^4}$, dimensionless quantity used in finite difference solution

II EXPERIMENTAL PROGRAM

1. Description of Test Slab

The test slab, shown in Fig. 1, had over-all dimensions of 15 x 15 ft. in plan and was 3 in. thick. Supports were placed on 7 ft. centers in both directions. The test slab represented about a 1/3 scale model of actual slabs found in practice and it was designed

in accordance with the "beam theory" as presently used in design. A steel plate with a bearing area of 6 x 6 in. was used at each of the exterior supports. A rocker and roller arrangement, as detailed in Fig. 2, permitted the necessary rotations and horizontal movements so that no restraints were introduced at each of these support points. At the center support a 9 x 9 in. bearing plate was used with a support assembly which permitted rotations in two directions but no horizontal movement. Since the center support had to carry the greatest reaction, the 9 x 9 in. bearing plate was necessary to minimize the possibility of a shear failure at this support.

The slab was post-tensioned with 12 cables in each direction. The cables were spaced 15 in. on center. Each cable consisted of a 1/4 in. high strength steel wire greased and placed in a plastic tube to provide for post-tensioning. Specially designed end anchorages for the one wire cables were used so as to enable accurate measurements of the amount of prestress in each cable. Details of these end anchorages are shown in Fig. 3. The profile for all of the cables running in both directions was the same and is shown in Fig. 4.

In addition to the prestressing steel, two layers of 2 by 2 in. No. 14 gage wire mesh were placed over each support to cover an area 18 in. sq. This steel was included to help prevent the possibility of local failures at the supports.

2. Fabrication

The slab was cast in place. Referring to Fig. 1 and Fig. 5 channels were first bolted to the floor along each line of supports,

18 x 36 in. cylindrical concrete pedestals were then placed on top of these channels at the support points, this was followed by the placement of the rocker and roller assemblies on top of the concrete pedestals. Forms were next constructed in the standard manner so that the soffit was at the final elevation of the slab. Prestressing cables were then placed in position using specially designed chairs so that a close tolerance could be achieved in the location of the cable profile. The wire mesh was then placed at each of the support points. The concrete was delivered ready-mixed from a central batching plant and placed into the forms. A little over 2 cubic yards was required for the entire slab. The concrete was vibrated internally with 1-3/4 in. diameter internal vibrators. The slab was cured moist with wet burlap for 10 days and then left air dry until testing. At an age of 13 days the slab was prestressed to 25% of its final value. At 100% the steel was stressed to 153,000 psi at the jacking end. After stressing all cables to 25% of the final value the forms were removed. Prestressing to 25% was required to prevent any cracking under dead load alone. The instrumentation was then placed on the slab. As part of the test program the slab was later taken to 50% and then 100% of the final prestressed value to measure the effect of prestressing. This will be described later. Once the forms had been removed and the instrumentation had been placed the remainder of the loading frame as shown in Fig. 5 was erected.

3. Materials

Concrete for the slab was designed to possess a minimum strength

of 5,000 psi at 28 days as measured by 6 x 12 in. clyinders. The mix contained 7 sacks of Type I Santa Cruz cement per cubic yard of concrete. The water-cement ratio was 5.7 gals. per sack. The aggregate consisted of Livermore Valley sand and gravel having a maximum size of 3/4 inches. Batch proportions by weight based on saturated surface dry conditions were:water, 0.51; cement, 1.00; sand, 2.05; gravel, 2.56. Slump was 5 in. and placement of the concrete took approximately 35 minutes. Sieve analyses for the aggregates used are given in Table 1.

Table 1 - Sieve Analysis of Aggregates

Kind of Aggregate	Percentage Retained on Sieve											Fineness Modulus
	1"	3/4"	1/2"	3/8"	#4	#8	#16	#30	#50	#100	#200	
Sand	-	-	-	-	0	16	45	62	83	94	97	3.00
Gravel	0	4	46	75	98	-	-	-	-	-	-	6.77

Control specimens were cured in the same manner as the slab. Three cylinders were tested in compression at 7, 14, 22, and 28 days. One cylinder was tested at 43 days. Average values for the compressive strength, modulus of elasticity, and Poisson's ratio for these cylinders are given in Table 2. A typical stress-strain diagram for the concrete is shown in Fig. 6 and a strength-age curve is given in Fig. 7. Three 6 x 6 x 20 in. beams were tested under third point loading on an 18 in. span, at 14 and 28 days. Average values for the moduli of rupture as obtained for these beams are also listed in Table 2.

Table 2 - Properties of Concrete

Age, days	7	14	22	28	43
Compressive strength of 6 x 12 in. cylinders, psi	3590	4337	4985	5455	5940
Secant modulus of elasticity at 1000 psi	-	3.40×10^6	-	3.50×10^6	-
Poisson's ratio	-	0.14	-	0.14	-
Modulus of rupture of 6 x 6 x 20 in. beams on 18 in. span under third point loading, psi	-	540	-	480	-

As mentioned earlier each prestressing cable consisted of a single 1/4 in. diameter high-strength steel wire. The wire was greased and encased in a plastic tube to prevent bonding to the concrete. Six samples of the prestressing wire were tested in tension on a 10 inch gage length and the following average values were found: proportional limit, 170 ksi; yield point as measured by the 0.2 percent offset method, 218 ksi; ultimate strength, 253 ksi; modulus of elasticity, 29,400 ksi; and percent elongation, 6.7 percent. A typical stress-strain curve for the wire is shown in Fig. 8.

4. Method of Loading

Cable prestress was applied by means of a 30-ton capcity hydraulic jack which had been accurately calibrated.

For the slab loading it was desired to provide for a uniform load on each of the four panels independently. This was accomplished by the use of four plastic air bags placed between the top of the slab and a 1/2 in. plywood sheathing which was supported by the steel frame

shown in Fig. 5. Each of the bags covered one panel or one-quarter of the total slab. By introducing air pressure into each of the bags independently the magnitude of the uniform load on each panel could be accurately controlled. The air pressure was introduced into the bags after it had been reduced in magnitude from that supplied by the compressed air system of the laboratory. The air pressure in each of the bags was measured by means of a water manometer. With the arrangement used the load on the slab could be controlled and measured to the nearest 2 or 3 psf.

This method of loading had been successfully used in earlier tests in the laboratory and once again it proved to be an excellent technique for producing uniform loadings.

5. Instrumentation

The instrumentation was designed to measure the following quantities.

a. Strains on top and bottom surfaces of the slab.

b. Force at ends of prestressing cable.

c. Strains in prestressing steel between the two ends.

d. Reactions at each support point.

e. Deflections at various locations.

A total of 48 - SR4, type A9, and 22 - SR4, type A1 strain gages were used to measure strains on the top and bottom surfaces of the slab. The A9 has a 6 in. gage length and the A1 has a 13/16 in. gage length. Both types functioned well. The location of these gages is shown in Fig. 9. It can be noted that it was only necessary to instrument one-eighth of the slab with strain gages, because of symmetry.

With this instrumentation all of the necessary strain data could be obtained.

The prestress force at the jacking end was measured for all cables initially by means of the pressure gage attached to the hydraulic jack. On six of the cables a simple dynamometer was attached at the non-jacking end so that the prestress force existing there could be measured. The location of these dynamometers are shown in Fig. 9. It can be seen that jacking and non-jacking ends were alternated along each edge of the slab. The dynamometer used is detailed in Fig. 3. It consisted of a 1-1/8 in. O.D. aluminum alloy tube with a wall thickness of 0.235 in. The tube could be passed over the end of the prestressing wire and its bearing washer, after which a 3/8 in. thick split washer could be inserted between the end of the tube and the bearing washer. Upon application of the prestressing force at the jacking end the bearing washer delivered a load to the aluminum dynamometer tube. This axial force was measured by means of a pair of SR4 type A5 strain gages mounted on the dynamometer. The dynomometer was capable of measuring this force to the nearest 20 lbs.

In order to get a record of the prestress force at several points along the length of the cables two SR4, type A12 gages were mounted directly onto each of the six cables which had dynamometers at the ends. The location of these gages is shown in Fig. 9. The procedure used in mounting these gages was as follows: 1) prior to the placement of the concrete a short length of the plastic tube was cut off at each gage location; 2) the prestressing wire was then cleaned thoroughly in this

region and the SR-4 gage mounted; 3) the gage was covered carefully with a water proofing compound; 4) a sheet metal shield was then placed around the wire; this shield protected the gage during the placing of the concrete and permitted movement of the wire during the tensioning operation; 5) the shield was sealed at each end on to the plastic tube by means of a water proofing compound. These gages worked well throughout the entire test program.

Reactions at each support point were measured by pressure meters. A schematic drawing of the typical pressure meter is shown in Fig. 2. Each pressure meter consisted of a pair of 6 in. diam. by 3/4 in. steel plates with a 1/16 in. film of oil sealed between them. Oil pressure was measured by means of a standard pressure gage connected to the meter. These pressure meters were calibrated in a testing machine prior to their use with the slab and could measure a reaction to the nearest 35 lbs.

To obtain deflections at various points deflection gages were placed as shown in Fig. 9. These were simple dial gages bearing on the bottom surface of the slab. The dial gages had a least count of 0.001 in. Dial gages were used until the load approached its ultimate value after which they were removed. Deflections were then obtained at the center of each panel by level readings taken on graduated scales hung from the bottom of the slab.

6. Test Program

The test program was designed to study the distribution of moments and deflections and the behavior of the slab under the following loading conditions:

a. Effect of prestress alone.

b. Uniform live load on one panel only. (skip loading - elastic range).

c. Uniform live load on entire slab.

1. Up to cracking (elastic range)

2. Beyond cracking to ultimate load (plastic range)

For identification purposes the four panels of the slab were designated as PI, PII, PIII, PIV with P I being the instrumented panel. In each direction the center pair of cables and each pair of cables closest to an edge were designated as column strip cables while the remaining cables were designated as middle strip cables. Thus, in each direction, there were a total of six column strip cables and six middle strip cables. The test program is indicated in Table 3, which gives a chronological histroy of the various stages of loading.

Table 3 - Test Program

Date	Test No.	Stage	Load Data					
			Col. Strip Cable Pre-stress, lbs (At Jack)	Mid. Strip Cable Pre-stress, lbs (At Jack)	Panel Live Load, psf			
					PI	PII	PIII	PIV
2/4		Slab cast on forms	-	-	-	-	-	-
2/17		25% Prestress - Nominal (Forms still in place)	1960	1960	-	-	-	-
2/18		25% Prestress + dead load (Forms removed, dead load on from now on)	1960	1960	-	-	-	-
3/3	1a	50% C.S. - 25% M.S.	3750	1960	-	-	-	-
&	b	50% C.S. - 50% M.S.	3750	3750	-	-	-	-
3/4	c	100% C.S. - 50% M.S.	7500	3750	-	-	-	-
	d	100% C.S. - 100% M.S.	7500	7500	-	-	-	-
3/10	2a	Design load and repeat	7500	7500	0	0	0	0
&	&		7500	7500	80	80	80	80
3/11	2b		7500	7500	0	0	0	0
3/12	3	Skip loading	7500	7500	0	0	0	0
&			7500	7500	60	60	60	60
3/13	a		7500	7500	120	60	60	60
	b		7500	7500	60	120	60	60
	c		7500	7500	60	60	120	60
	d		7500	7500	60	60	60	120
			7500	7500	60	60	60	60
			7500	7500	0	0	0	0
3/14	4a	Cracking load and repeat	7500	7500	0	0	0	0
&	&		7500	7500	240	240	240	240
3/17	4b		7500	7500	0	0	0	0
3/18	5	Load to failure	7500	7500	0	0	0	0
			7500	7500	360	360	360	360

III THEORETICAL STUDIES

1. Elastic Plate Theory, Uniform Loads

One of the primary objectives of this study was to compare experimental results with theoretical analysis. Since a prestressed concrete slab can be expected to behave elastically prior to cracking the elastic theory of plates was used to predict the behavior of the slab.

The analytical determination of deflections and bending moments in an elastic plate involves the solution of the Lagrangian differential equation for plates with the appropriate boundary conditions. This differential equation is given by Timoshenko[3] and others as

$$\nabla^4 w = \frac{\partial^4 w}{\partial x^4} + 2\frac{\partial^4 w}{\partial x^2 \partial y^2} + \frac{\partial^4 w}{\partial y^4} = q/D \quad - - - \quad (1)$$

Where w = deflected surface of the plate

x, y = Cartesian coordinates

q = load on the plate

D = flexural rigidity of the plate = $\frac{Eh^3}{12(1-\mu^2)}$

After the solution of eq. (1) with the proper boundary conditions, the moments and shears are found by

$$M_x = -D\left(\frac{\partial^2 w}{\partial x^2} + \mu\frac{\partial^2 w}{\partial y^2}\right) \quad - - - - - - - \quad (2a)$$

$$M_y = -D\left(\frac{\partial^2 w}{\partial y^2} + \mu\frac{\partial^2 w}{\partial x^2}\right) \quad - - - - - - - \quad (2b)$$

$$M_{xy} = +D(1-\mu)\frac{\partial^2 w}{\partial x \partial y} = -M_{yx} \quad - - - - - \quad (2c)$$

$$Q_x = -D \frac{\partial}{\partial x}\left(\frac{\partial^2 w}{\partial x^2} + \frac{\partial^2 w}{\partial y^2}\right) \quad - - - - - - \quad (2d)$$

$$Q_y = -D \frac{\partial}{\partial y}\left(\frac{\partial^2 w}{\partial x^2} + \frac{\partial^2 w}{\partial y^2}\right) \quad - - - - - - \quad (2e)$$

$$V_x = Q_x - \frac{\partial M_{xy}}{\partial y} \quad - - - - - - - - \quad (2f)$$

$$V_y = Q_y + \frac{\partial M_{yx}}{\partial x} \quad - - - - - - - - \quad (2g)$$

where M_x, M_y = bending moments per unit length acting on the yz and xz planes of an element, respectively.

M_{xy}, M_{yx} = torsional moments per unit length acting on the yz and xz planes of an element, respectively.

Q_x, Q_y = vertical shears per unit length acting on the yz and xz planes of an element respectively.

V_x, V_y = total equivalent shearing forces on the yz and xz planes of an element respectively.

μ = Poisson's ratio.

It is often advantageous to reduce eq. (1) to two second order differential equations. Using the notation

$$M = \frac{M_x + M_y}{1 + \mu} \quad - - - - - \quad (3)$$

eqs. (2a) and (2b) become

$$\nabla^2 w = \frac{\partial^2 w}{\partial x^2} + \frac{\partial^2 w}{\partial y^2} = -\frac{M}{D} \quad - - - \quad (4a)$$

and eq. (1) becomes

$$\nabla^2 M = \frac{\partial^2 M}{\partial x^2} + \frac{\partial^2 M}{\partial y^2} = -q \qquad - \quad - \qquad (4b)$$

For a plate supported by concentrated forces eq. (1) or eqs. (4a) and (4b) cannot be solved explicitly because of the rather complicated boundary conditions. Various approximate methods are available for the solution; one of the simplest in concept is the method of finite differences. The finite difference method substitutes finite elements for infinitesimal elements and reduces the solution of a differential equation to the solution of a set of linear simultaneous equations. A detailed discussion of this method and finite difference expressions for various derivatives can be found in a book by Salvadori and Baron[4].

a. First Approximation

A simple example illustrates the method of solution described above. One-eighth of a plate, 2a by 2a in plan with a thickness h, supported by 9 equidistant columns and uniformly loaded is shown below. Only one-eighth of the plate need be considered for this case because of symmetry. A coarse mesh with finite elements having $\lambda = a/2$ is chosen. For each point on the slab (o, a, b, A, B, C) finite difference equations representing eq. (4a) can be written. For points o, a, b finite difference equations representing eq. (4b) can be written. Eq. (4b) cannot be used for support points A, B, and C, because the load on these elements is not q but q + r where r is the reaction. The following notation is used so that all equations will be in a non-dimensional form.

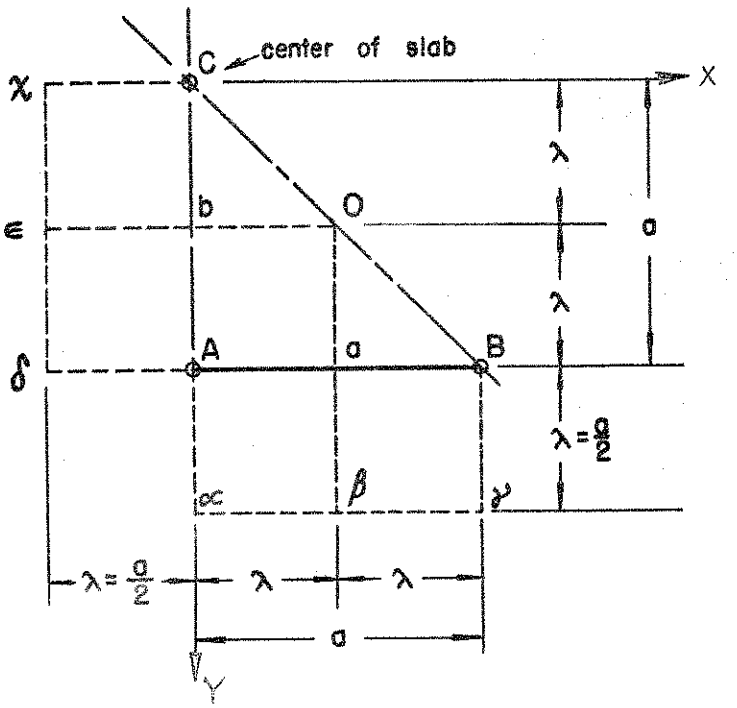

Coordinate System for the Plate

$$U = \frac{M}{q \lambda^2} \qquad - - - - - - \qquad (5)$$

$$Z = \frac{wD}{q \lambda^4} \qquad - - - - - - \qquad (6)$$

$$\begin{aligned}
2 Z_a + 2 Z_b - 4 Z_o &= - U_o \\
Z_A + Z_o + Z_B + Z_\beta - 4 Z_a &= - U_a \\
Z_\varepsilon + Z_C + Z_o + Z_A - 4 Z_b &= - U_b \\
Z_\delta + Z_b + Z_a + Z_\alpha - 4 Z_A &= - U_A \\
2 Z_a + 2 Z_\gamma - 4 Z_B &= - U_B
\end{aligned} \qquad - - - - \qquad (7)$$

$$
\left.
\begin{aligned}
&2\,Z_{\chi} + 2\,Z_{b} - 4\,Z_{c} = -\,U_{c} \\
&2\,U_{a} + 2\,U_{b} - 4\,U_{o} = -\,1 \\
&U_{A} + U_{o} + U_{B} + U_{\beta} - 4\,U_{a} = -\,1 \\
&U_{\varepsilon} + U_{C} + U_{o} + U_{A} - 4\,U_{b} = -\,1
\end{aligned}
\right\} \quad - - - \quad \text{(7 Cont.)}
$$

Eqs. (7) must be solved together with the appropriate boundary conditions. Along boundary x = 0 the slope in the x - direction, $\frac{\partial w}{\partial x}$, and the shear, V_x, must be equal to zero. Along boundary y = a the moment about the x - axis, M_y, and the shear, V_y, must be equal to zero because of the free boundary. In addition, the deflections at A, B, and C must be zero. Expressing these conditions in finite difference equations, we have

$$Z_{b} - Z_{\chi} = 0 \qquad - - - - - - - - - \qquad (8)$$

$$Z_{o} - Z_{\varepsilon} = 0 \qquad - - - - - - - - - \qquad (9)$$

$$Z_{a} - Z_{\delta} = 0 \qquad - - - - - - - - - \qquad (10)$$

$$U_{o} - U_{\varepsilon} = (1 - \mu)\left[(Z_{b} - 2\,Z_{o} + Z_{a}) - (Z_{\chi} - 2\,Z_{\varepsilon} + Z_{\delta})\right] \qquad (11)$$

$$Z_{\alpha} - 2\,Z_{A} + Z_{b} = -\,\mu\,(Z_{a} - 2\,Z_{A} + Z_{\delta}) \qquad - - - - \qquad (12)$$

$$Z_{\beta} - 2\,Z_{a} + Z_{o} = -\,\mu\,(Z_{B} - 2\,Z_{a} + Z_{A}) \qquad - - - - \qquad (13)$$

$$U_{B} = 0 \qquad - - - - - - - - - - - \qquad (14)$$

$$U_{\beta} - U_{o} = (1 - \mu)\left[(Z_{\gamma} - 2\,Z_{\beta} + Z_{\alpha}) - (Z_{a} - 2\,Z_{o} + Z_{b})\right] \qquad (15)$$

$$Z_{A} = 0 \qquad - - - - - - - - - - - \qquad (16)$$

$$Z_{B} = 0 \qquad - - - - - - - - - - - \qquad (17)$$

$$Z_{C} = 0 \qquad - - - - - - - - - - - \qquad (18)$$

Eqs. (7) through (18) can be solved simultaneously to obtain the moments and deflections of the plate. The results are tabulated in Table 4.

Table 4 - Theoretical values obtained from plate theory for a 2a x 2a plate uniformly loaded. Mesh size $\lambda = a/2$ Poisson's ratio = 0.15.

x	y	$\frac{M_x}{qa^2}$	$\frac{M_y}{qa^2}$	$\frac{M_{xy}}{qa^2}$	$\frac{wD}{qa^4}$	Reactions $\frac{R}{qa^2}$
0	0	-0.126800	-0.126800	0	0	1.288
0	a/2	-0.042228	0.101444	0	0.013782	
0	a	-0.095724	0	-	0	0.504
a/2	a/2	0.074672	0.074672	0	0.021128	
a/2	a	0.095724	0	0.005742	0.012241	
a	a	0	0	-	0	0.174

b. Second Approximation

The accuracy of the solution can be improved by using a finer mesh than that of the preceding example. The procedure is exactly the same, the only difference being that the number of equations which must be solved in order to obtain a solution becomes larger. Table 5 gives values obtained for a mesh size of $\lambda = a/4$.

The results from this second approximation are compared to experimental results in Figs. 38 through 49. It should be noted that the test slab differed slightly from the plate considered in the above theory since a 6-in. overhang extended on all sides of the test slab resulting in a 15 x 15 ft. test slab. The plate considered in the theory had its supports at the edges and center of a 14 x 14 ft. plate. The effect of the overhang is small when considering moments and deflections and is thus neglected in these comparisons. In comparing reactions, however, allowance is made for

Table 5 - Theoretical values obtained from plate theory for a 2a x 2a plate uniformly loaded. Mesh size λ = a/4. Poisson's ratio = 0.15.

x	y	M_x/qa^2	M_y/qa^2	M_{xy}/qa^2	wD/qa^4	Reactions R/qa^2
0	0	-0.244823	-0.244823	-	0	1.392
0	a/4	-0.103491	-0.020946	0	0.006653	
0	a/2	-0.047029	0.095041	0	0.010974	
0	3a/4	-0.062828	0.093176	0	0.008767	
0	a	-0.165722	0	-	0	0.513
a/4	a/4	0.009894	0.009894	-0.024335	0.010062	
a/4	a/2	0.012630	0.073556	-0.005780	0.012933	
a/4	3a/4	0.015403	0.068211	0.017557	0.011222	
a/4	a	0.025270	0	0.038170	0.005298	
a/2	a/2	0.060725	0.060725	-0.001875	0.014790	
a/2	3a/4	0.065263	0.055515	0.004664	0.013347	
a/2	a	0.087249	0	0.009825	0.008980	
3a/4	3a/4	0.059463	0.059463	-0.010779	0.011831	
3a/4	a	0.081135	0	-0.021322	0.007084	
a	a	0	0	-	0	0.139

the difference by adding to each of the theoretical exterior reactions an amount equal to the load on an area 6 in. wide and 7.0 ft. long. The center reaction is assumed unaffected.

c. Richardson's Extrapolation

The accuracy of the theoretical results obtained from the first and second appoximations can be increased by Richardson's extrapolation procedure. This procedure is described by Salvadori[4]. The "h^2 - extrapolation formula" is given as

$$k'_{ij} = \frac{n_j^2 k_j - n_i^2 k_i}{n_j^2 - n_i^2} \quad - - - - \quad (19)$$

where $k'_{i,j}$ = extrapolated value of K

K = true value of quantity

k_i, k_j = approximate values of K for n_i and n_j, respectively

n_i, n_j = number of sub-intervals in approximation = $\frac{a}{\lambda}$

For the two approximations which are tabulated in Table 4 and 5, $n_1 = 2$ and $n_2 = 4$, therefore

$$k'_{1,2} = \frac{4^2 k_2 - 2^2 k_1}{4^2 - 2^2} = \frac{4}{3} k_2 - \frac{1}{3} k_1 \quad - \quad - \quad - \qquad (19')$$

Table 6 shows the extrapolated values obtained from the two approximations.

Table 6 - Theoretical values obtained from plate theory for a 2a x 2a plate uniformly loaded. Extrapolation from $n_1 = 2$, $n_2 = 4$ Poisson's ratio = 0.15.

x	y	M_x/qa^2	M_y/qa^2	M_{xy}/qa^2	wD/qa^4	Reactions R/qa^2
0	0	-0.284164	-0.284164	-	0	1.427
0	a/2	-0.048629	0.092907	0	0.010038	
0	a	-0.189055	0	-	0	0.516
a/2	a/2	0.056076	0.056076	-0.007707	0.012677	
a/2	a	0.084424	0	0.011186	0.007893	
a	a	0	0	-	0	0.127

Because of the time involved in solving the simultaneous equations no better approximations were attempted. A solution using a third approximation with a sub-interval of $\lambda = a/8$ would have required the solution of 101 linear simultaneous equations.

The second approximation with subinterval $\lambda = a/4$, which involved the solution of 33 linear simultaneous equations, was solved with the aid of the IBM 701 computer. No programming was necessary as a standard routine was available for the solution of 45 or less linear simultaneous equations.

The actual machine time required to solve the 33 equations was less than a minute. When programs are available to solve larger size matrices the finite difference solution of the plate equation will become a simple and fast approach as it is an easy matter to set up a problem in finite difference form.

2. Elastic Beam Theory, Uniform Loads

Present design of continuous prestressed concrete lift slabs is usually based on the behavior of beams.[2] The slab is considered to be a continuous beam in each direction. For the purpose of design in one direction the supports normal to this direction are considered to be continuous rather than point supports. When designing in the other direction, a similar assumption is made. The problem thus reduces to the analysis of a continuous beam in each direction. The beam width is normally taken equal to the panel width. The total moments obtained in this way for a panel width are then distributed to the middle and column strips to account for the fact that the supports are actually point supports instead of continuous supports as assumed in the analysis. For example, 45% of the total moment may be assumed to be carried by the middle strip while 55% of the total moment is assumed to be carried by the column strips. The test slab in this investigation was designed on the basis of the elastic beam theory.

The bending moments for a two span continuous beam uniformly loaded are obtained quite easily and are presented below.

Comparisons between the beam theory moments and the experimental results are shown in Figs. 38 through 42 in which the calculated beam theory moments for a panel width are shown distributed uniformly to the column and middle strips.

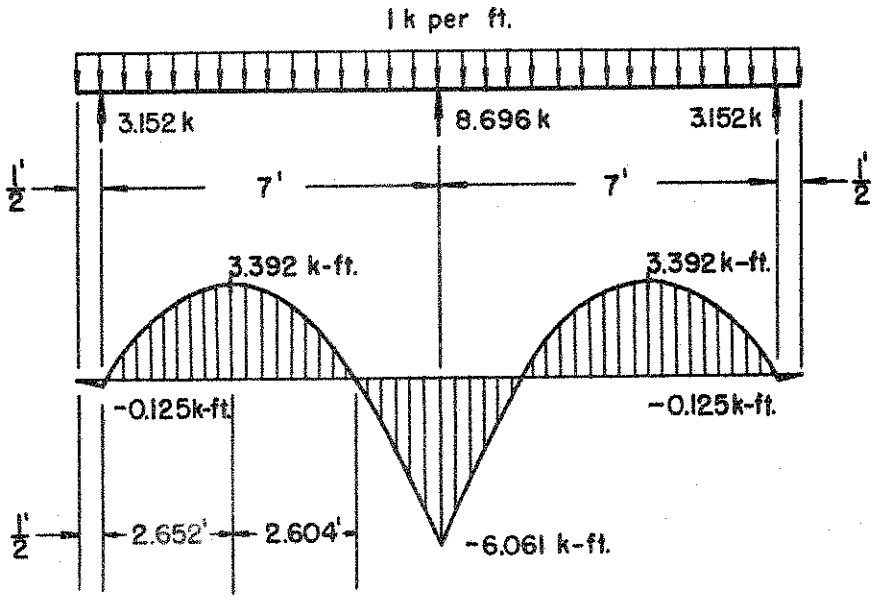

Moment Diagram due to Uniform Load of 1 kip per ft.

The deflection at the center of a panel can be approximated by use of the beam theory. The usual method is to superimpose deflections due to beams in two directions. For example, the deflection at the center of a panel is calculated by adding the deflections at the center of two beams, a one ft. wide beam passing over the columns and another one ft. wide beam orthogonal to the first and passing through the center of the panel. Each beam is loaded with a uniform load per ft. of q.

For a slab similar to the test slab, the deflection at the center of the panel, under a uniform load q, calculated by the beam theory is:

$$\Delta = 0.125 \frac{qa^4}{Eh^3} \qquad - \quad - \quad - \quad - \quad - \qquad (20)$$

The same deflection from the plate theory, for $\mu = 0.15$, is:

$$\Delta = 0.149 \frac{qa^4}{Eh^3} \quad - \quad - \quad - \quad - \quad - \quad - \quad - \quad (21)$$

A comparison between deflections from the beam theory and the plate theory is shown in Fig. 10 for slabs having various edge conditions. Data for the deflection of a panel on 4 columns and a typical interior panel may be found in references 3 and 4.

3. Elastic Beam Theory, Prestressing.

If the slab is assumed to be a continuous beam in each direction the moments and stresses induced by prestressing can be calculated by converting the forces produced by the prestressing into equivalent loads.[2] The loading and the corresponding moment diagram is shown on the next page for the cable profile shown in Fig. 4.

Comparisons with experimental results are shown in Figs. 13 through 17 for the case of an equal prestress force in all cables of 6840 lbs per cable.

4. Design Load and Cracking Load from Beam Theory.

By combining the effect of uniform load and prestressing, the design and the cracking load can be determined. The design load capacity of prestressed concrete slabs is usually based on a criterion that the allowable tensile stress equals zero or some limited value, such as 100 or 200 psi. The cracking load of the slab is usually assumed to occur when the computed tensile stress in the concrete reaches the modulus of rupture as determined from plain concrete control beam specimens.

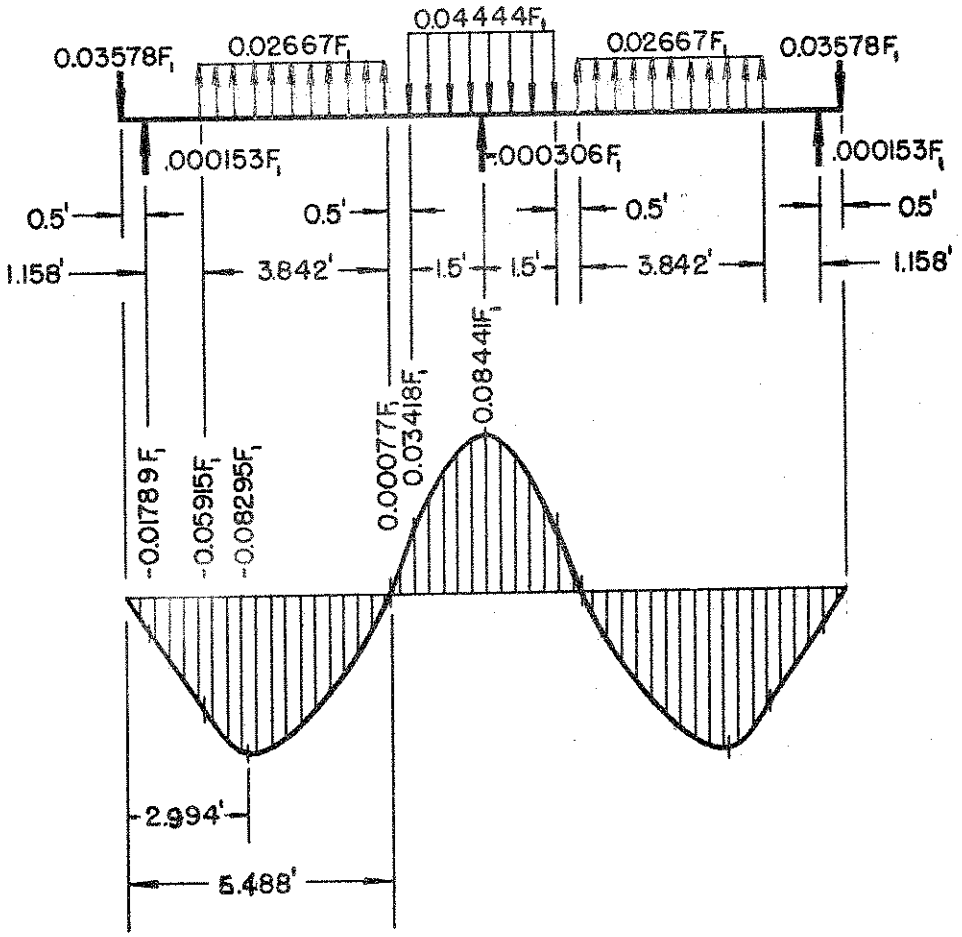

Loads and Moments Due to Prestress, F_1,
where F_1 = Prestress Force per ft. of width

According to the above beam theory, the live load design capacity for the test slab based on no tensile stress in the concrete was found to be 76 psf for a prestress force in all cables of 6840 lbs per cable. The live load for cracking based on a modulus of rupture of 480 psi and a prestress force of 6840 lbs per cable was 194 psf.

5. Ultimate Load

The ultimate load capacity of the slab can be calculated from the yield line theory for slabs. Because of the nature of the prestressing the yield line pattern shown below can be assumed.

An assumption must be made as to the stress in the prestressing steel at ultimate. Because the cables are unbonded, it is unlikely

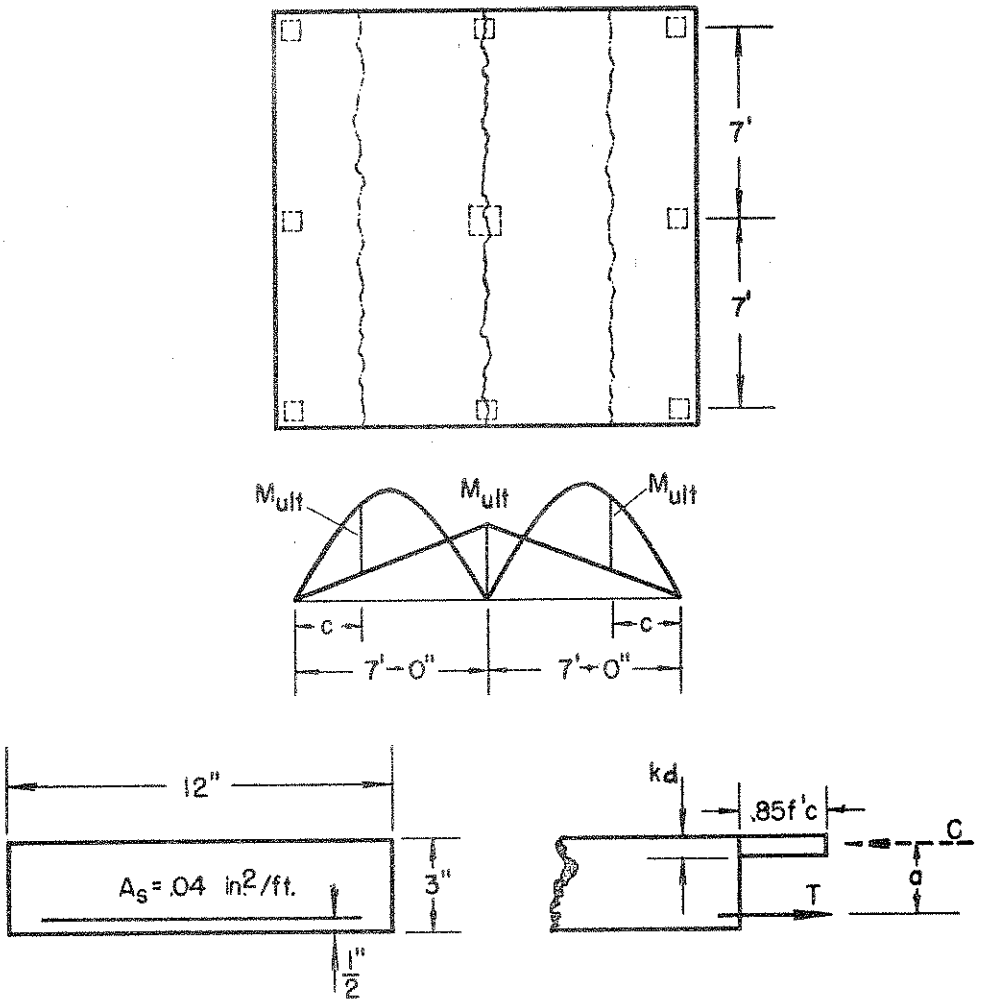

Ultimate Strength Theory

that the steel stress will reach its ultimate or even its yield strength. In the calculations which follow a steel stress of 200 ksi at ultimate load is assumed, which yields an ultimate live load capacity of 356 psf.

$f'_c = 6000$ psi

$T = f_s \times A_s = 200 \text{ ksi} \times 0.04 = 8$ kips

$C = kd \times b \times 0.85 f'_c = kd \times 12 \times 0.85 \times 6 = T = 8$ kips

$kd = 0.131$ in. $\qquad a = 2.5 - \frac{0.131}{2} = 2.435$ in.

$M_{ult} = 8 \times 2.435 = 19.5$ kip-in.

$c = 0.414\ L = 0.414 \times 7 = 2.9$ ft. (from plastic analyses of continuous beam)

$$w_{ult} = \frac{2\ M_{ult}}{c^2} = \frac{11.6\ M_{ult}}{L^2} = \frac{11.6}{49 \times 12} \times 19.5 \times 1000 = 385$$

$w_{DL} = 3/12 \times 150 = 38$

w_{LL} = ultimate = 347 psf

IV EXPERIMENTAL RESULTS AND DISCUSSION

1. General

Experimental results for the effect of four different types of loading on the slab were obtained. These were as follows:

a. Equal prestress in all cables. (uniform prestress case)

b. Unequal prestress in cables, (1.8:1 ratio of prestress between column and middle strips).

c. Uniform live load on one panel only. (skip loading)

d. Uniform live load on all four panels. (uniform load case)

The effects of the various loadings were determined separately. The results are presented almost entirely in the form of curves. Generally, for each of the cases indicated above, the following information was obtained.

a. From strain measurements on slab surface:

1. Prestress or load vs. strain curves.

2. Stresses and moments at various sections in the elastic range.

b. From deflection measurements:

1. Prestress or load vs. deflection curves.

2. Deflected shapes of various sections in the elastic range.

3. Contour map of the deflected surface of the slab in the elastic range.

c. From measurements of the reactions at supports:

1. Prestress or load vs. reaction curves.

2. Distribution of load to supports.

d. From measurements of forces and strains in the prestressing steel:

1. Loss of prestress due to friction.

2. Increase in steel stresses due to load.

During the live load tests the prestress in all cables was the same and averaged 6840 lbs. per cable or 140 ksi.

Generally, the prestress force referred to is the average prestress force in the steel rather than the jacking force.

The sum of the reactions obtained from the reaction meters agreed to within 2% of the load as measured by the manometers for all loads less than 240 psf; however, for higher loads close to the ultimate the difference was as high as 6%. In all cases the total load indicated by the reactions meters was less than that indicated by the manometer readings. This difference was attributed to the pressure drop between the manometers and the air bags as air pressure was being introduced at higher loads. For this reason the total load on the slab used in all calculations was determined from the sum of the reaction measurements rather than from the manometer readings.

The stresses and moments in the elastic range were found by first plotting the observed data as prestress or load vs. strain curves. The strains at a certain prestress or load were then taken from these curves and plotted at various sections taken through the gage locations. Then the stresses at these sections were calculated from the strains by using Hooke's Law:

$$\sigma_{x_{T,B}} = \frac{E}{1-\mu^2}\left(\varepsilon_{x_{T,B}} + \mu\varepsilon_{y_{T,B}}\right) \quad - \quad - \quad (22)$$

$$\sigma_{y_{T,B}} = \frac{E}{1-\mu^2}\left(\varepsilon_{y_{T,B}} + \mu\varepsilon_{x_{T,B}}\right) \quad - \quad - \quad (23)$$

The subscripts T and B refer to the top and bottom surface, respectively. The bending moments at the sections were then calculated from:

$$M_x = \frac{\left(\sigma_{x_B} - \sigma_{x_T}\right) h^2}{12} \quad - \quad - \quad - \quad - \quad - \quad (24)$$

$$M_y = \frac{\left(\sigma_{y_B} - \sigma_{y_T}\right) h^2}{12} \quad - \quad - \quad - \quad - \quad - \quad (25)$$

Curves for M_x represent the bending moment distribution along a section x = a constant, $-7.5 \leq y \leq 7.5$. The system of coordinates used is shown in Fig. 9. The gross bending moment at a section is therefore the area under the M_x curve, $\Sigma M_x \cdot \Delta y$. Since each of the reactions was measured independently, the gross bending moment at a section could also be calculated by the principles of statics to obtain a check between the strain measurements and the reaction measurements. This latter value is represented by the term "Statics: M" in the curves for the moments.

2. Effect of Equal Prestress in all Cables (Uniform Prestress Case).

A typical prestress vs. strain curve is plotted in Fig. 11 for uniform prestress. The curve shows that the slab behaved elastically during prestressing.

The stresses, σ_x and σ_y, acting across and along section x = 0 are shown in Fig. 12 for the full prestress of 6840 lbs. per cable. The stresses were calculated using the 28 day cylinder modulus of elasticity of 3,500,000 psi and a Poisson's ratio of 0.14. The average stress in the concrete as measured by the strain gages was 253 psi compression. However, the average stress in the concrete should only have been 152 psi compression as calculated by P/A, for the prestress force of 6840 lbs. per cable. This same discrepancy was noted at all of the measured sections for this case of uniform prestress.

This was the only major discrepancy encountered in the entire test program. The cause of this discrepancy is not known. It is unlikely that errors in strain measurement could have caused this discrepancy. At full prestress the measured compressive strains would have to be decreased by 25 micro-inches and the measured tensile strains would all have to be increased by 25 micro-inches in order to obtain agreement. Errors in strain measurements are more likely to be accidental in nature; therefore, it is not believed that the strains were in error by this amount.

The modulus of elasticity of the slab may have been different from the cylinder modulus of 3,500,000 psi that was used for the calculations. If all of the discrepancy was attributed to the modulus a modulus of 2,100,000 psi would have been required. This modulus would seem to be too low for a concrete age of 28 days.

The Poisson's ratio used also affects the calculation of the average stress in the slab. This error is probably small since a change in the Poisson's ratio from 0.14 to 0 changes the average stress by only 14%. The likelihood that the Poisson's ratio was closer to zero than to 0.14 is small.

The elapsed time from the start of prestressing to the taking of the readings was only about 2 hours; therefore the effects of shrinkage and creep should have been negligible.

Perhaps the true reason for this discrepancy is a combination of all of the above effects.

The moments produced by the equal prestress of 6840 lbs. per cable are plotted in Figs. 13 through 17. M_x is the bending moment distribution across the section whereas M_y is the bending moment diagram along the section. Only one-half of the total width of the section is shown since the moments are symmetrical about the centerline of the slab. The difference between the gross moments as measured by the strain gages and as obtained from statics using measured reactions and cable forces range from 5 to 26%. The moments calculated from the measured reactions and cable forces are very sensitive to the cable location. A change in the cable location of 0.1 in. would eliminate the differences between the two calculated moments.

Also plotted in Figs. 13 through 17 are theoretical values for bending moments as obtained from the beam theory. It can be noted that there is good agreement between theoretical and experimental values at all sections indicating that the beam theory is fairly accurate in predicting the moments for this case.

The measured deflections due to uniform prestress are shown in Figs. 18, 19, and 20. In Fig. 19 the experimental points are plotted along with deflected shapes calculated by the beam method for comparison. Again the agreement between theoretical and experimental values is good. The maximum deflection of the slab due to uniform prestress was 0.052 in. upward as shown in Fig. 20.

The reactions induced by the uniform prestress were quite small as shown in Fig. 21.

Fig. 22 shows the loss of prestress in the cables due to friction for nominal values of 25, 50, and 100% of full prestress. Theoretical values are based on the usual formula for loss due to cable friction. It can be noted that there is a considerable scatter of the experimental data for

the various cables. At full prestress the average loss was about 15% in the total length of 15 ft.

3. Effect of 1.8:1 Ratio of Prestress Between Column Strip and Middle Strip.

Fig. 23 shows experimental values for the moments at three sections caused by prestressing the cables in the column strips nominally twice as much as the cables in the middle strips. The average force in the column strip cables was 6840 lbs. each while the average force in the middle strip cables was 3320 lbs. each. The width of column and middle strips by definition is 1/4 x 14 x 12 = 42 in. With the cable spacing used it can be found that the total force delivered to the column strip over the outer row of columns, the middle strip, and the column strip over the center row of columns is 19.2, 10.0, and 16.4 kips respectively. The net effect has been termed a nominal 1.8:1 ratio of prestress.

A modulus of elasticity of 3,500,000 psi and a Poisson's ratio of 0.14 was used for the calculation of moments from strain readings.

A comparison between the moment distribution caused by the 1:1, 1.8:1 ratios of prestress and by uniform load over the entire slab are shown in Fig. 24. In order to make a proper comparison the total prestress in each direction was made equal for the two ratios of prestress. At section x = 0, the total gross moment due to the uniform load of q = 85 psf would be equal to the total gross moment produced by either ratio of prestress. Thus either combination of prestress and load would produce a gross moment of zero at this section.

Fig. 25 shows the deflected shape of the slab due to the 1.8:1 ratio of prestress. For the same total prestress as in the 1:1 case the maximum

deflection would be 0.047 in. upward for the 1.8:1 prestress as compared to 0.052 in. upward for the 1:1 prestress.

4. Effect of Live Load on One Panel Only (Skip Loading).

No theoretical calculations were made for this case, thus all of the results presented are based on experimental values obtained from the test program.

The moments due to a uniform load of 100 psf on one panel are shown in Figs. 26 through 28. A modulus of elasticity of 4,150,000 psi and a Poisson's ratio of 0.14 was used for the calculations. In both the skip load and the uniform load case, the modulus of 4,150,000 psi was used rather than the cylinder modulus of 3,500,000 psi in order to maintain consistency between the gross moments as calculated from strain measurements and the gross moments as calculated from the equations of statics using the reaction measurements.

Referring to Table 3 it can be seen that the maximum effect measured for live load in one panel was for a load of 60 psf. However, for purposes of comparison with the case of a 100 psf uniform live load on all four panels all of experimental values for the skip loading case were increased by a ratio of 100:60 before drawing the curves.

The difference between the gross moments calculated from the strain measurements and from statics using the reaction measurements is due primarily to the size of the strain readings. In many of the gages the strains were in order of 5 to 10 micro-inches per inch for the load of 60 psf.

Comparing Figs. 13 through 17 for uniform prestress with Figs. 26 through 28 for skip load, the skip load moments in the loaded panel are

counteracted very well by the prestressing moments. In the unloaded panels, however, the moments tend to add, causing an increase in tensile stresses already existing. At x = - 5.25, y = 3.5 the top fiber stresses caused by full prestress, 100 psf live load on one panel and dead load are +40, + 50, and - 65 psi, repsectively, the total tensile stress being + 25 psi, a relatively small value.

The deflections due to the load on one panel are shown in Figs. 29 through 31. The maximum deflection in the loaded panel was about 5 times the maximum deflections in the unloaded panels.

The load-reaction curves and the load distribution curves are shown in Figs. 32 and 33. It is noted that the load on the 6 in. overhang tended to equalize the reactions at the boundaries of the loaded panel.

5. Effect of Uniform Load on all Four Panels (Uniform Load Case)

The general behavior of the slab with a uniform load on the entire slab can be deduced from the typical load-strain curves shown in Figs. 34 through 37. Because of the test arrangement a visual inspection for cracks on the top surface of the slab during the test could not be made. However the first tensile crack, as indicated by strain readings, seems to have occurred over the center support at a live load of 100 psf. This crack was localized and did not pass through the gage 6 in. away from the center support (gage point 13) until the load reached 160 psf.

The first visual observation of cracks occurred at a load of 290 psf. Cracks were then observed at the edges of the slab directly over the center supports.

The first cracks on the bottom of the slab were observed at a load of 330 psf. They began at the edges of the slab at the mid-span of the panels

and extended inward about 2 ft. At a load of 347 psf a crack 1/8 in. wide extended across the bottom of the slab from the east edge to the west edge 52 in. from the north edge of the slab. At 356 psf a similar crack occurred in the north-south direction 36 in. from the west edge of the slab.

Ultimate failure occurred at a live load of 362 psf with the center support punching through the slab. The failure occurred directly around the edges of the 9 by 9 in. center support at a shear angle of about 45°. The crack pattern at ultimate is shown in Fig. 53.

The moments caused by the uniform load in the elastic range are shown in Fig. 38 through 42. The agreement between the moments calculated from the strain measurements, $\Sigma M_x \cdot \Delta y$, and the moments calculated by statics from the reaction measurements, "Statics:M", is very good.

At sections x = 0, 1.75, 3.5 and 5.25 ft the differences are 0.7, 75.0, 0.8, and 0.4%. At section x = 1.75 ft. where the difference is 75% the gross moment obtained from statics is very sensitive to reaction measurements. A change of 2% in the reactions would reduce the difference to zero. No values for M_x are plotted at section x = 7.0 ft. since strains in the x direction were not measured at this section. The gross moment on this section is quite small, being equal to 94 lb-ft.

By inspecting Figs. 38 through 42 a comparison between the experimental moments obtained from strain measurements and theoretical moments obtained by the elastic plate theory may be made. Agreement again is good, the only major discrepancy exists for the moments near the center support, i.e., at x = 0, y = 0. At this point it can be seen that the theoretical value obtained using Richardson's extrapolation procedure tends to approach the experimental value. This indicates that if a finer mesh were used in the finite difference

solution the theoretical and experimental values would probably be in close agreement at this point. From the above comparisons it can be stated that the elastic plate theory can be used to accurately predict the magnitude and distribution of moments in a prestressed concrete slab loaded within the elastic range.

The experimental moments may also be compared to the theoretical moments obtained by the beam theory. Since the beam theory assumes a uniform moment across the width of the slab the M_y curve is the same in Figs. 38 through 42. It is apparent that at sections of high moment such as x = 0 the distribution of the experimental moments M_x is not uniform across the section, and that some distribution of the gross moment obtained by the beam theory should be made, with a higher percentage going to the column strips than the middle strips.

Stresses were not plotted for the uniform load case, since the stresses in psi are simply 2/3 of the moments in ft. lbs per ft. (from Eqs. 24 and 25), if the top fiber stress is assumed equal to the bottom fiber stress. Figs. 34 through 37 show that the bottom fiber strains in general were not equal to the top fiber strains but the differences were quite small in most cases. The differences represent axial forces which may be due to increases in cable forces due to loading or to axial forces induced by the loading.

The load-deflection curves for the panel centers are shown in Fig. 43. Elastic behavior of the slab can be noted until the load reached around 160 psf. The maximum deflection just prior to the serious cracking at a load of 347 psf was 0.24 in. The deflections increased sharply when the large cracks occurred.

Figs. 44 and 45 compares the measured deflections with theoretical plate deflections for a load of 100 psf. Agreement is very good when

theoretical values obtained using Richardson's extrapolation are compared with experimental values. Comparing the prestress deflections of Fig. 20 with the uniform load deflections of Fig. 45 shows that the slab would be nearly flat under the combined effect of the prestress, and a total load (dead plus live) of 100 psf.

Figs. 46 through 50 show the distribution of the load to the supports in the elastic and plastic ranges. Very little change in the distribution of load was observed between the elastic and plastic ranges. Direct comparison between Figs. 49 and 50 should not be made as Fig. 49 applies only to the live load while Fig. 50 includes the dead load and prestress as well as the live load.

The last measurements were taken at a live load of 356 psf although failure did not occur until the load reaches 362 psf. Observations of the deflections, reactions and steel strains were made as well as visual observations of the crack pattern. The crack pattern at failure is shown in Fig. 53.

The maximum deflection at a live load of 356 psf was 2.1 in. at the center of the northwest panel. The most serious cracking occurred in this panel.

The stress in the prestressing steel increased sharply when the serious cracks occurred as shown in the typical load-cable force curve of Fig. 51. Fig. 52 shows the cable stresses at a load of 356 psf together with the increase in cable stress from 0 to 356 psf. No particular distribution of stresses or increase in stresses can be noted. Comparing Fig. 52 with Fig. 53, the cable stresses were known only at the east-west crackline at the top of and through the center of the slab. The average cable stress in the steel at this crack line was 170 ksi.

The average cable stress required at all of the crack lines for a live load of 356 psf were calculated from the reaction measurements and are shown in Table 7. The reactions used for the calculations are shown in Fig. 50. The total load on the slab including dead load was 394 psf. The concrete stresses at the sections were assumed to be described by Whitney's rectangular stress block with f'_c = 5940 psi. At sections 1-1 and 2-2 which pass through the supports the contribution of 0.27 sq. in. of mild steel were mesh to the resisting moment was taken into account.

At section 1-1 where the cable stresses were measured, the average measured cable stress was 170 ksi compared to the calculated stress of 190 ksi required to resist the moment, a difference of 12% of the measured stress. Strain measurements were taken on only one-half of the cables. It is possible that the stresses in the unmeasured cables were higher than in the measured cables since the deflections in the panels affecting the unmeasured cables were much larger than the deflections in the panels affecting the measured cables. Also, section 1-1 passes through three reaction bearing plates. If these bearing plates are assumed bonded to the concrete and there contribution to moment capacity as part of a composite section is included in the moment calculations, the calculated cable stress would only be 180 ksi or 6% different from the measured stress.

Table 7 - Calculated Steel Stresses Required at Ultimate

(q_{LL} = 356 psf)

Section	Distance From Center of Slab ft.	Direction of Cracks	Calculated Gross Moment From Reaction Meas. lb-ft	Cable Stress Required to Resist. Moment ksi	Measured Cable Stress ksi
1-1	0	EW	-24,200	190	170(1)
2-2	0	NS	-26,400	210	(2)
3-3	3.17	EW	20,800	196	(2)
4-4	4.50	NS	19,200	160	(2)

(1) Average stress in 6 cables crossing section.

(2) Cable stresses not measured at these sections.

V SUMMARY AND CONCLUSIONS

1. General

In this investigation the behavior of a 15 x 15 ft slab, 3 in. thick, and supported at 9 points was studied analytically and experimentally. The studies made and the quantities determined for each case are listed below:

1. Equal prestress in all cables (uniform prestress case).
   a. Experimental moments, deflections, and reactions.
   b. Theoretical moments and deflections by the beam theory.
2. Unequal prestress in cables (1.8:1 ratio of prestress between column and middle strips).
   a. Experimental moments, deflections, and reactions.
3. Uniform live load on one panel only (skip loading).
   a. Experimental moments, deflections, and reactions.
4. Uniform live load on all four panels (uniform load case).
   a. Experimental moments, deflections and reactions within the elastic range.
   b. Experimental deflections, reactions, and cable stresses at ultimate load.
   c. Theoretical moments, deflections, and reactions in the elastic range by the elastic plate theory.
   d. Theoretical values for the design, cracking, and ultimate loads using the beam theory.

Utilizing the beam theory as usually practiced in present design methods, the live load design capacity based on no tension in the concrete was 76 psf; the live load for cracking based on a modulus of rupture of 480 psi was

was 194 psf; and the ultimate live load based on a steel stress of 200 ksi was 356 psf. These values were calculated for equal prestress in all cables.

Actual behavior of the slab observed during testing indicated very localized cracking on the top surface near the center support at a live load somewhere between 100 and 160 psf. First cracks on the bottom surface occurred at a live load of 330 psf. The maximum deflection just prior to serious cracking at 347 psf was only 0.20 in. The slab failed at a live load of 362 psf. Just prior to failure the maximum deflection was 2.1 in.

2. Elastic Plate Theory

Considering the case of uniform live load on the entire slab a number of conclusions may be drawn. Relatively good agreement was obtained between experimental values and theoretical values found by the elastic plate theory. Even with a relatively course approximation of $\lambda = a/4$, using the finite difference procedure, the plate theory gave moments within 10% of experimental values except over the center support and at other points where the moments are small and thus unimportant. Over the center support it is believed that if λ is taken equal the column (or collar size in a lift slab), theoretical values would compare favorably with experimental values. One foot away from the center support the plate theory moments, using $\lambda = a/4$, were practically equal to the experimental values. The comparison between the experimental and theoretical deflections by the plate theory was equally good.

Since the agreement was good for the case described above it can be concluded that the elastic plate theory should be valid for predicting the behavior of a prestressed concrete slab under any type of loading within the elastic range.

3. Cracking Load

The cracking load for continuous slabs has little practical significance since initial cracking is very localized at points of high moment. This was demonstrated during the test where the load producing the first cracks over the center support was doubled without any signs of distress or widespread cracking in the slab. Tensile cracks occurred at experimental stresses of about 400 to 700 psi, indicating that the modulus of rupture (480 psi) could be used together with the elastic plate theory to predict the cracking load within these limits.

The physical behavior of the slab was ideal as a structure. Deflections and cracks were small up to a live load of 347 psf. Ample warning was given of impending failure by the opening of large cracks and a large increase in the magnitude of the deflections. Final failure occurred when the center support punched through the slab at a live load of 362 psf.

4. Ultimate Strength

The ultimate load carrying capacity of the test slab was closely estimated by means of the beam method. It appears that this method will yield accurate results provided the crack line pattern at failure is similar to that assumed in the beam method. One other difficulty lies in the estimation of the steel stress at failure, although this can generally be estimated within certain limits.

5. Beam Method of Analysis

Theoretical moments and deflections obtained by the beam theory may be compared with those obtained experimentally for the cases of uniform prestress and uniform load over the entire slab.

A comparison of the magnitude and distribution of calculated theoretical moments by the beam theory with those obtained experimentally for the "uniform prestress case" indicates fairly good agreement with little variation in moments ascross a section. Deflections obtained by the beam theory also compare well with experimental values.

When the "uniform load case" is considered the beam theory does not accurately predict the magnitude of moments at specific locations. This is due to the fact the beam theory assumes a uniform distribution of moments across any section while actually the magnitude of the moments varies considerably across a section. For example, at a section through the center support (i.e., at x = 0), for a load of 100 psf the beam theory yields a uniform moment across the section of 606 ft. lb/ft. while the actual moments measured during the test for this load were a maximum of 1800 ft.lb/ft. over the center support and a minimum of 170 ft.lb/ft. at a distance of 4 ft. from the center support. While this discrepancy exists regarding the distribution of moments the total moment across a section calculated by the beam method is within 15% of that obtained experimentally, at all significant sections.

A quantitative study of these results indicates that for elastic behavior under uniform load the total negative moment calculated by the beam theory should be distributed approximately 75% to the column strips and 25% to the middle strips, while the total positive moment calculated by the beam theory should be distributed approximately 60% to the column strips and 40% to the middle strips. Thus the ratio of 55/45% common in present practice should be greatly modified. A heavier concentration of cables in the column strips should be used to obtain a better elastic behavior of the slab.

Deflections under uniform load given by the beam theory are within 15% of those obtained experimentally or by the elastic plate theory. Since the proper value of E_c to use is difficult to ascertain this appears to be accurate enough for predicting elastic deflections for design purposes.

6. Partial Live Load (Skip Loading)

Experimental values for moments and deflections were obtained for load on one panel only but no attempt was made to solve the problem analytically. It is believed that the elastic plate theory will yield correct values for these quantities. The beam theory does not appear to be applicable for this loading case, except as a rough approximation.

For the design live load acting on one panel in combination with dead load and uniform prestress, small but relatively insignificant tensile stresses were produced in the slab.

VI. References

1. Scordelis, A. C., Pister, K. S., and Lin, T. Y., "Strength of a Concrete Slab Prestressed in Two directions", ACI JOURNAL, Vol. 28, No. 3, September, 1956, pp. 241-256.

2. Lin, T. Y., "Design of Prestressed Concrete Structures", John Wiley & Sons, New York, 1955, pp. 324-344.

3. Timoshenko, S., "Theory of Plates and Shells", McGraw-Hill Book Company, New York and London, 1940.

4. Salvadori, M. G., and Baron, M. L., "Numerical Methods in Engineering", Prentice Hall, Inc., New York, 1952.

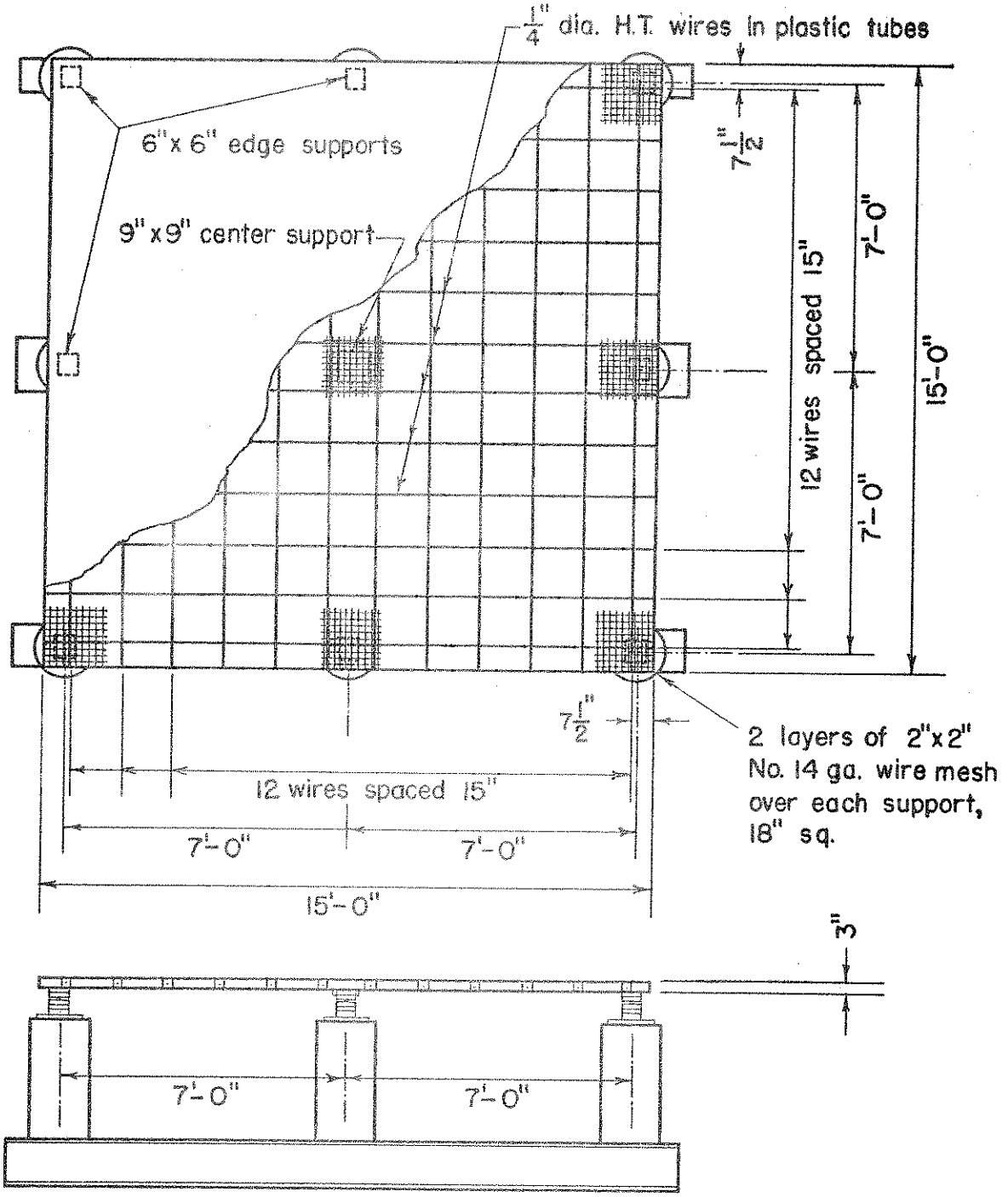

FIGURE 1. PLAN and ELEVATION of SLAB, SHOWING STEEL ARRANGEMENT

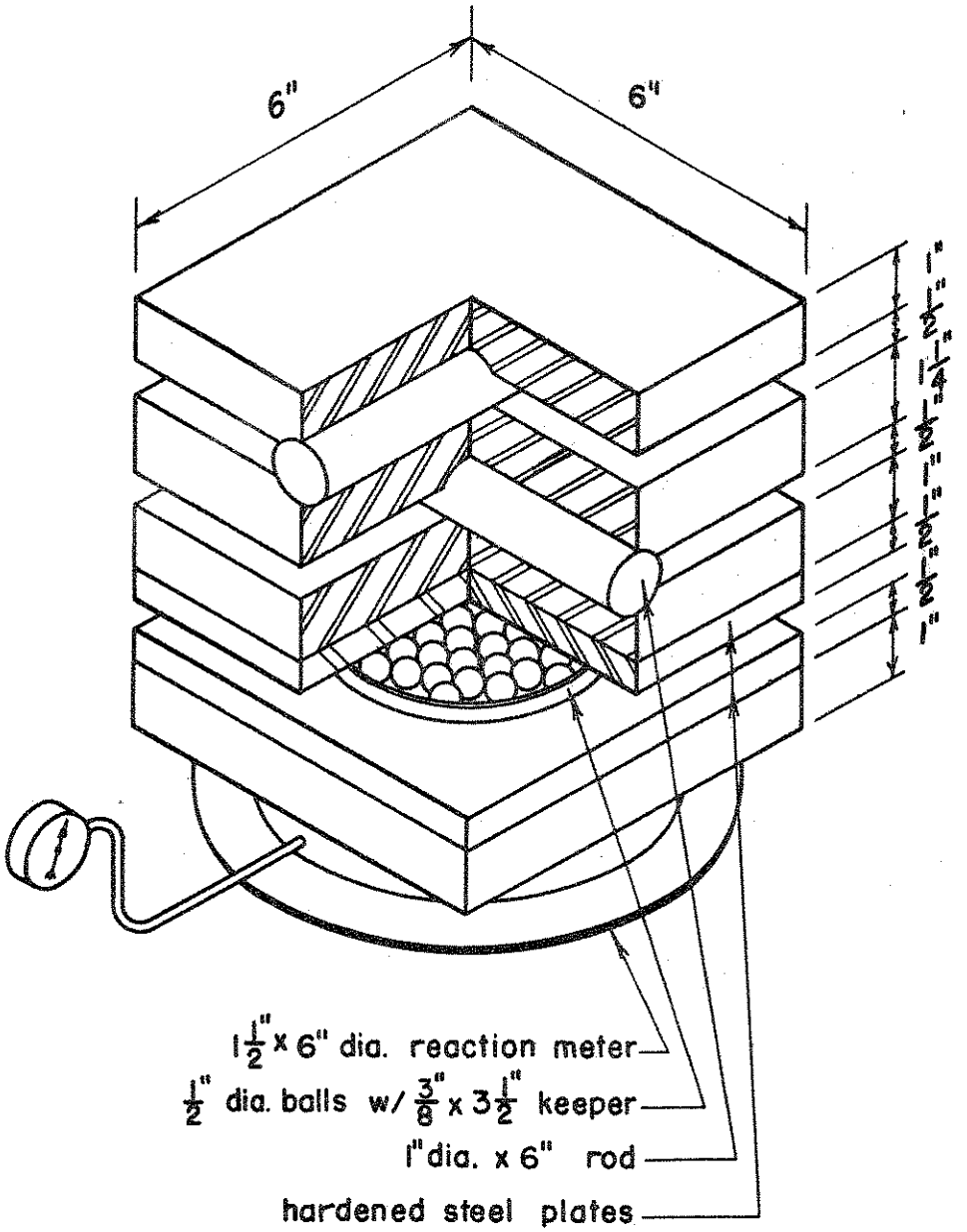

FIGURE 2. DETAIL of SUPPORT ASSEMBLY

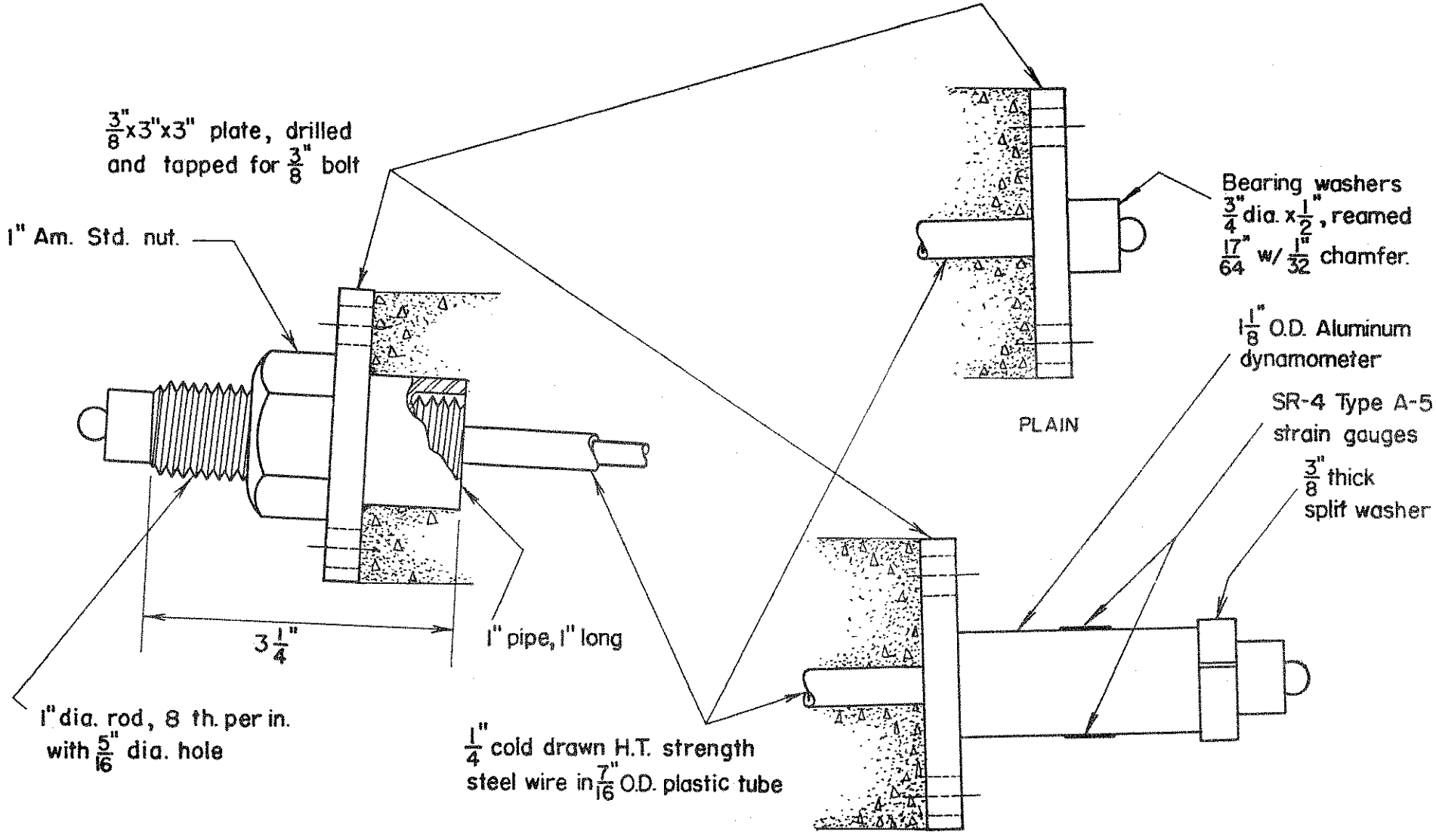

FIGURE 3. DETAILS of END ANCHORAGES and CABLE DYNAMOMETERS

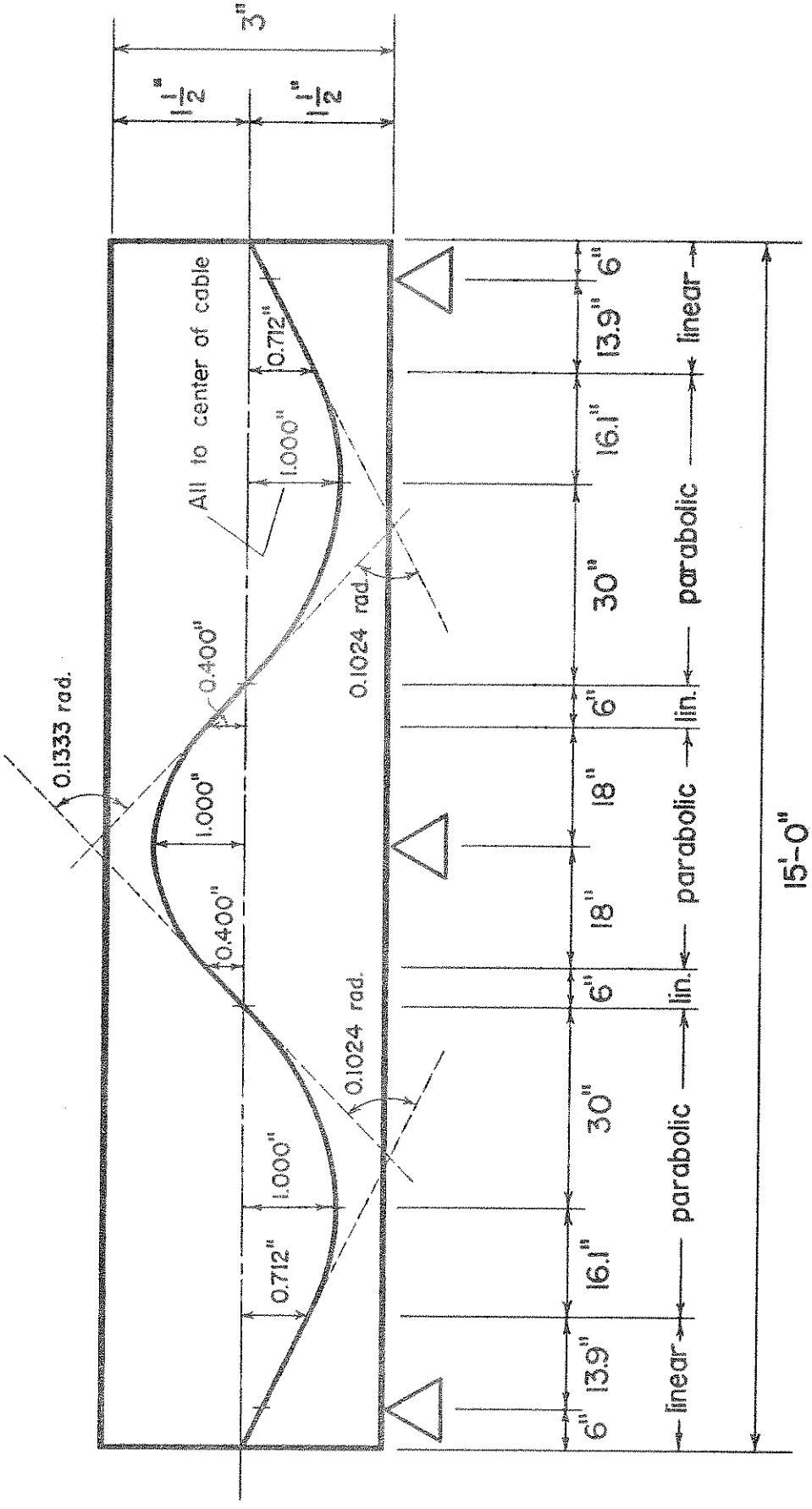

FIGURE 4. TYPICAL CABLE PROFILE

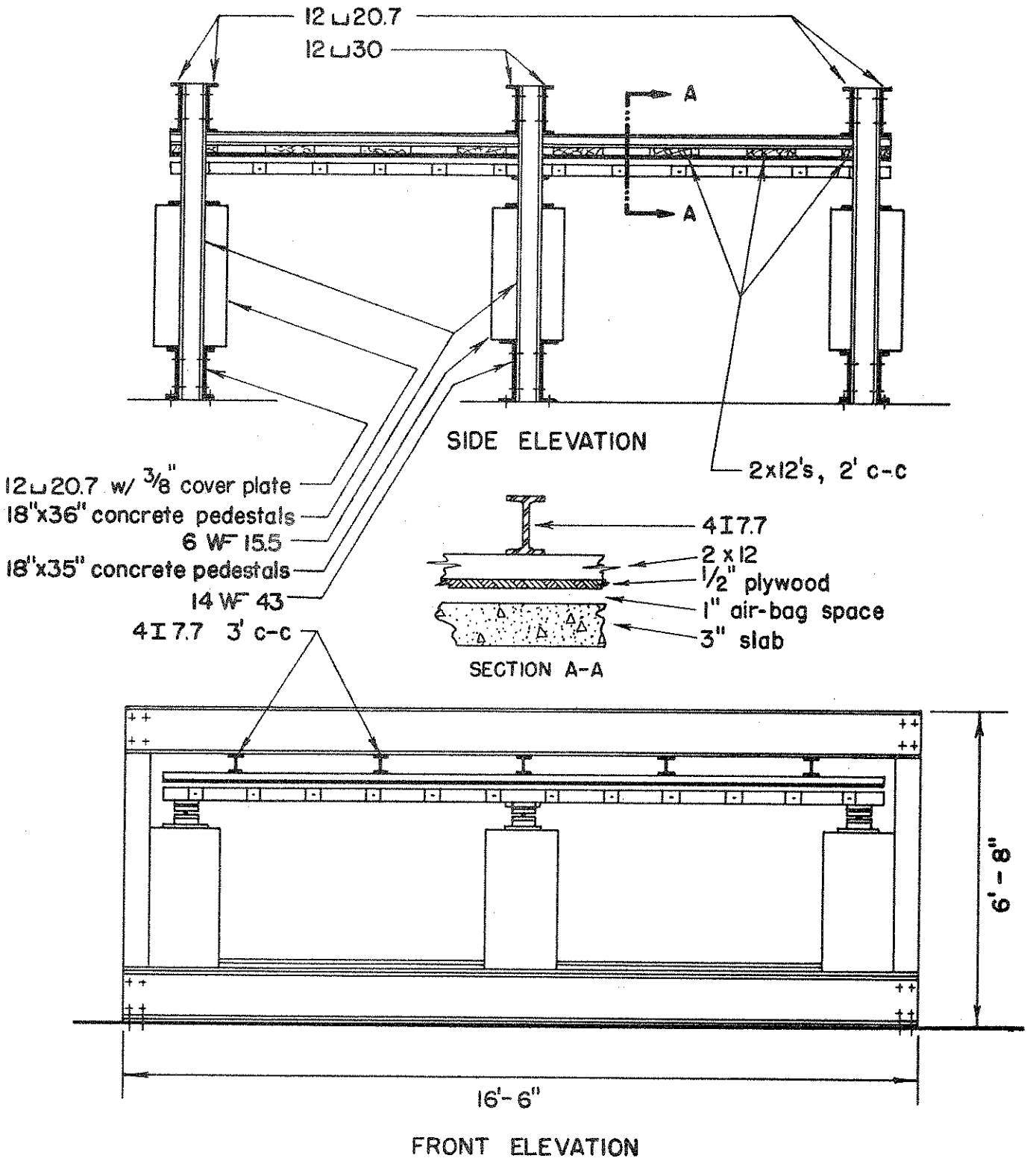

FIGURE 5. LOADING FRAME

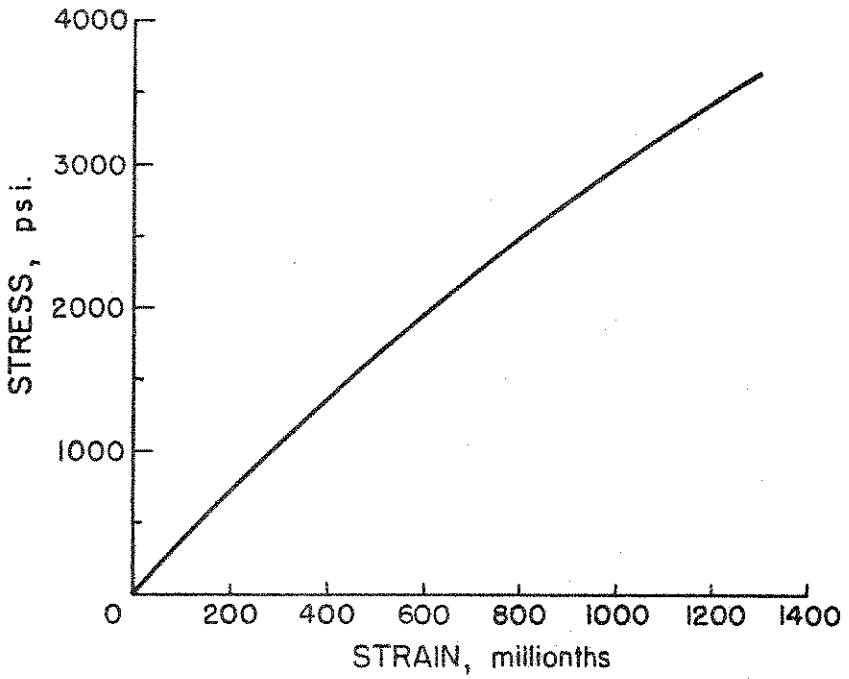

FIGURE 6. TYPICAL STRESS-STRAIN CURVE for 6" x 12" CONCRETE CYLINDER at AGE 28 days

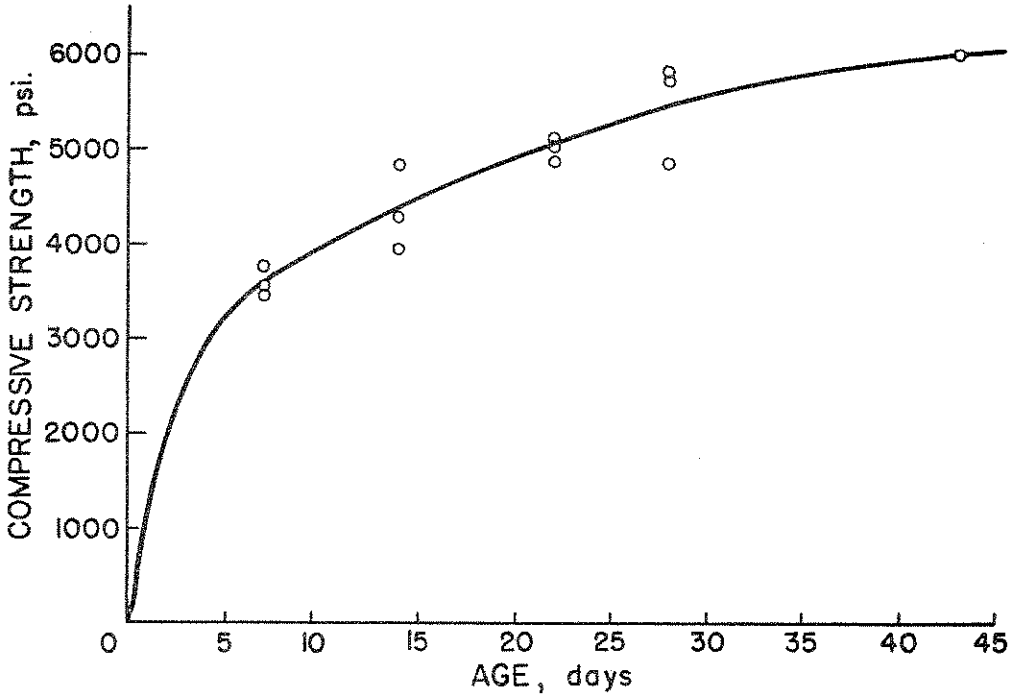

FIGURE 7. AGE-COMPRESSIVE STRENGTH RELATIONSHIP for 6" x 12" CONCRETE CYLINDERS

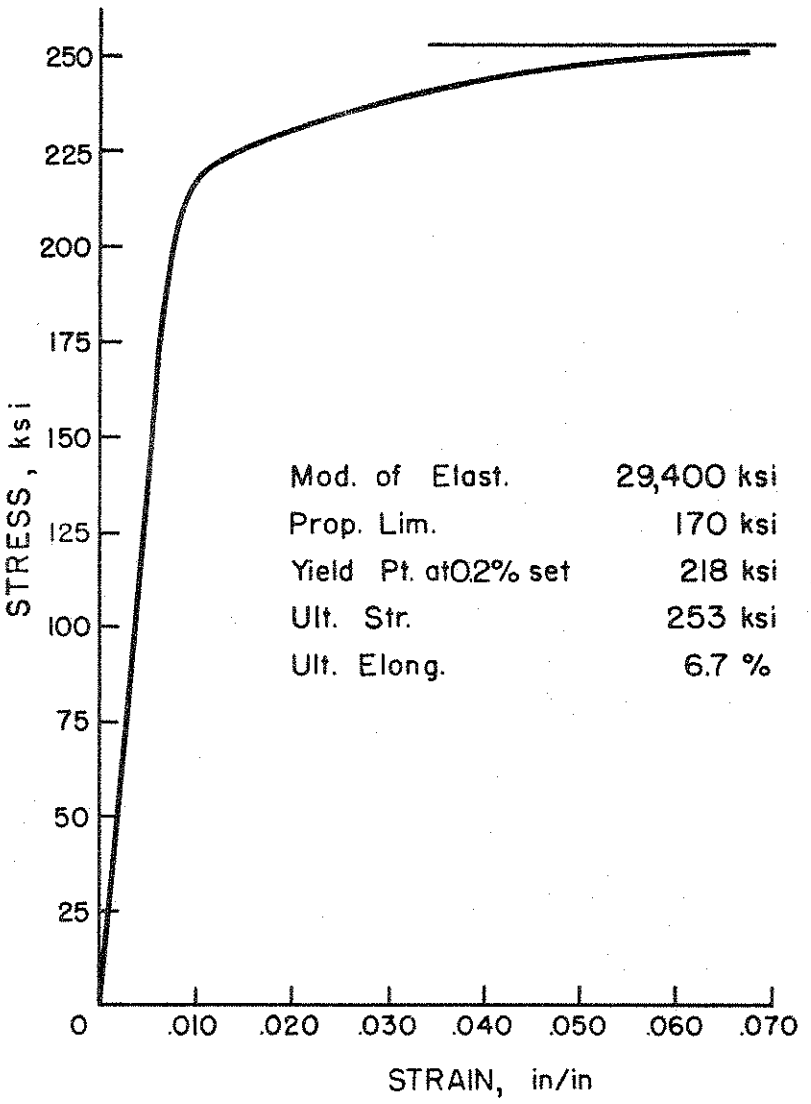

FIGURE 8. TYPICAL STRESS-STRAIN CURVE for $\frac{1}{4}$" dia. PRESTRESSING STEEL

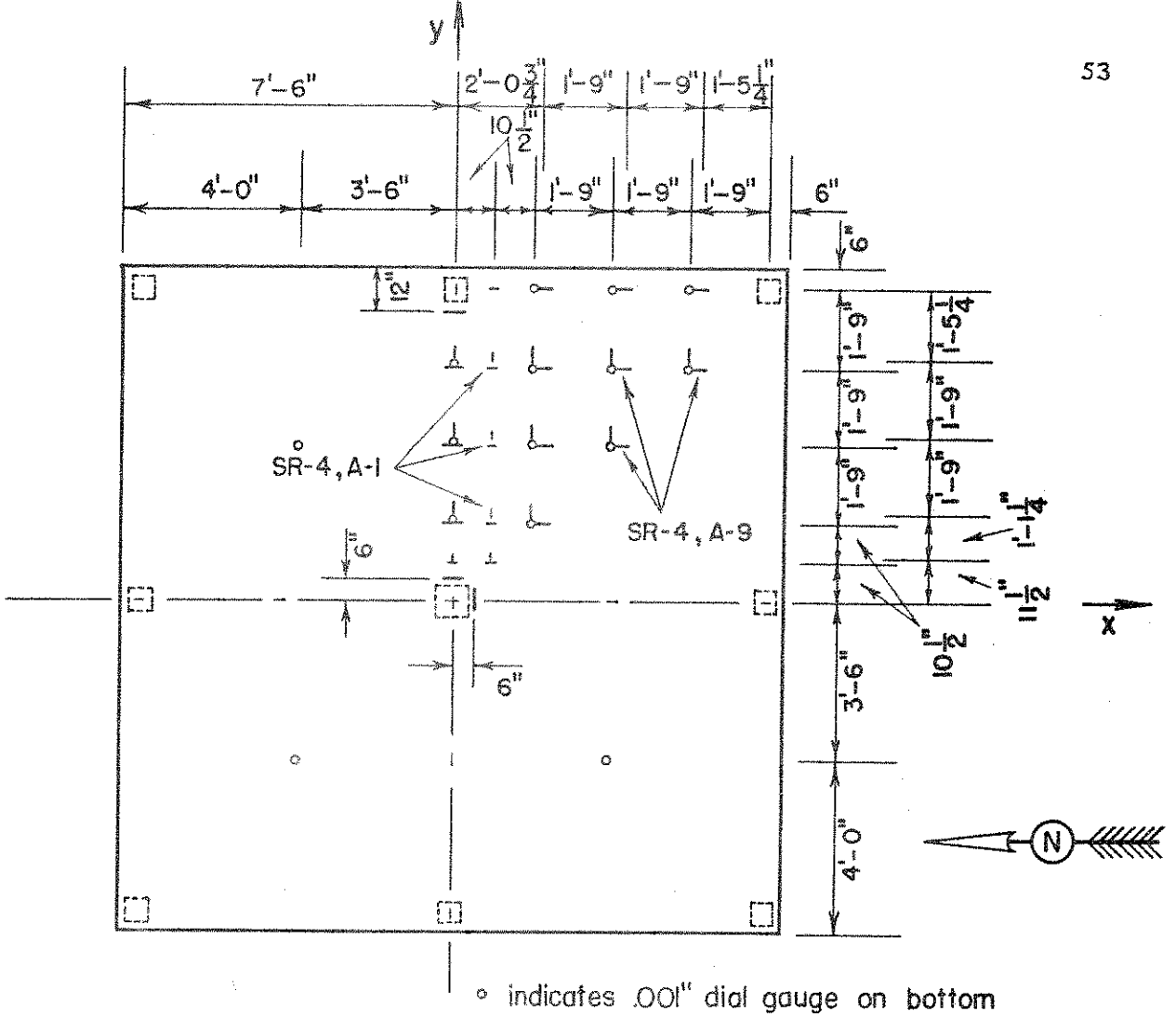

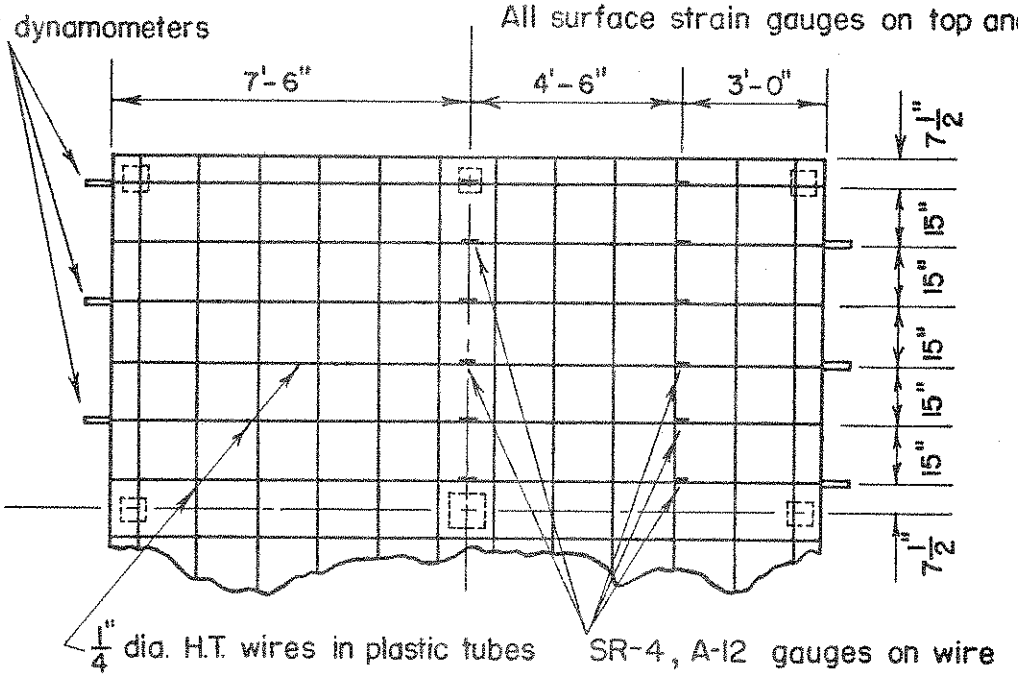

FIGURE 9. LOCATION of GAUGES

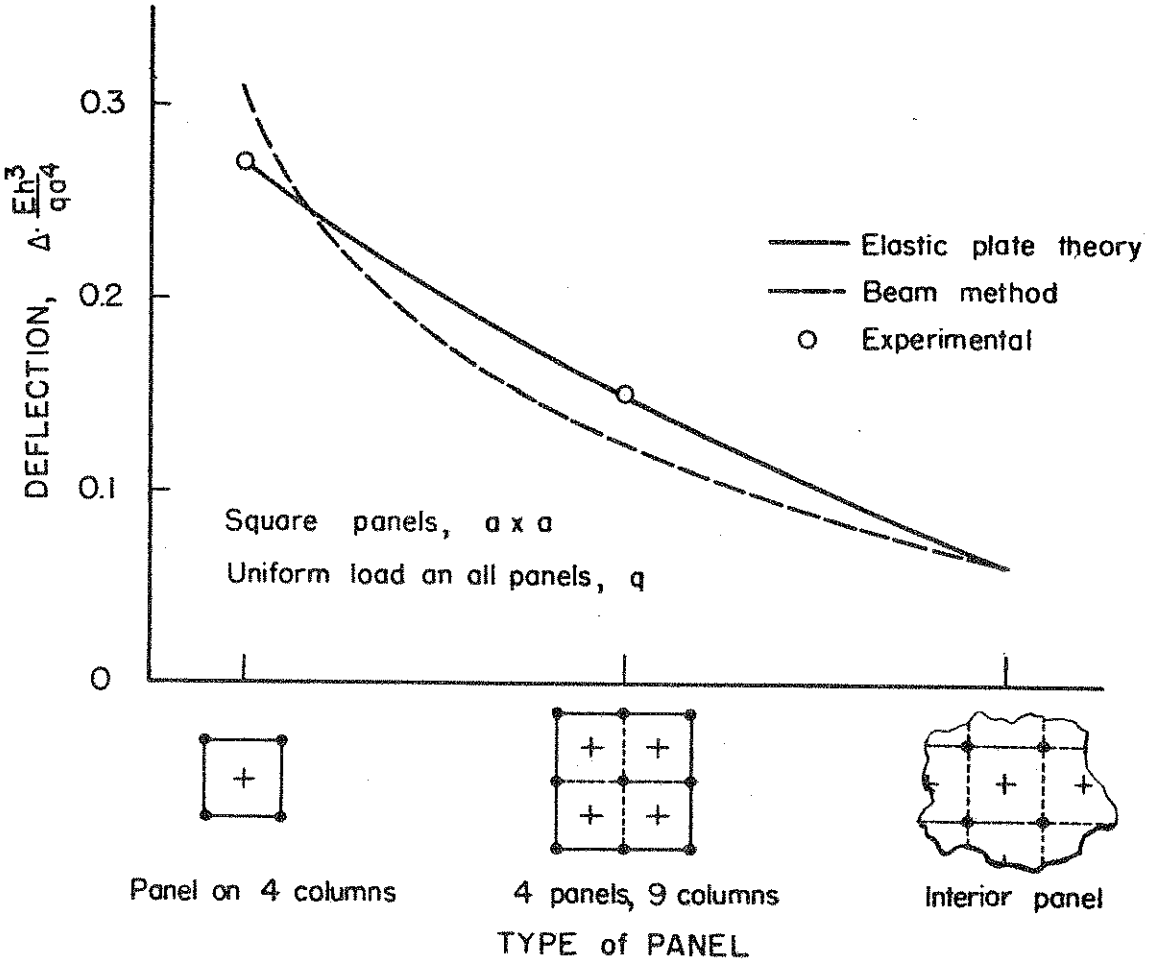

FIGURE 10. COMPARISON of DEFLECTIONS at CENTER of PANEL by PLATE THEORY and APPROXIMATE BEAM METHOD for UNIFORM LOAD

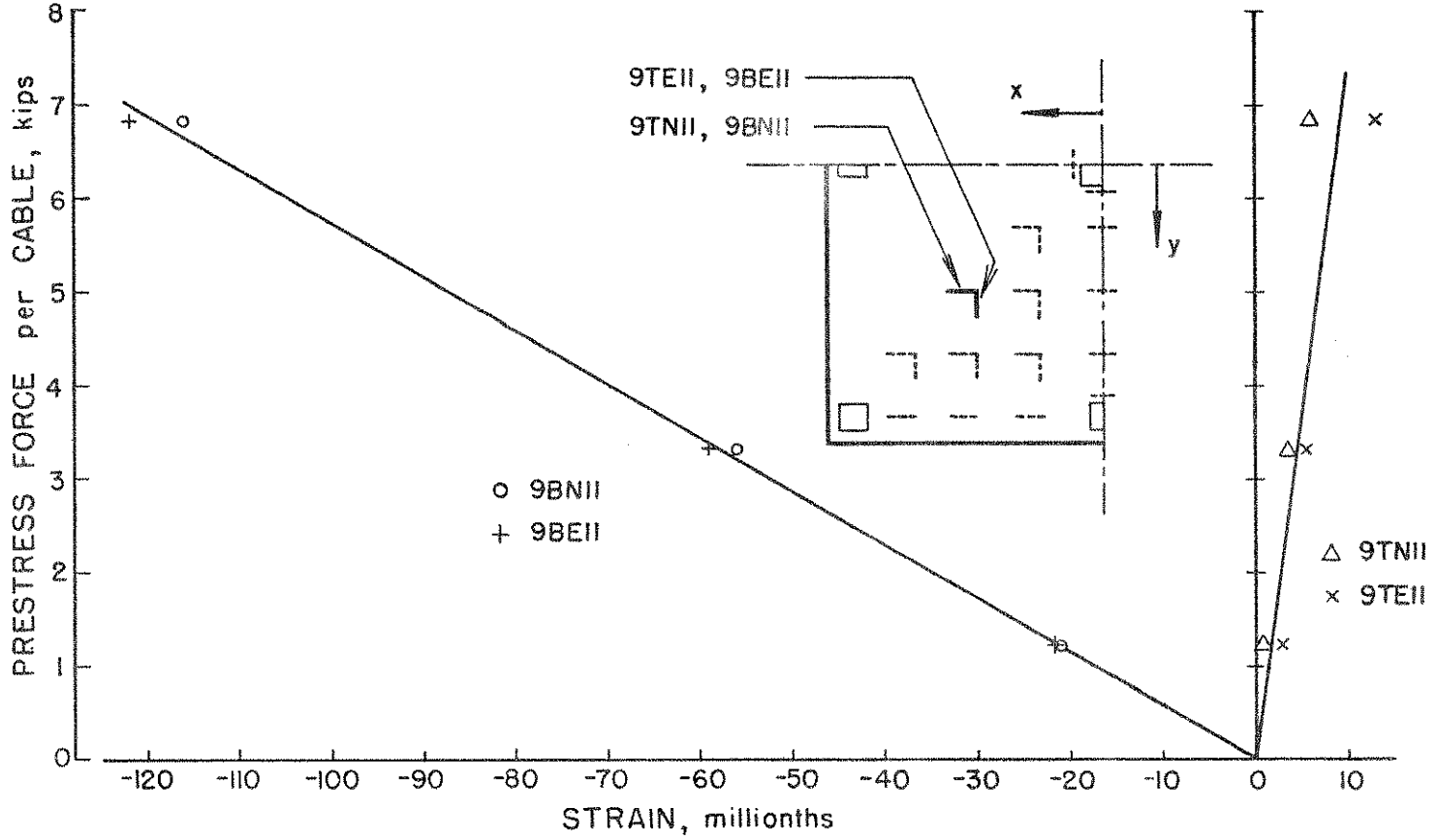

FIGURE 11. PRESTRESS FORCE *vs* STRAIN at GAUGE POINT 11
(EXPERIMENTAL VALUES for UNIFORM PRESTRESS CASE)

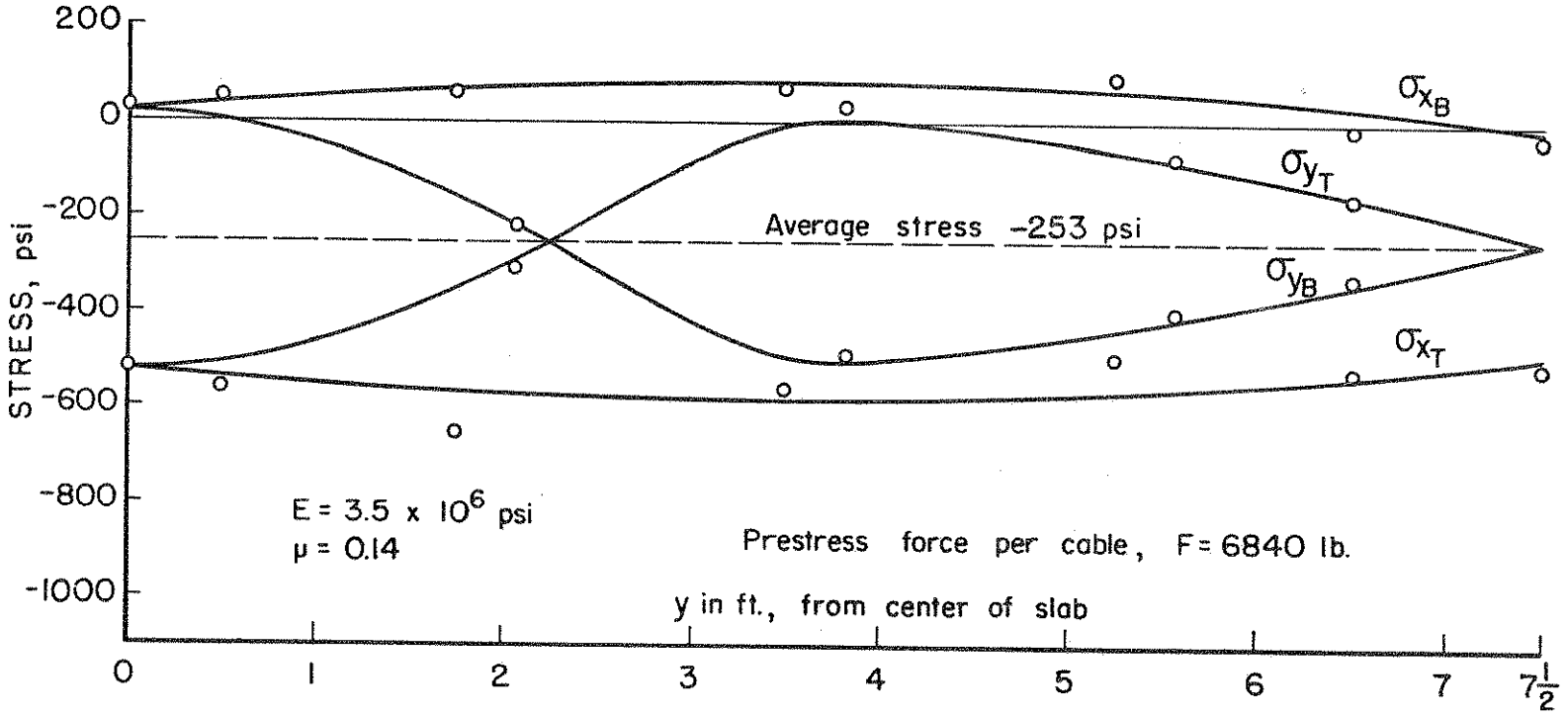

FIGURE 12. STRESSES DUE TO UNIFORM PRESTRESS at x = 0 ft. (EXPERIMENTAL VALUES ONLY)

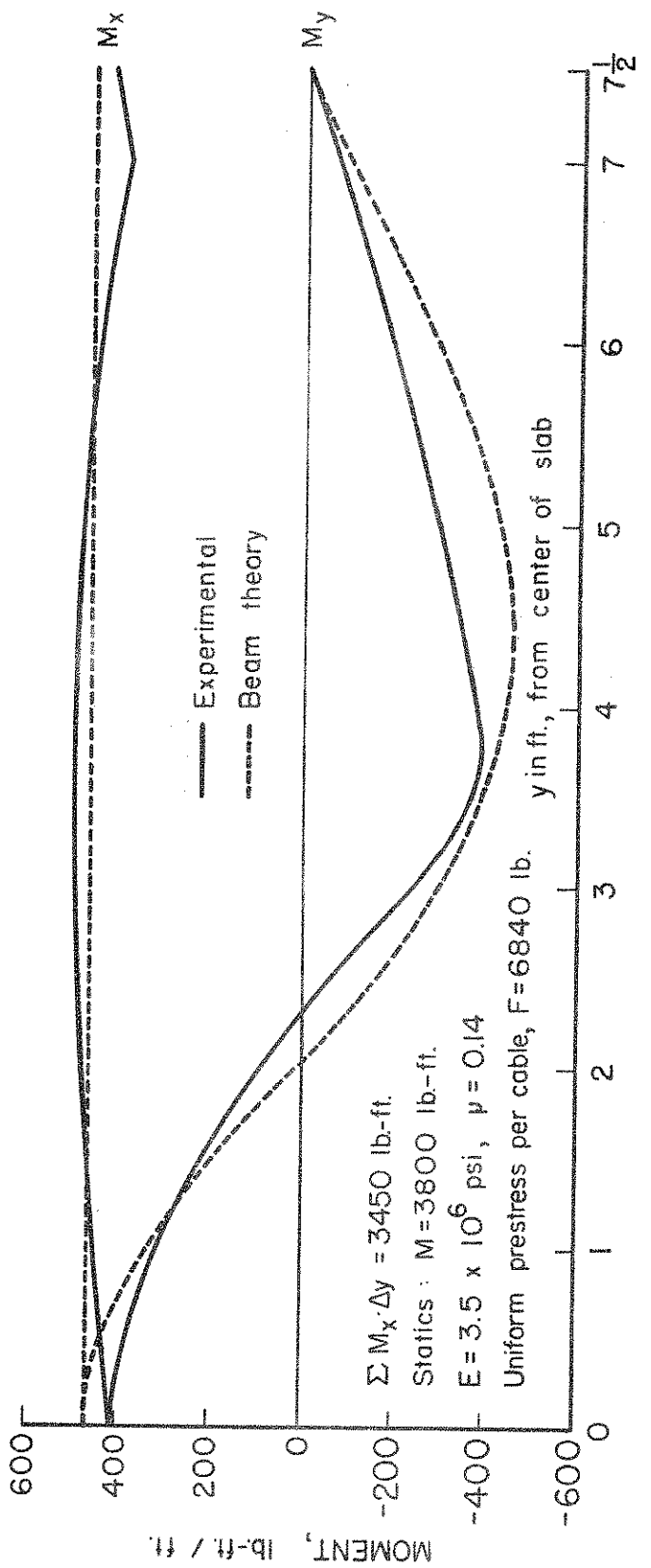

FIGURE 13. MOMENTS DUE TO UNIFORM PRESTRESS at x = 0 ft.

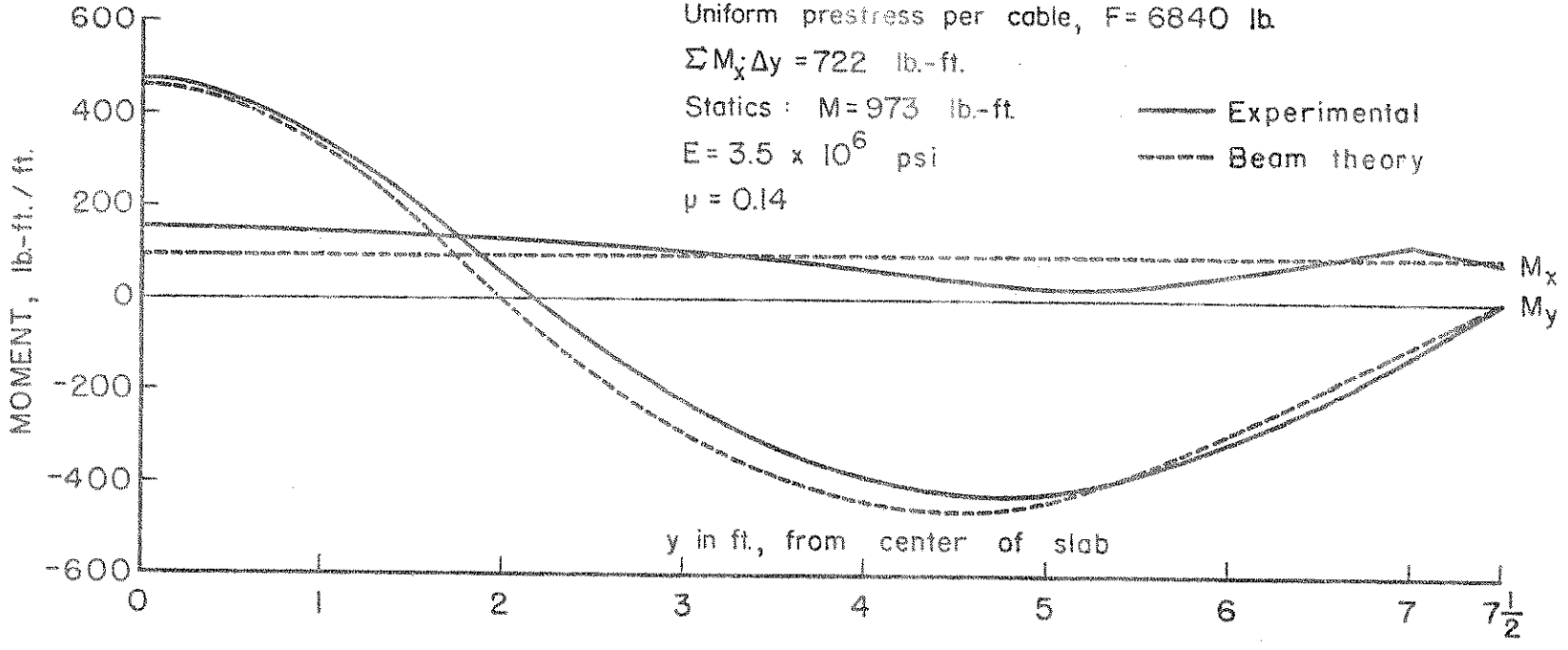

FIGURE 14. MOMENTS DUE TO UNIFORM PRESTRESS at x = 1.75 ft

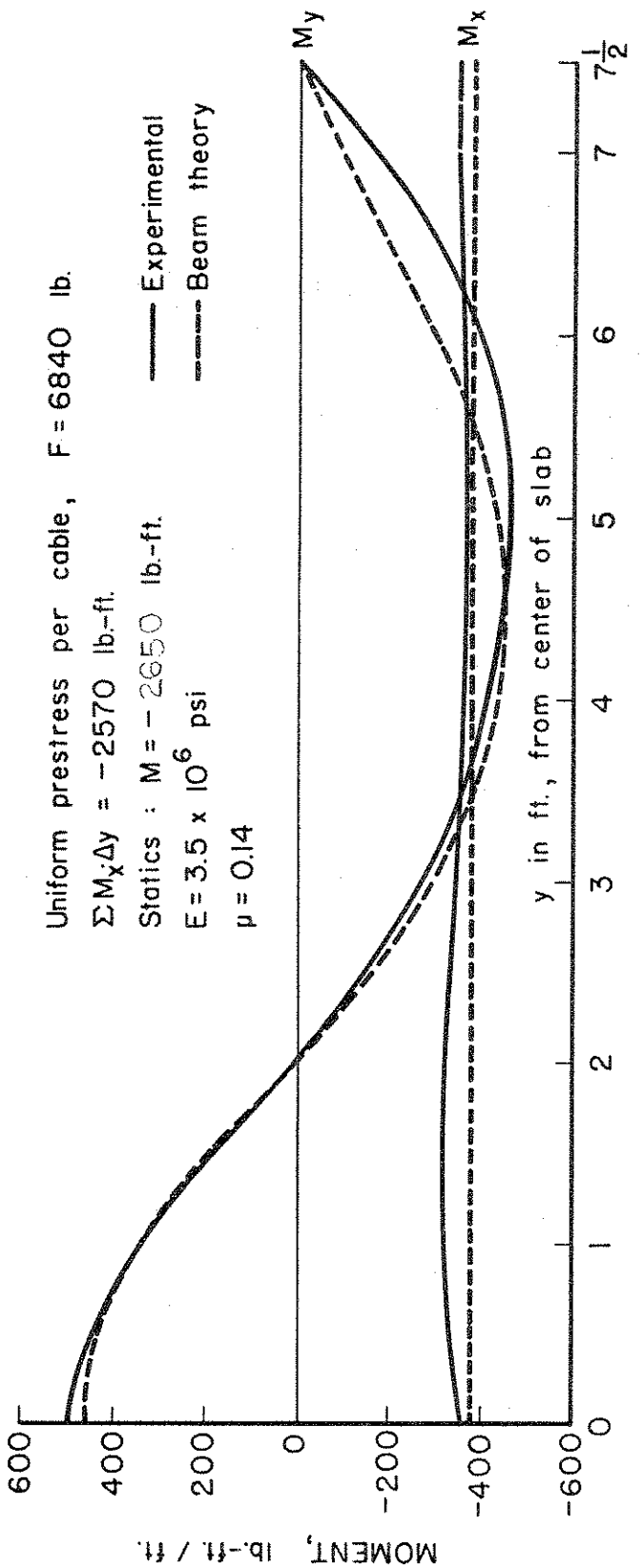

FIGURE 15. MOMENTS DUE TO UNIFORM PRESTRESS at x = 3.5 ft.

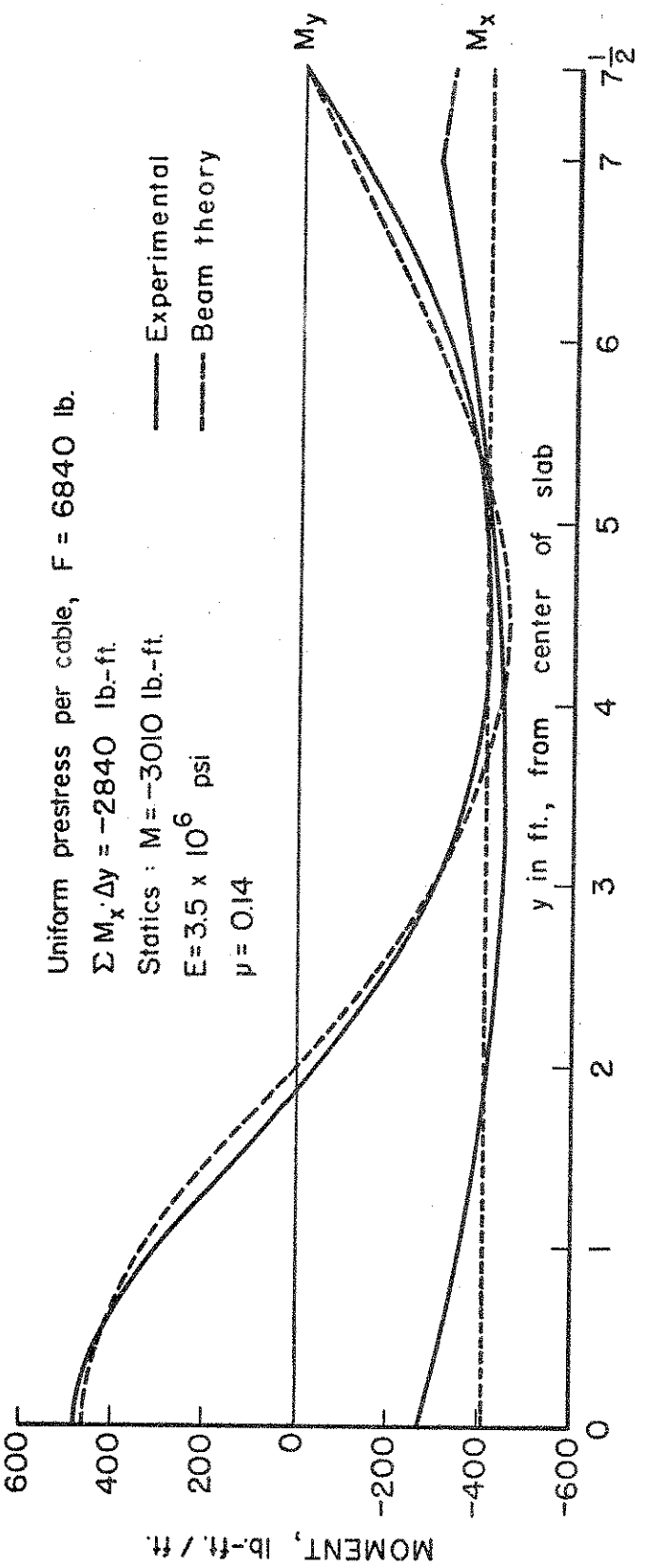

FIGURE 16. MOMENTS DUE TO UNIFORM PRESTRESS at x = 5.25 ft.

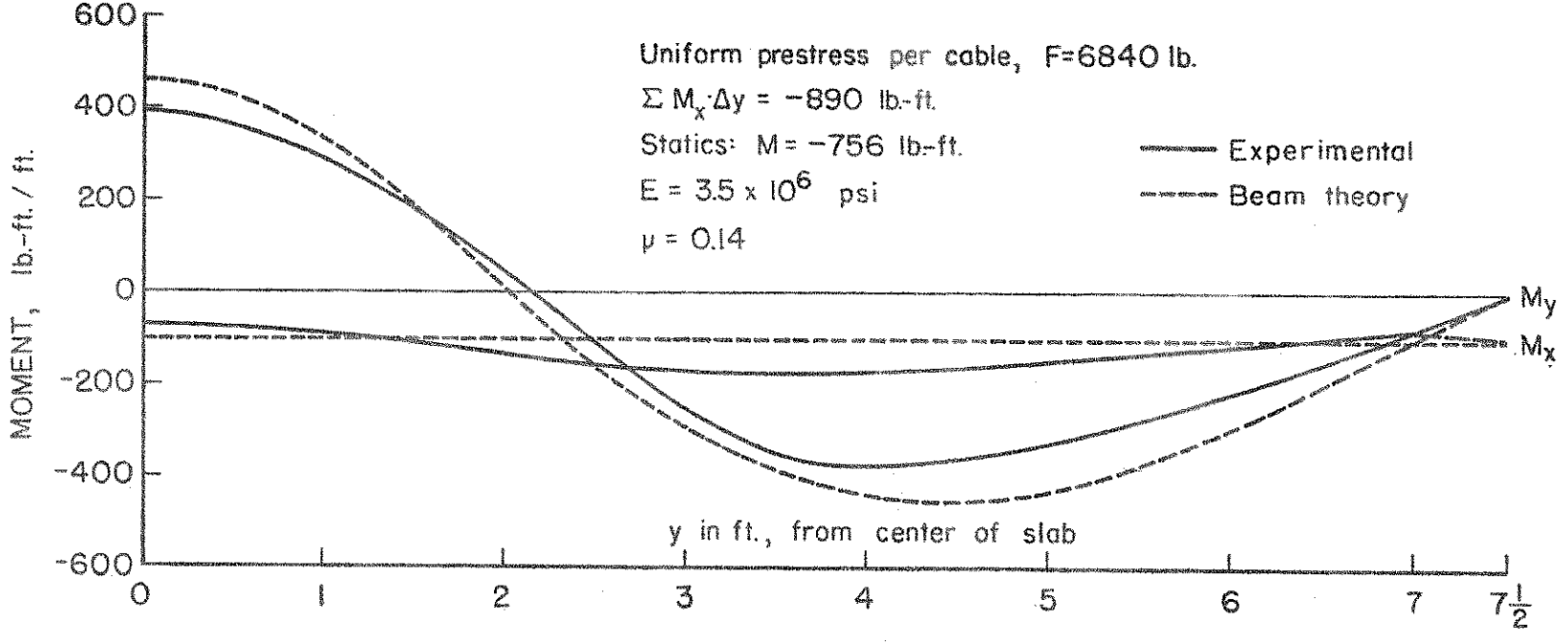

FIGURE 17. MOMENTS DUE TO UNIFORM PRESTRESS at x = 7.0 ft.

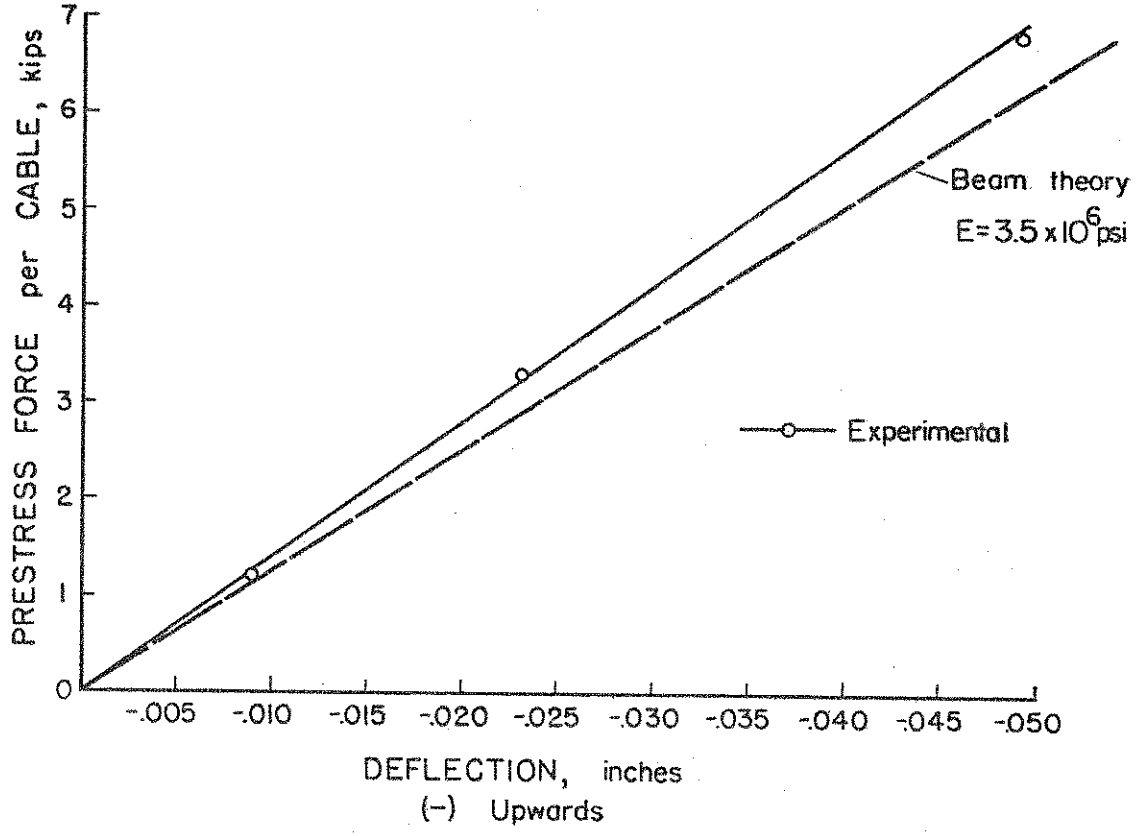

FIGURE 18. PRESTRESS FORCE *vs* DEFLECTION at CENTER of PANEL
(for UNIFORM PRESTRESS CASE)

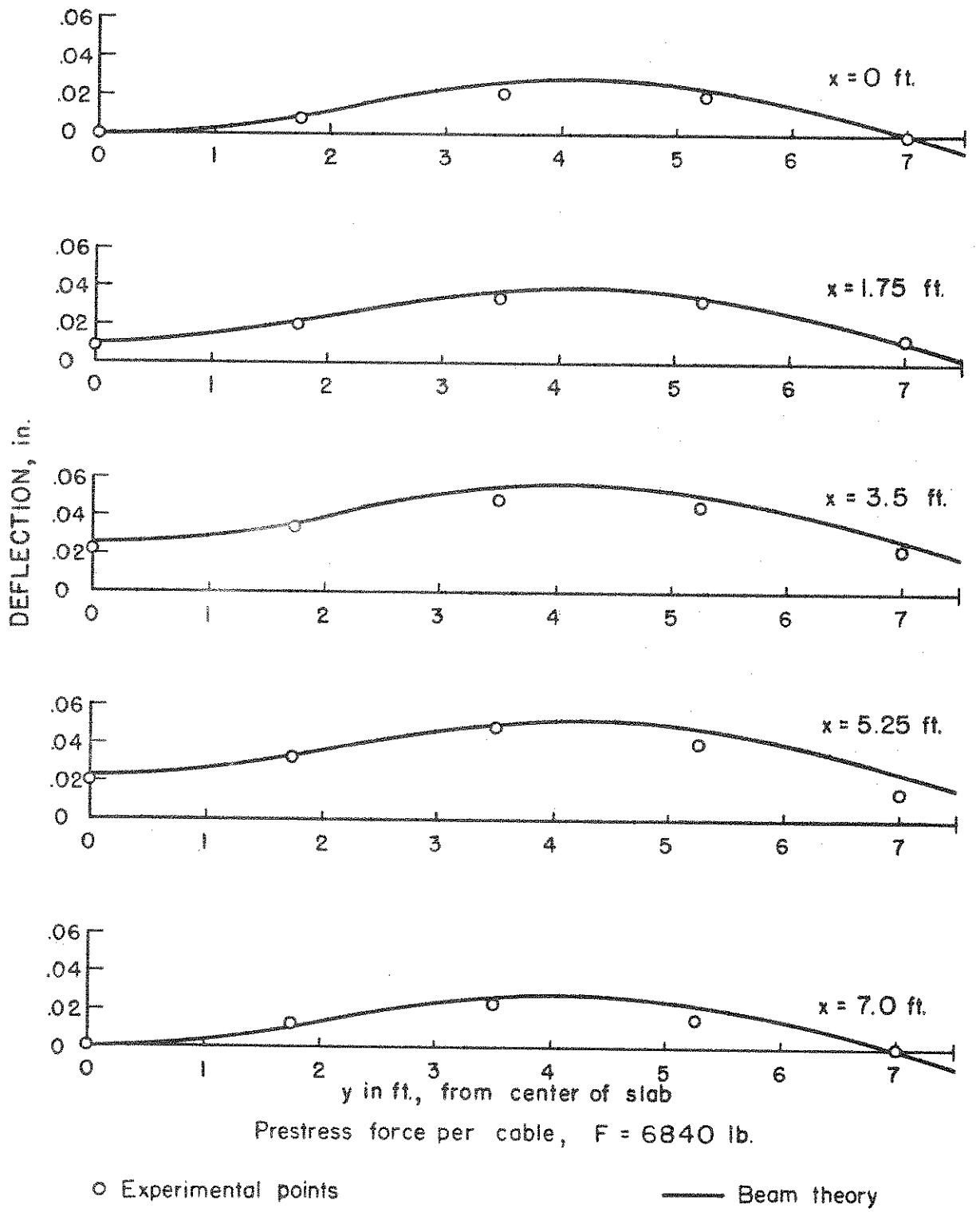

FIGURE 19. DEFLECTED SHAPES DUE TO UNIFORM PRESTRESS

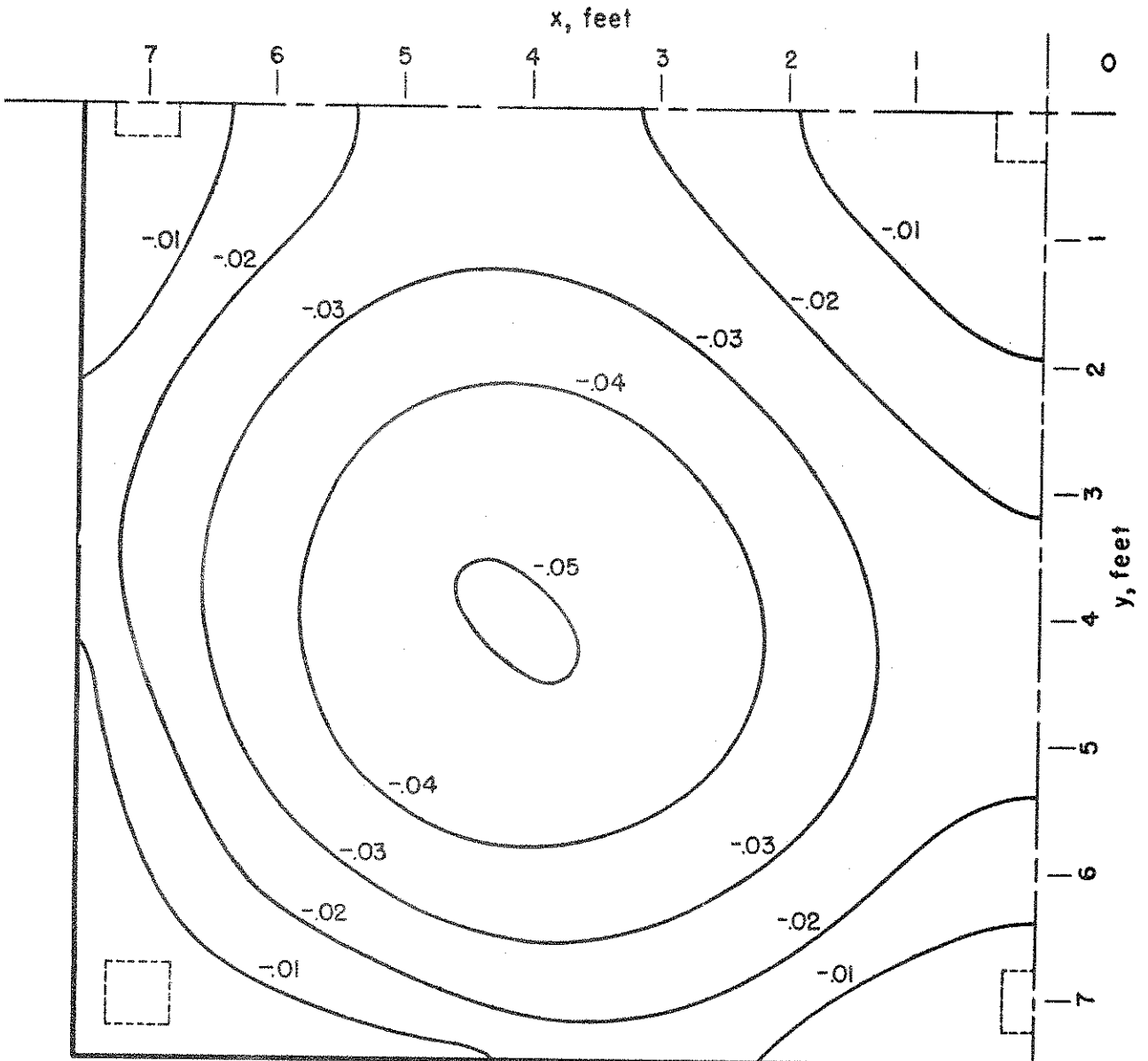

FIGURE 20. EXPERIMENTAL DEFLECTIONS DUE TO PRESTRESS (for UNIFORM PRESTRESS CASE)

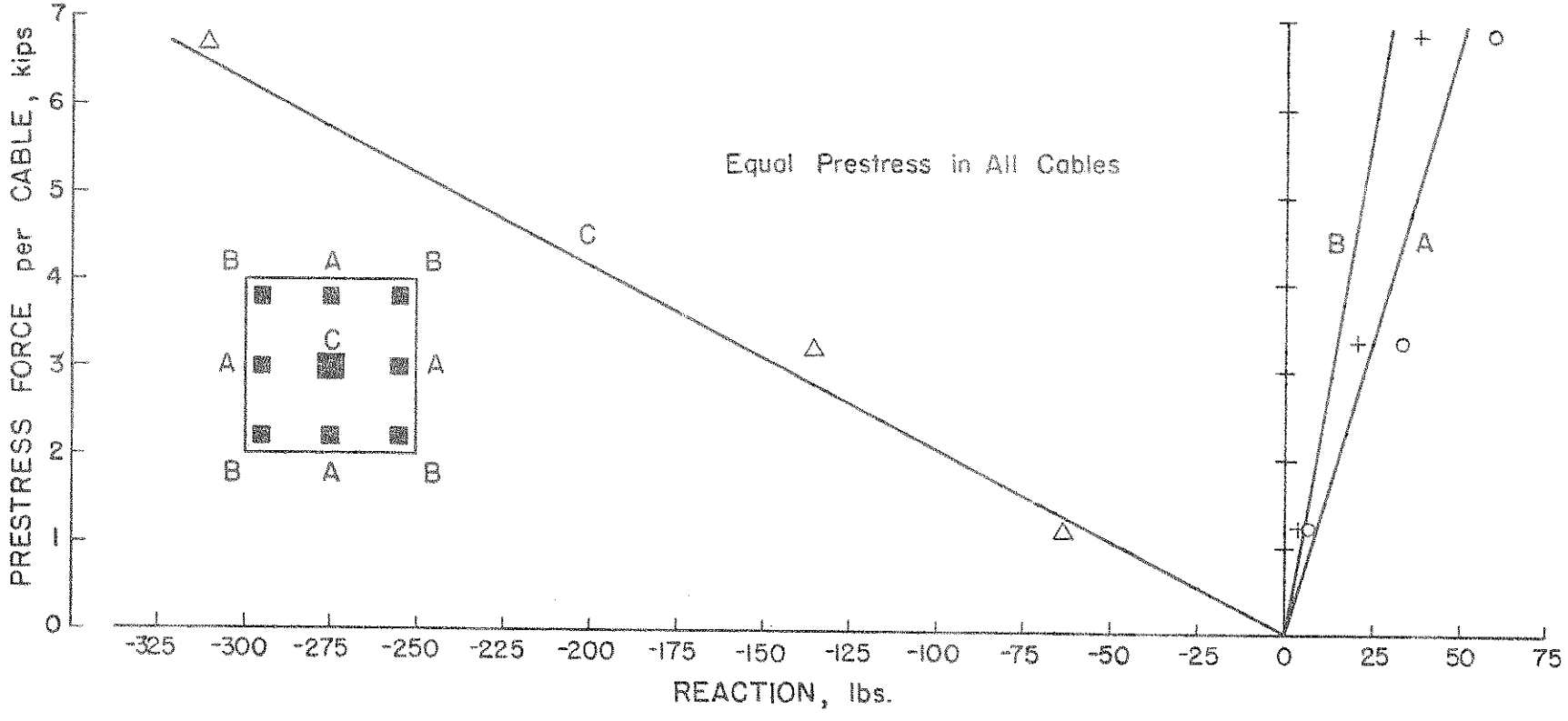

FIGURE 21. PRESTRESS FORCE *vs* REACTION
(EXPERIMENTAL VALUES for UNIFORM PRESTRESS CASE)

$$\frac{F_2}{F_1} = \epsilon^{-\mu\Theta - KL}$$

where F_2 and F_1 are forces in steel at pts. 2, 1
ϵ is natural log base
μ is coefficient of friction
Θ is angular change or curvature in radians
K is coefficient for wobble effect per ft.
L is length of cable in ft.

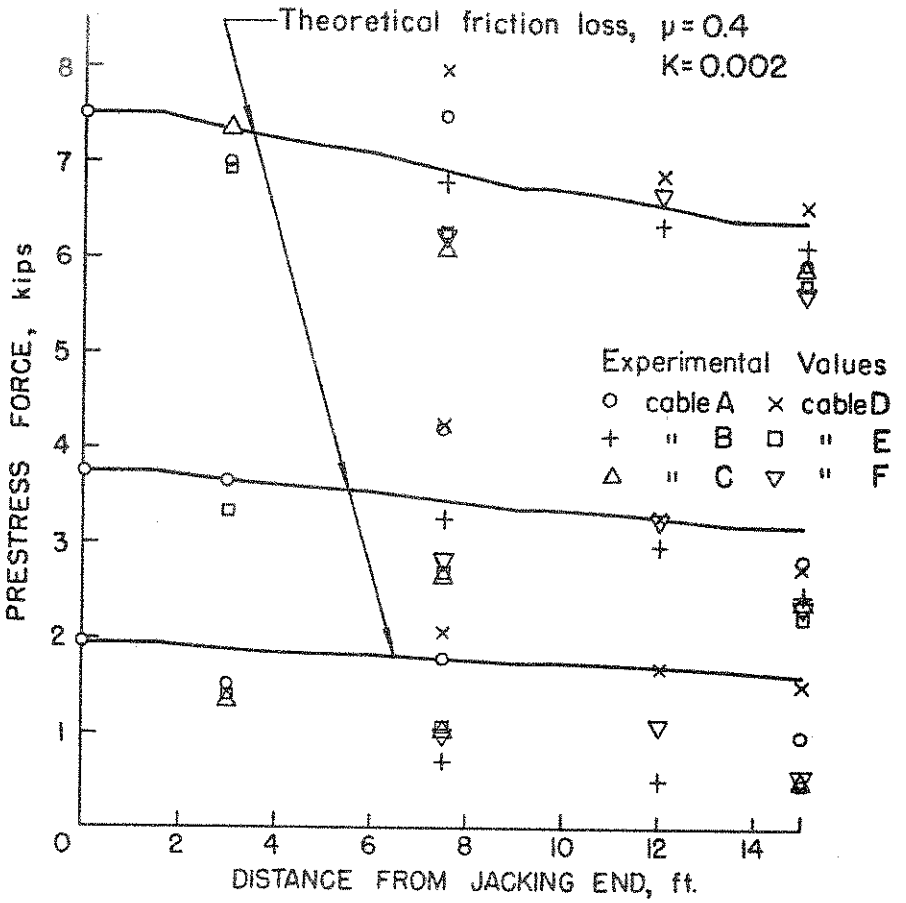

FIGURE 22. LOSS of PRESTRESS due to CABLE FRICTION

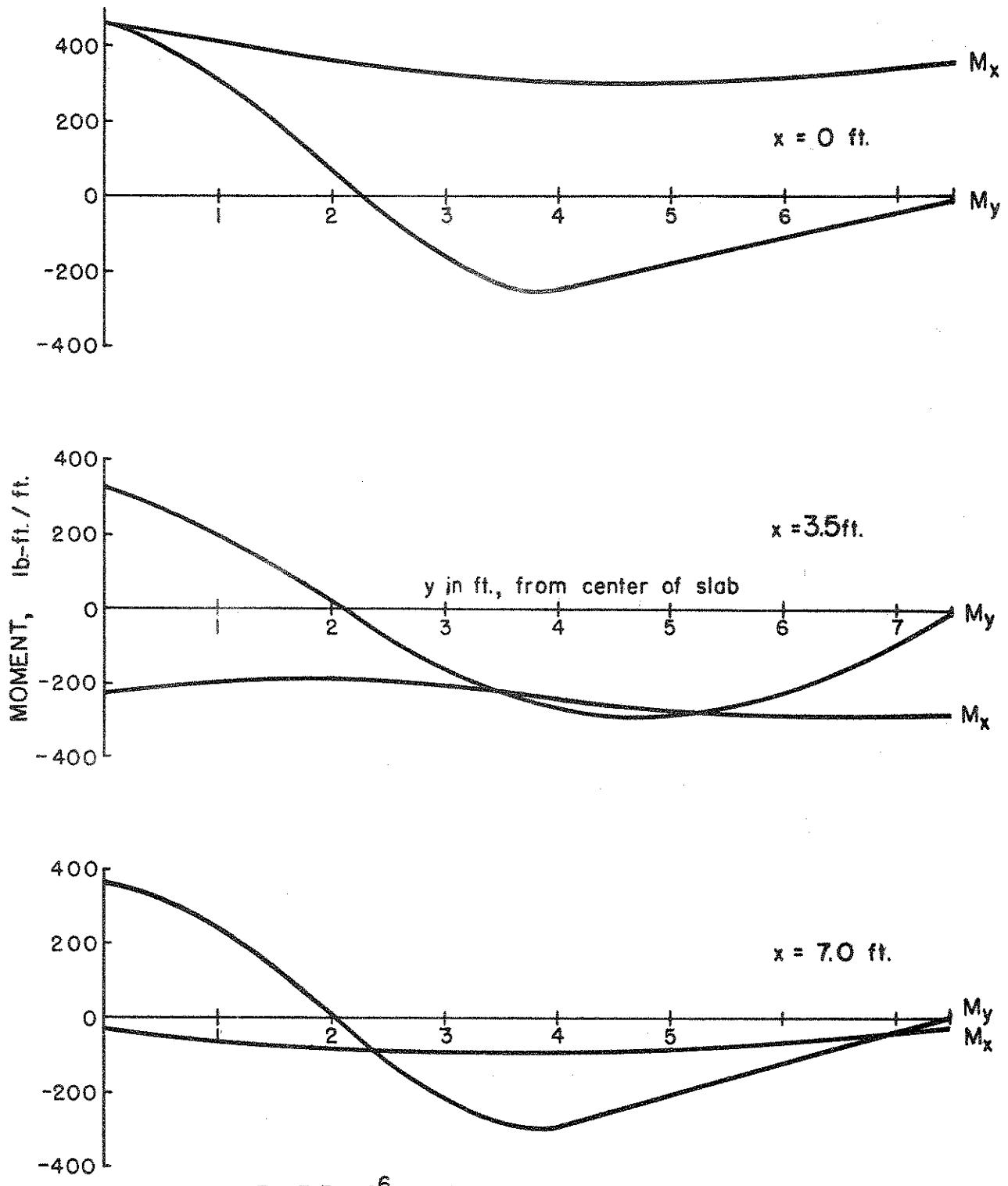

$E = 3.5 \times 10^6$ psi $\mu = 0.14$

Prestress force per cable: column strip, $F_{cs} = 6840$ lb.

middle strip, $F_{ms} = 3320$ lb.

FIGURE 23. MOMENTS DUE TO 1.8:1 PRESTRESS at x = 0, 3.5 & 7.0 ft (EXPERIMENTAL VALUES ONLY)

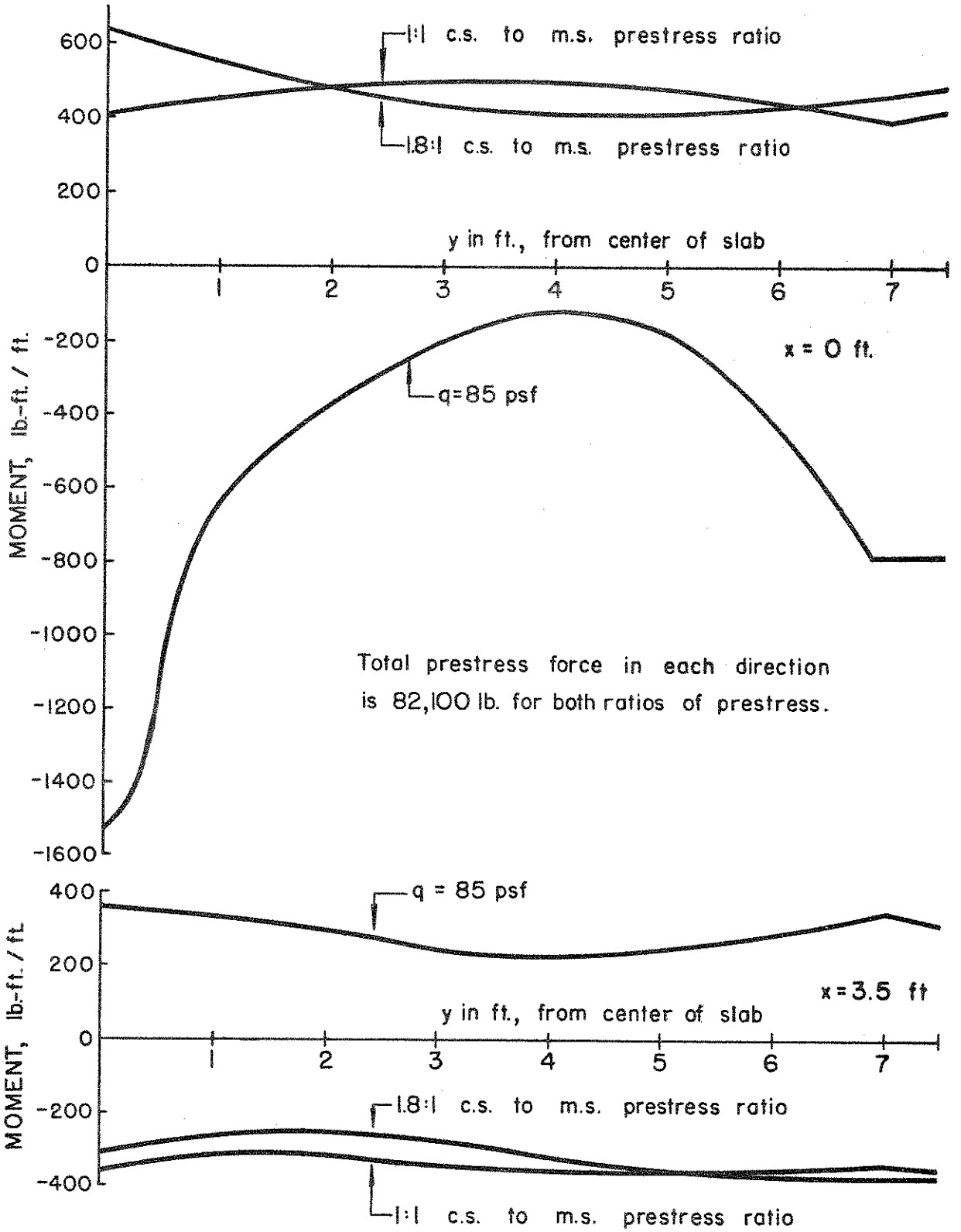

FIGURE 24. COMPARISON of MOMENT DISTRIBUTION DUE TO 1:1 PRESTRESS, 1.8:1 PRESTRESS, and UNIFORM LOAD on ENTIRE SLAB (EXPERIMENTAL VALUES ONLY)

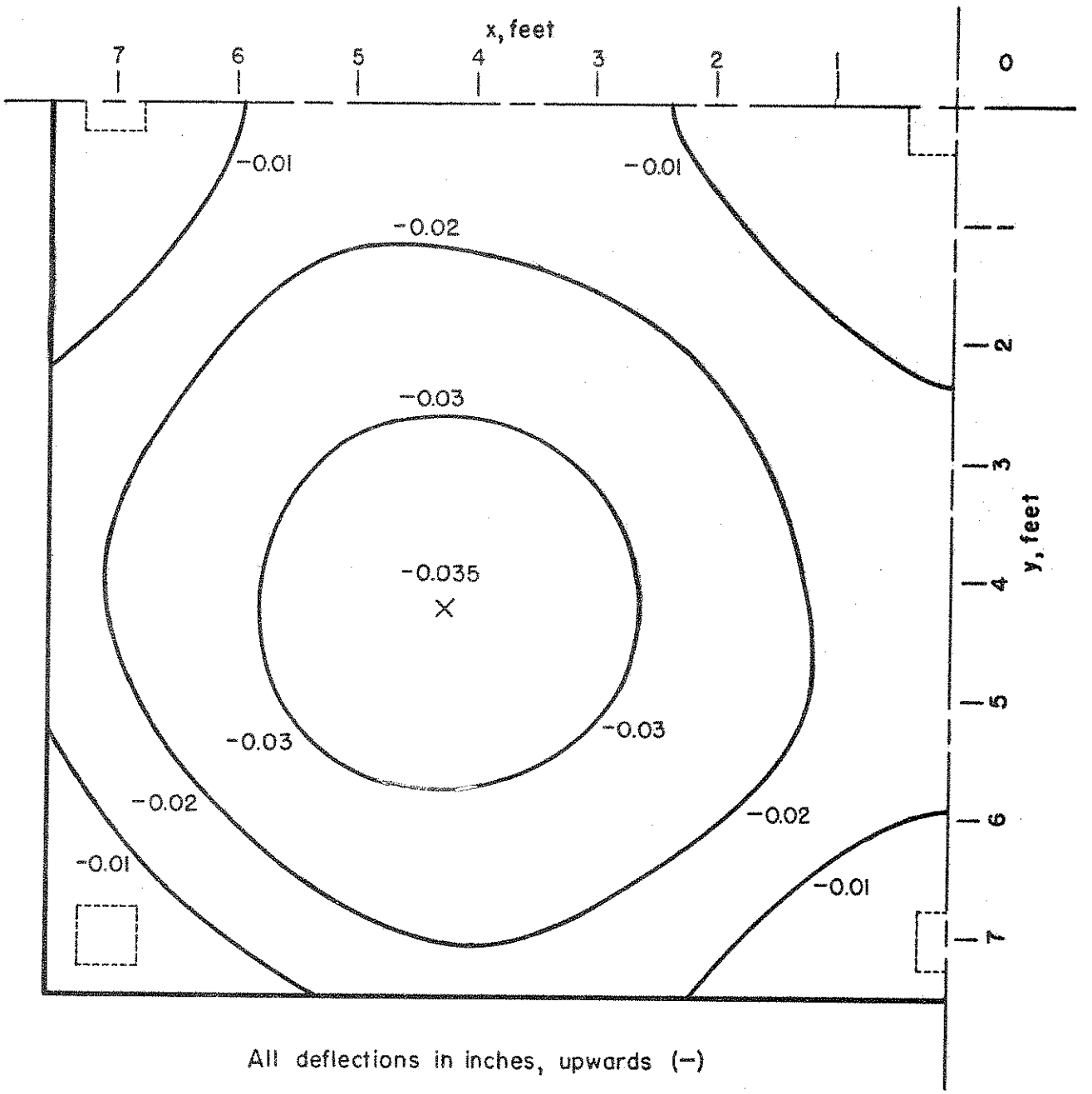

All deflections in inches, upwards (−)

Prestress force per cable, column strip F_{cs} = 6840 lb.
middle strip F_{ms} = 3320 lb.

FIGURE 25. EXPERIMENTAL DEFLECTIONS DUE TO 1.8:1 PRESTRESS

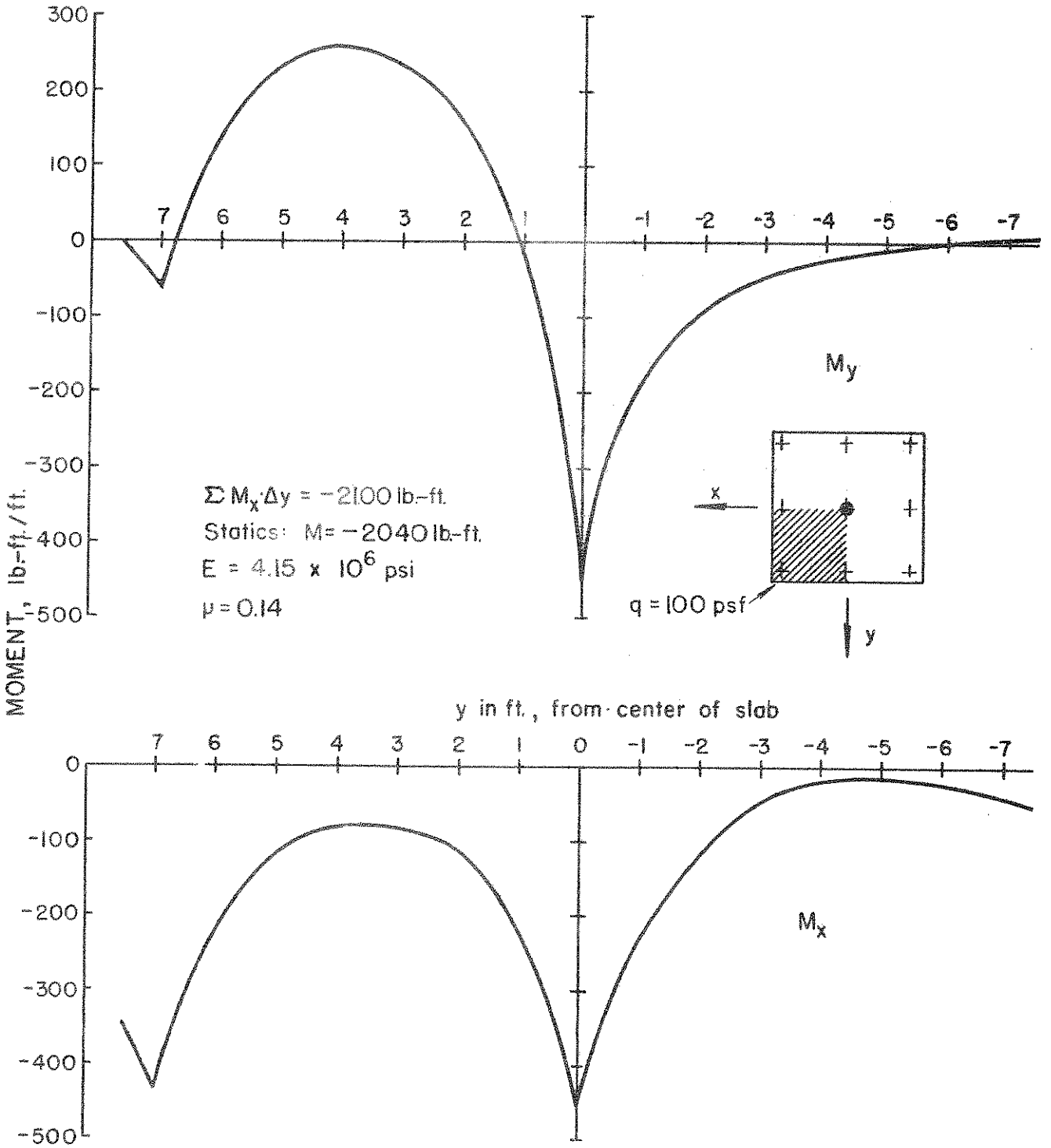

FIGURE 26. MOMENTS DUE TO LOAD on ONE PANEL at x=0 ft. (EXPERIMENTAL VALUES ONLY)

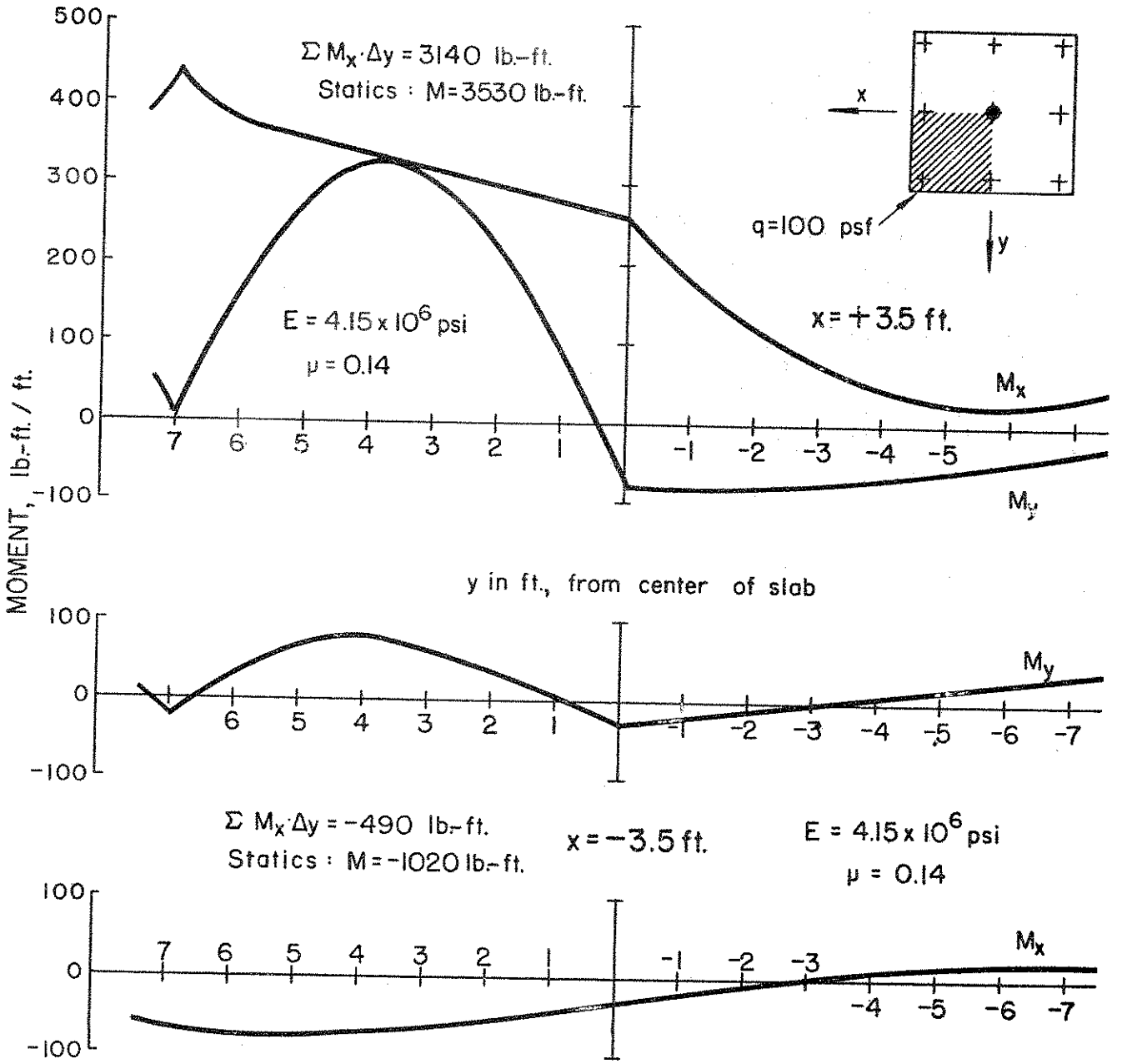

FIGURE 27. MOMENTS DUE TO LOAD on ONE PANEL at x=±3.5 ft. (EXPERIMENTAL VALUES ONLY)

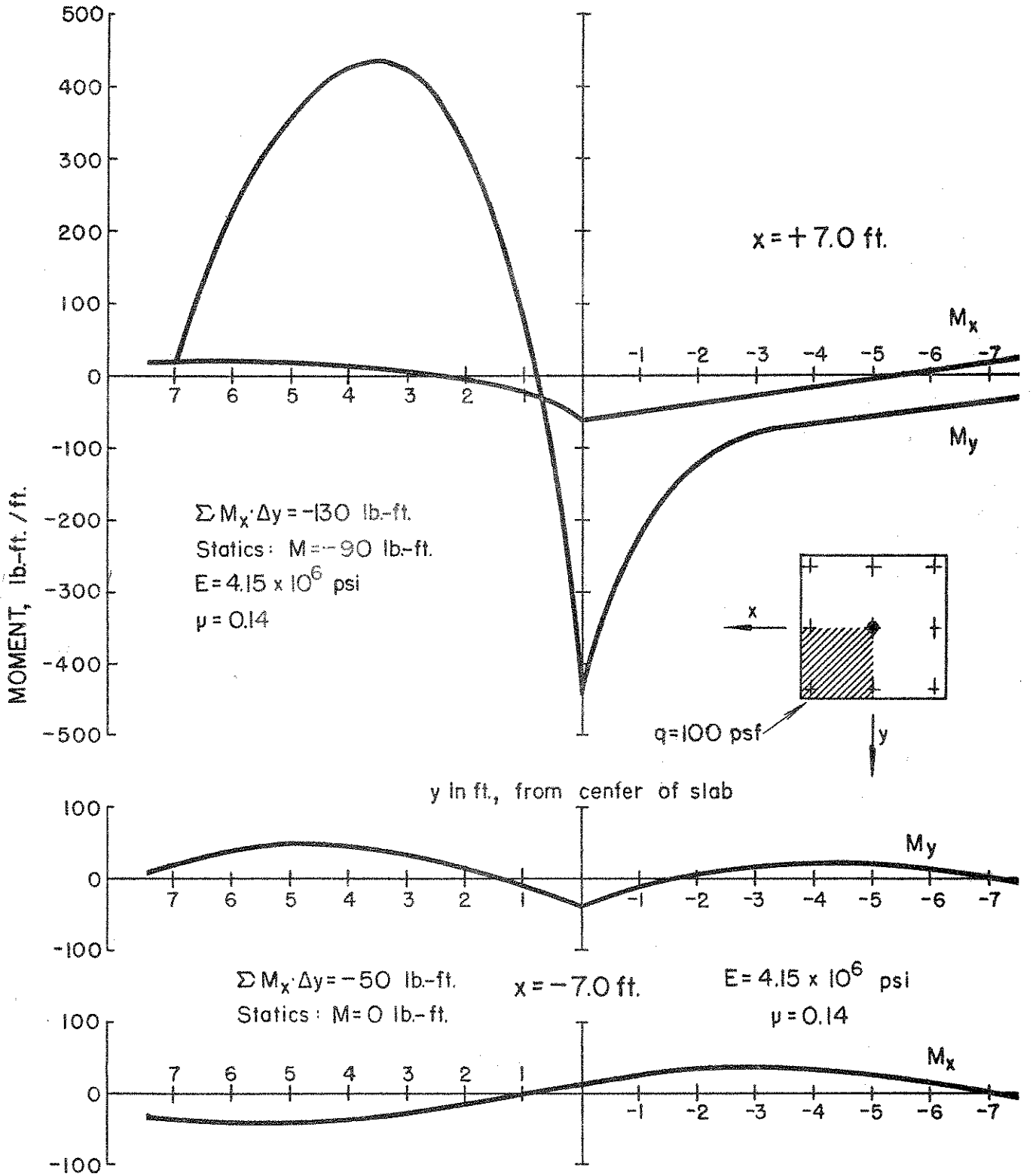

FIGURE 28. MOMENTS DUE TO LOAD on ONE PANEL at x = ±7.0 ft. (EXPERIMENTAL VALUES ONLY)

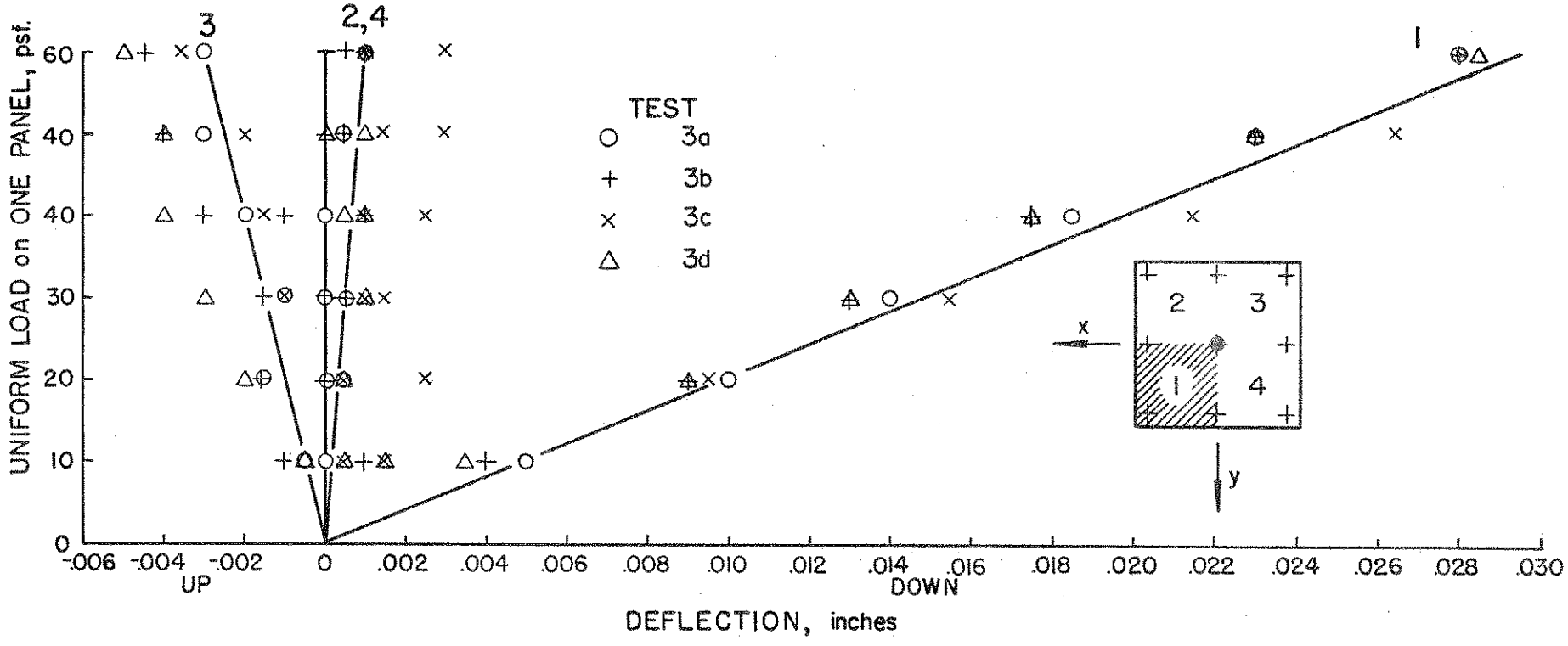

FIGURE 29. EXPERIMENTAL LOAD *vs* DEFLECTION CURVES at CENTER of PANEL for UNIFORM LOAD on ONE PANEL

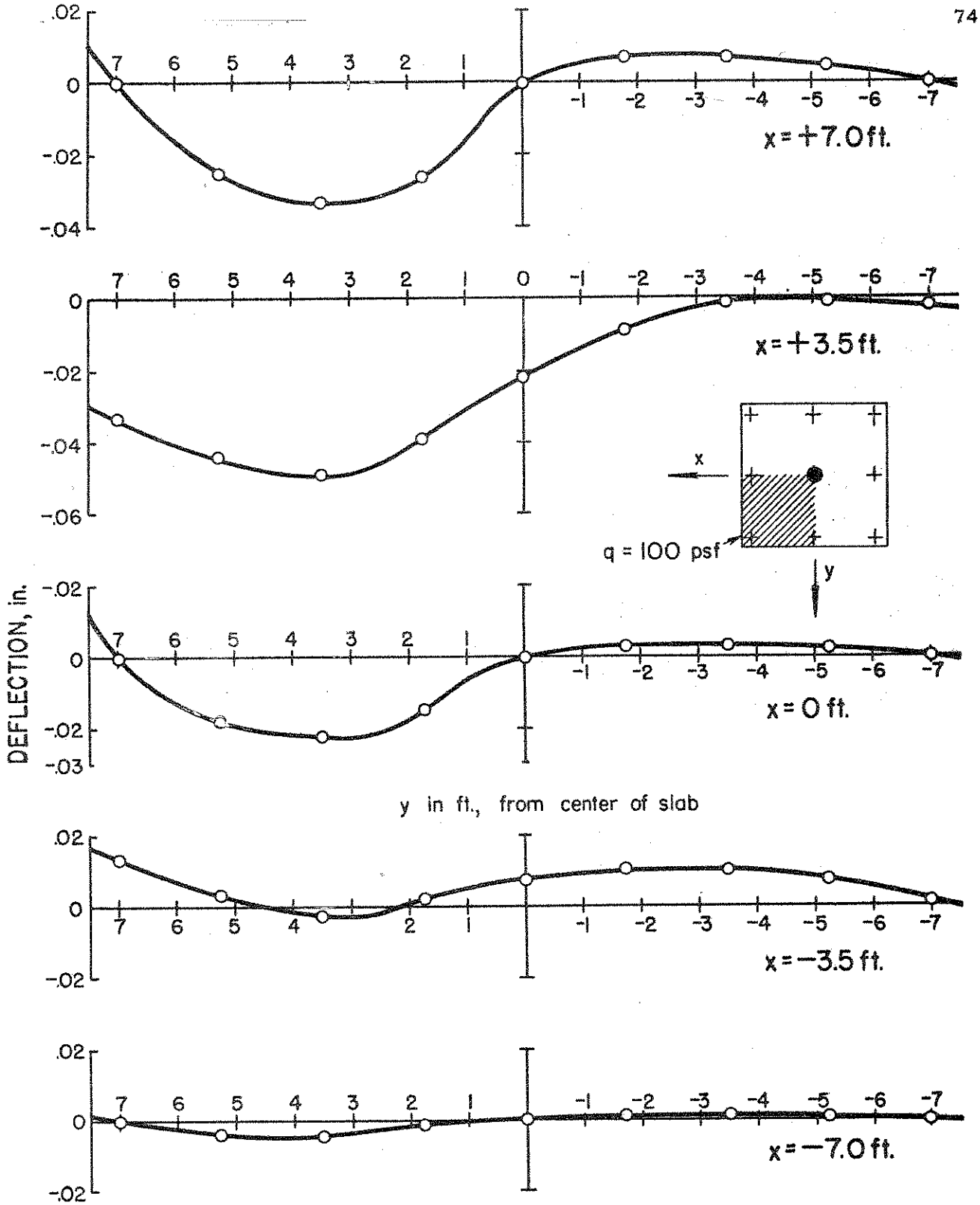

FIGURE 30. EXPERIMENTAL DEFLECTIONS DUE TO LOAD on ONE PANEL

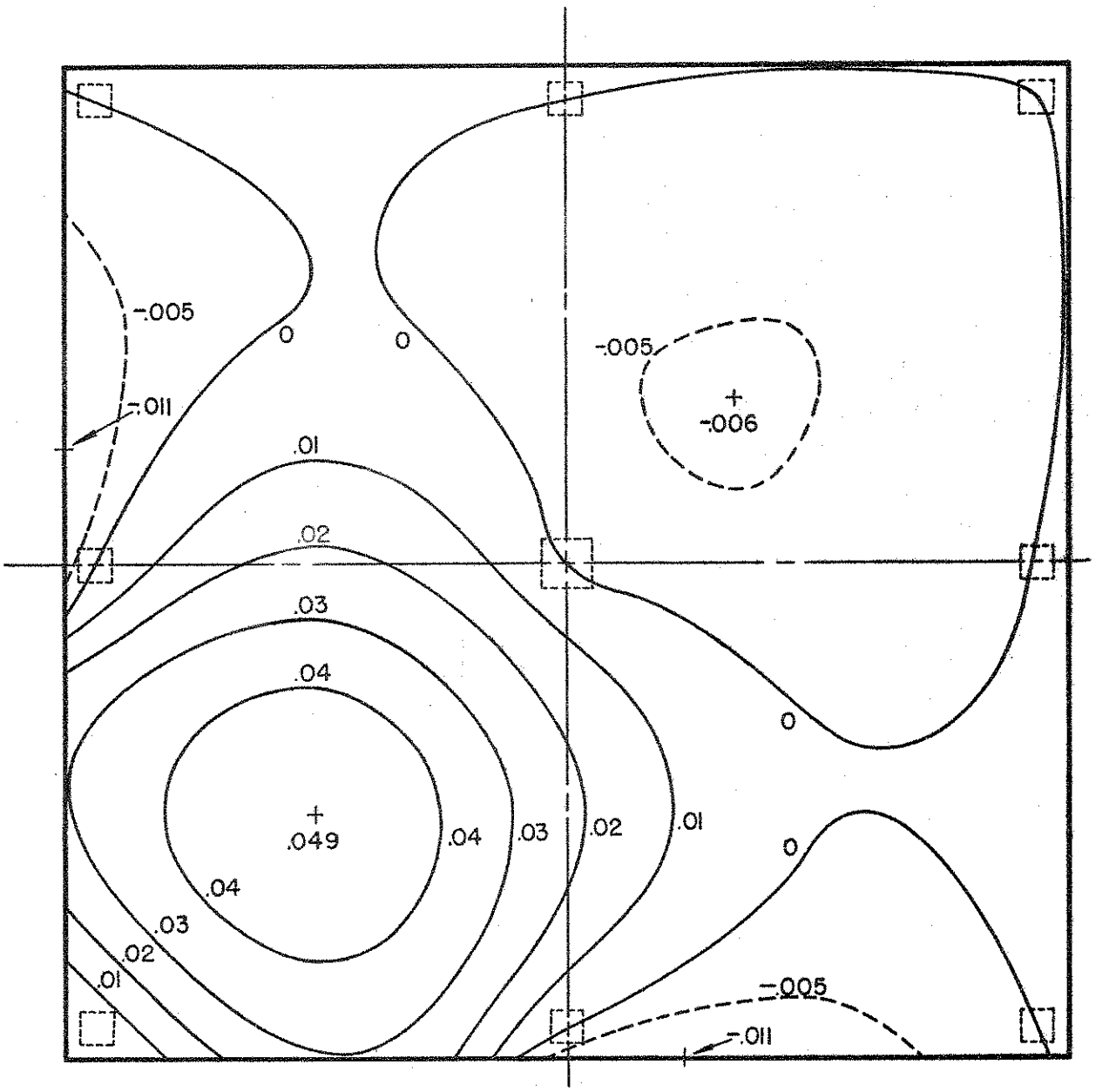

All deflections in inches, positive direction downward

FIGURE 31. EXPERIMENTAL DEFLECTIONS DUE TO UNIFORM LOAD of 100 psf on ONE PANEL

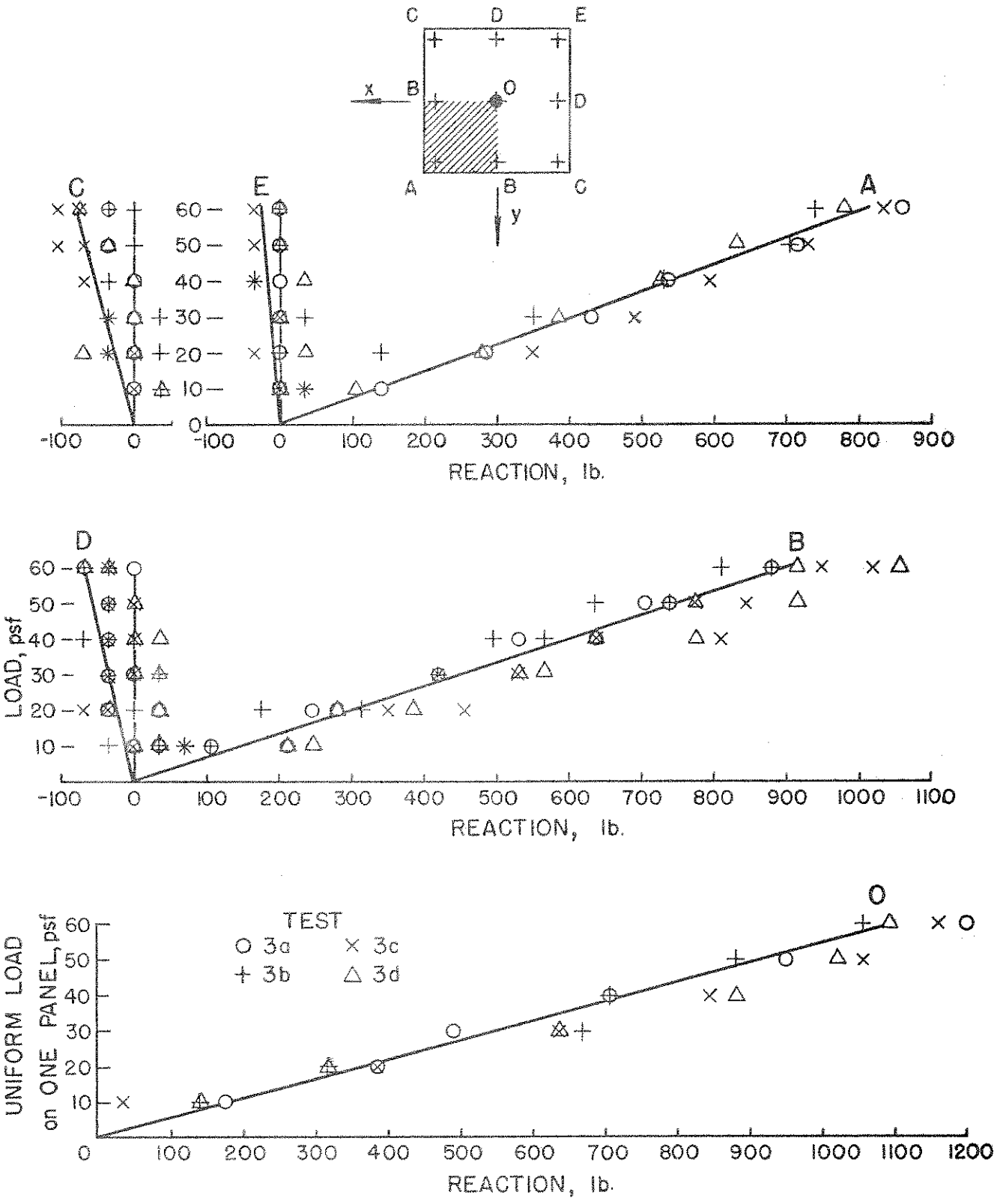

FIGURE 32. REACTIONS DUE TO UNIFORM LOAD ON ONE PANEL (EXPERIMENTAL VALUES ONLY)

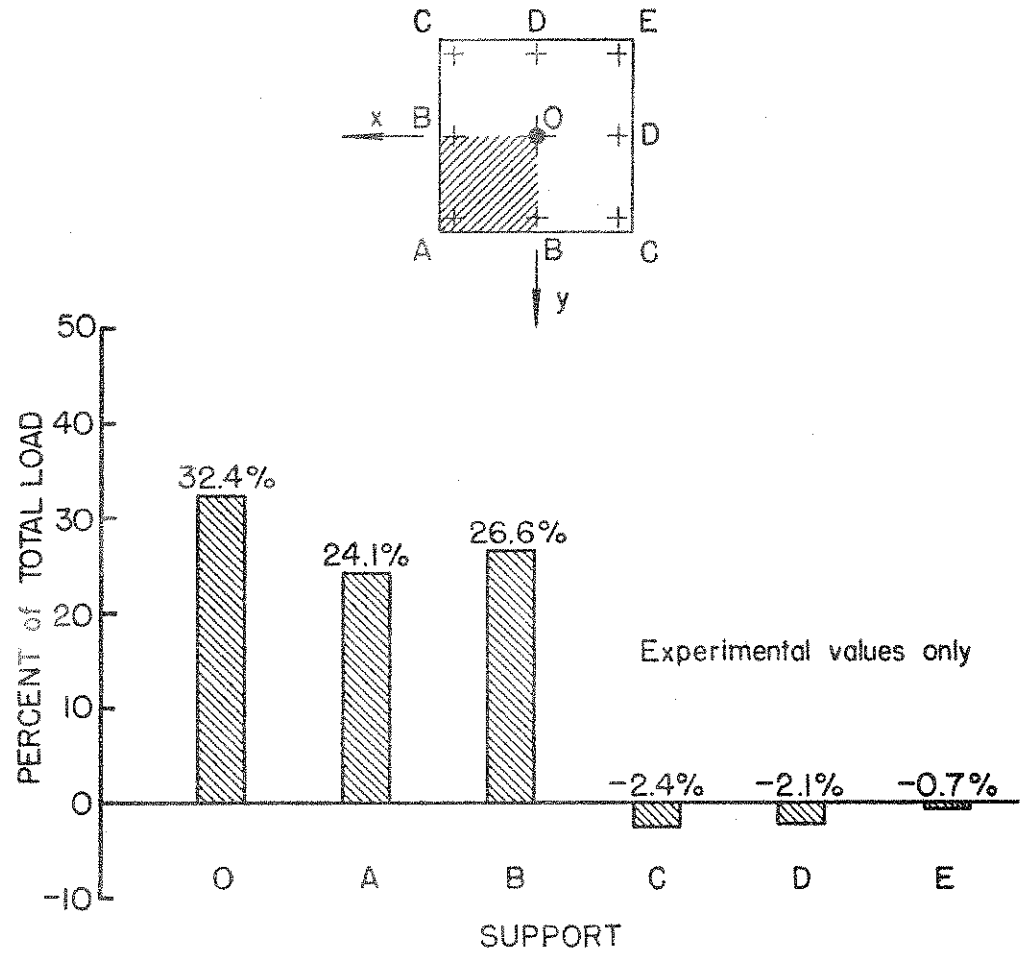

FIGURE 33. DISTRIBUTION of LOAD to SUPPORTS for UNIFORM LOAD on ONE PANEL, ELASTIC RANGE

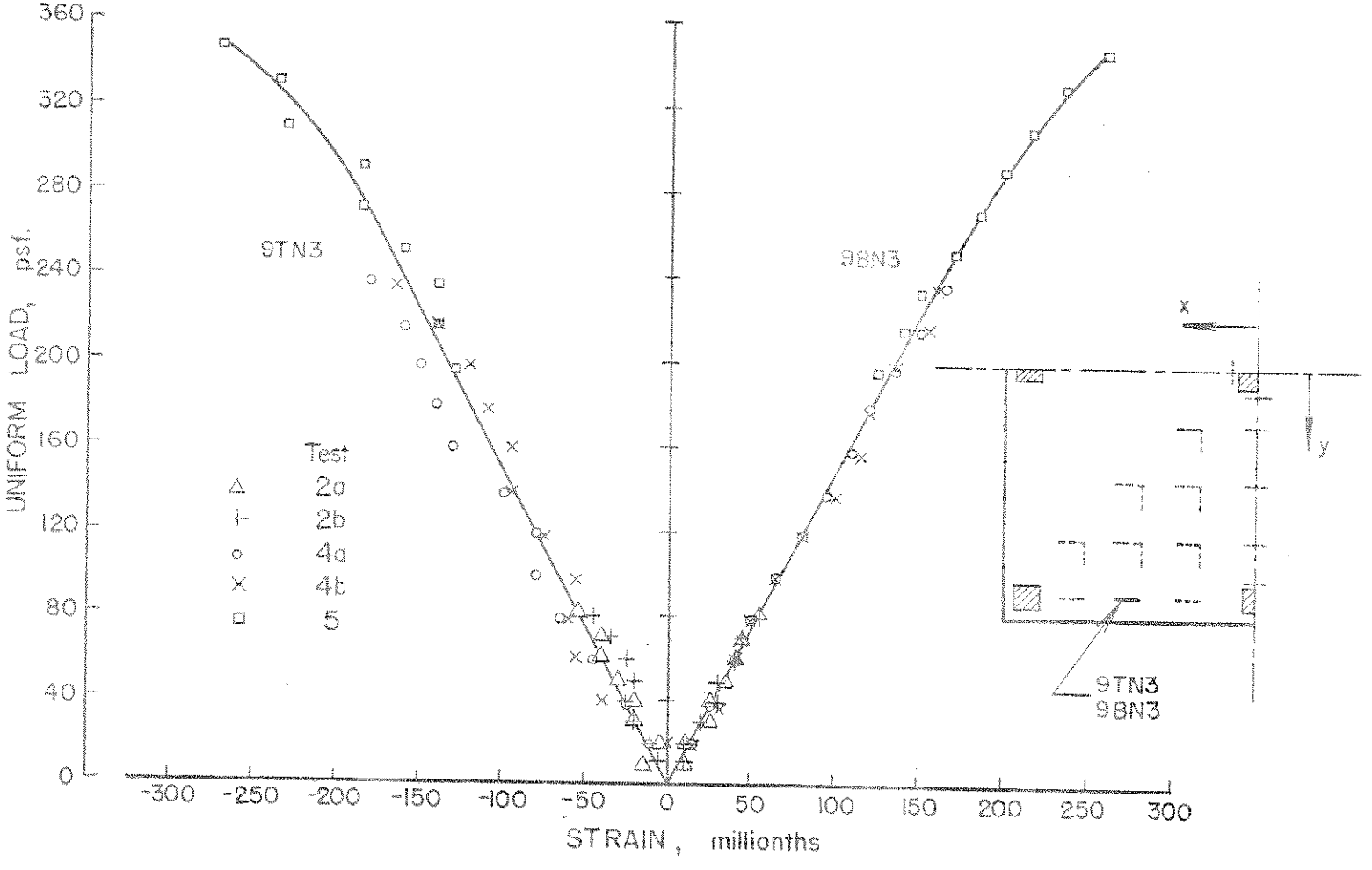

FIGURE 34. UNIFORM LOAD *vs* STRAIN for GAUGE POINTS 9BN3 & 9TN3 (EXPERIMENTAL VALUES ONLY)

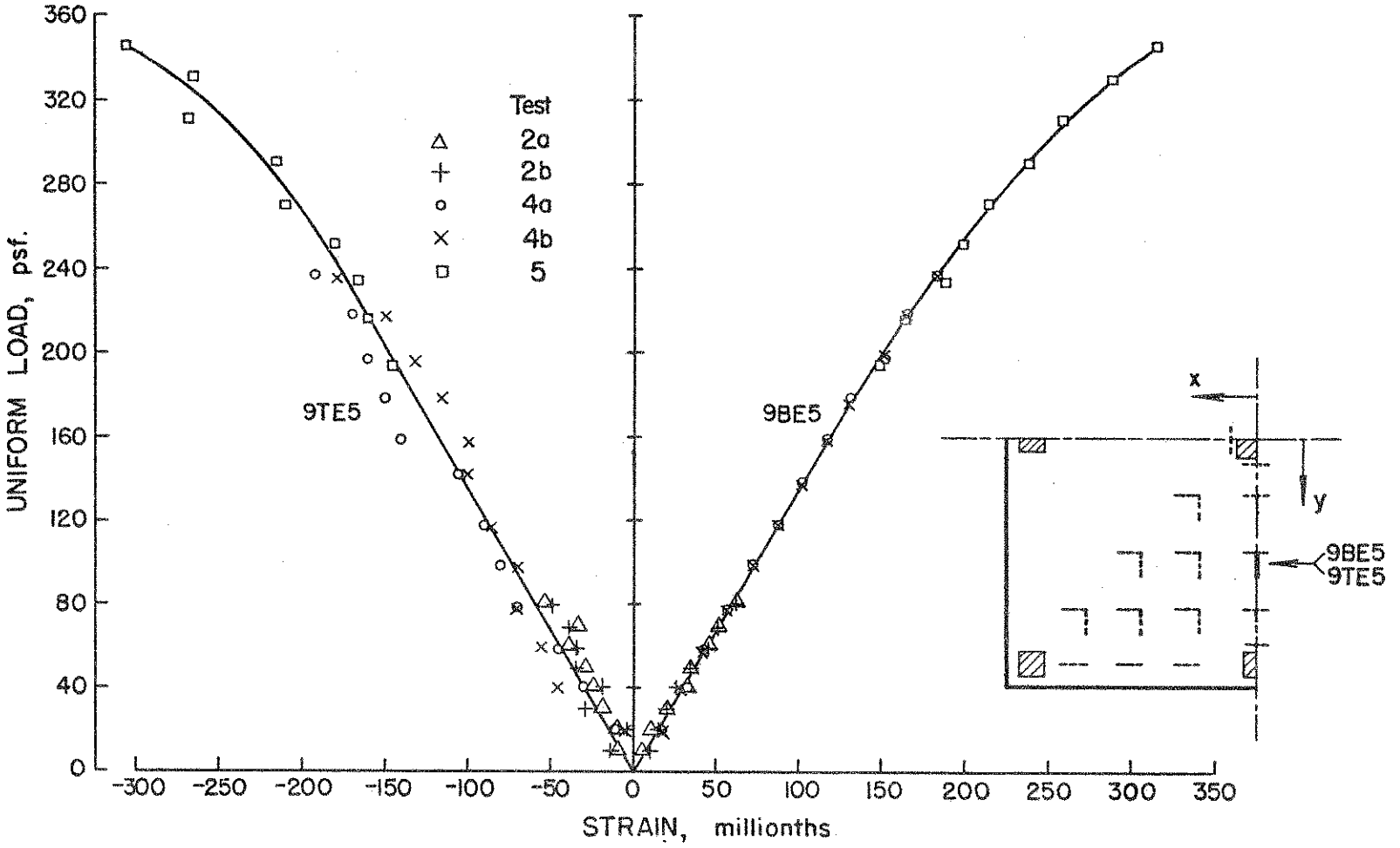

FIGURE 35. UNIFORM LOAD *vs* STRAIN for GAUGE POINTS 9BE5 & 9TE5 (EXPERIMENTAL VALUES ONLY)

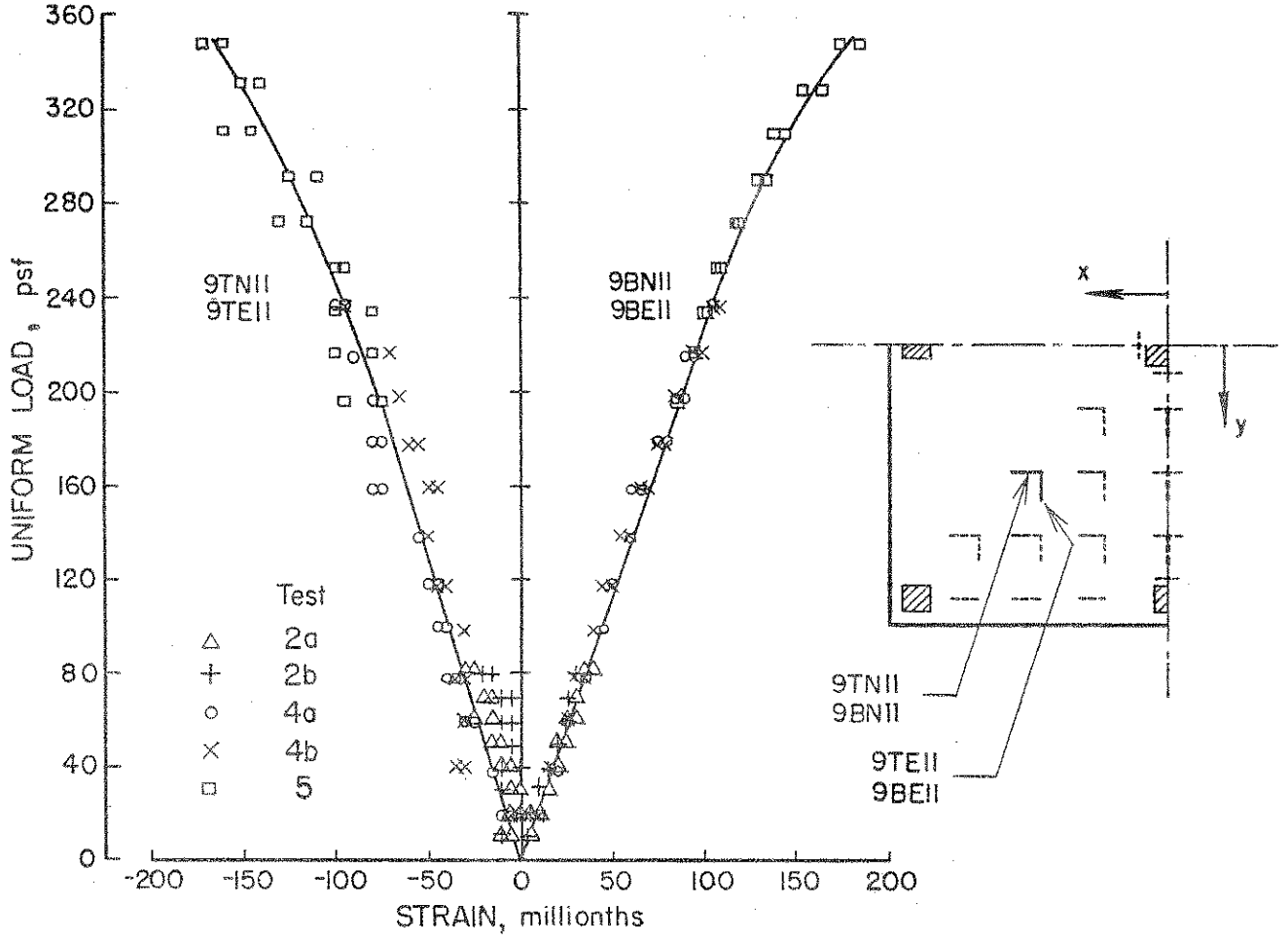

FIGURE 36. UNIFORM LOAD *vs* STRAIN for GAUGE POINT 11 (EXPERIMENTAL VALUES ONLY)

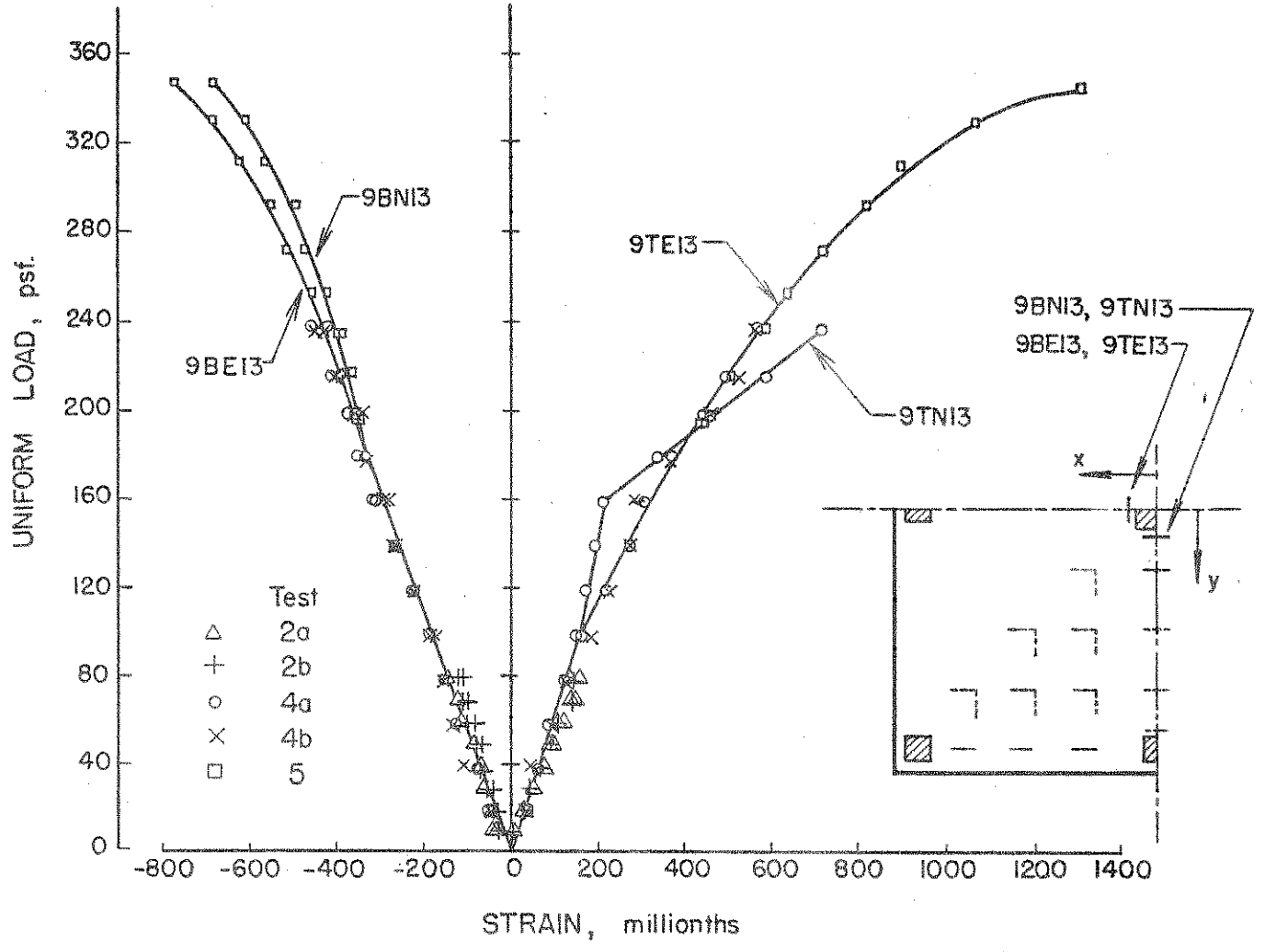

FIGURE 37. UNIFORM LOAD *vs* STRAIN for GAUGE POINT 13 (EXPERIMENTAL VALUES ONLY)

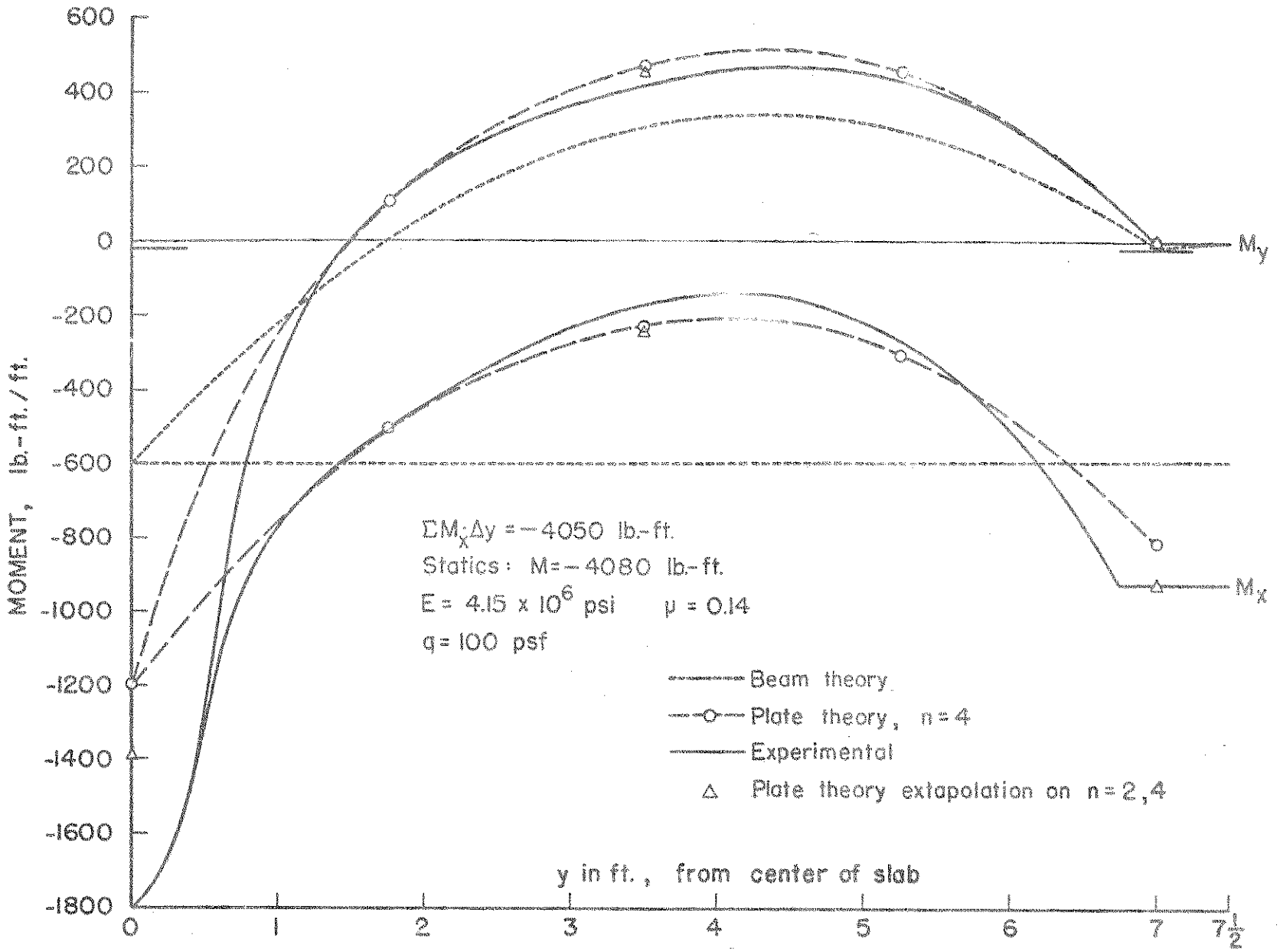

FIGURE 38. UNIFORM LOAD MOMENTS at x = 0 ft.

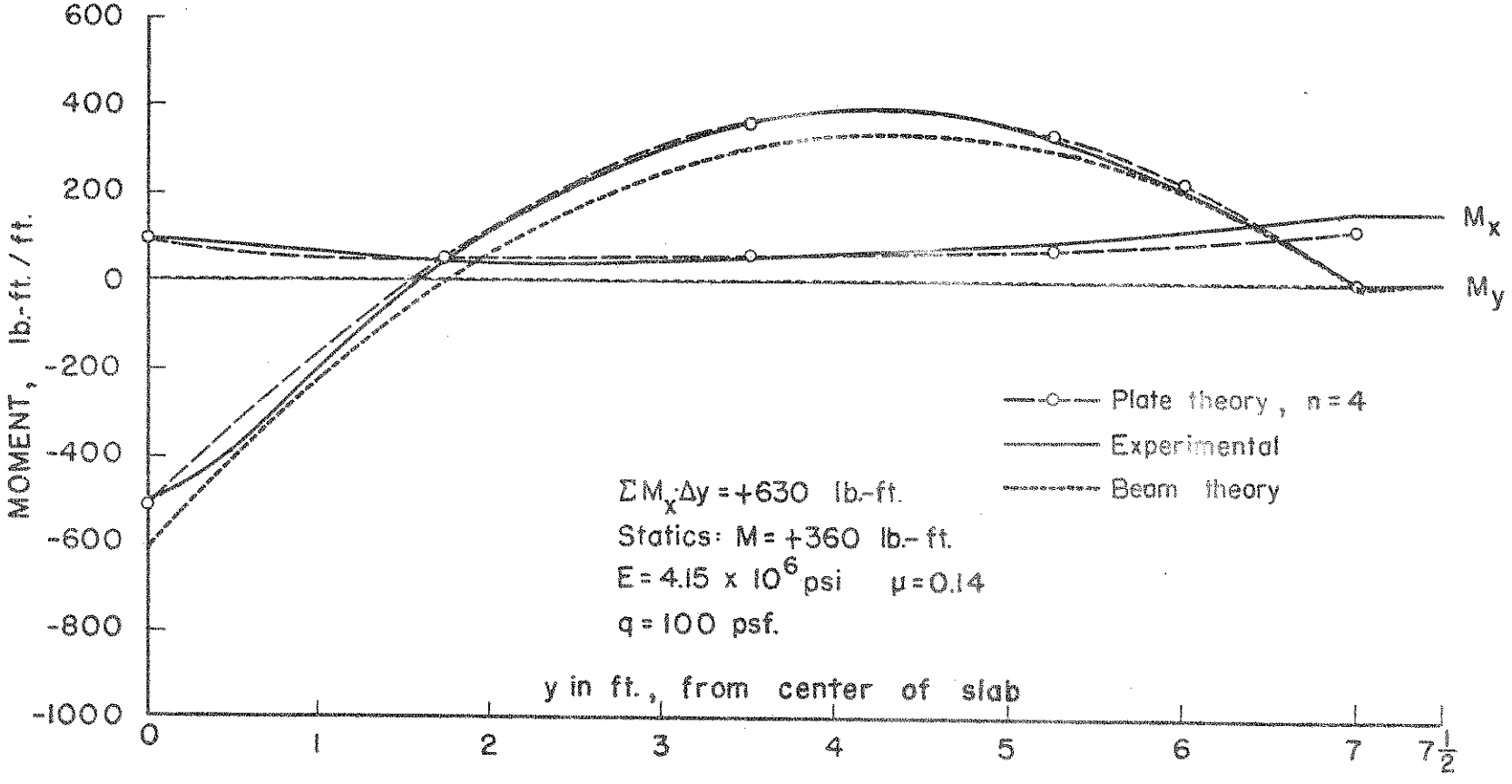

FIGURE 39. UNIFORM LOAD MOMENTS at x = 1.75 ft.

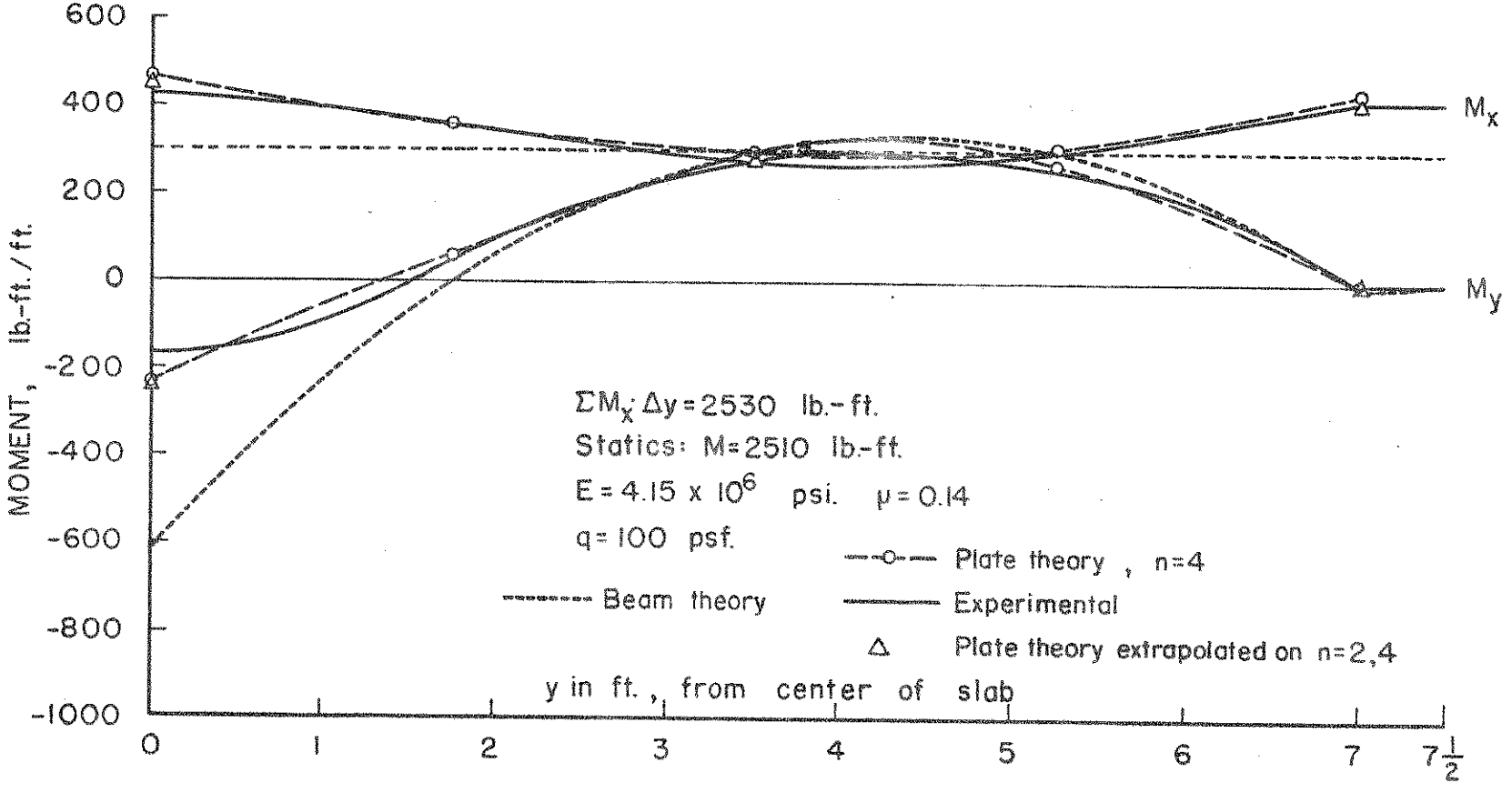

FIGURE 40. UNIFORM LOAD MOMENTS at x = 3.5 ft.

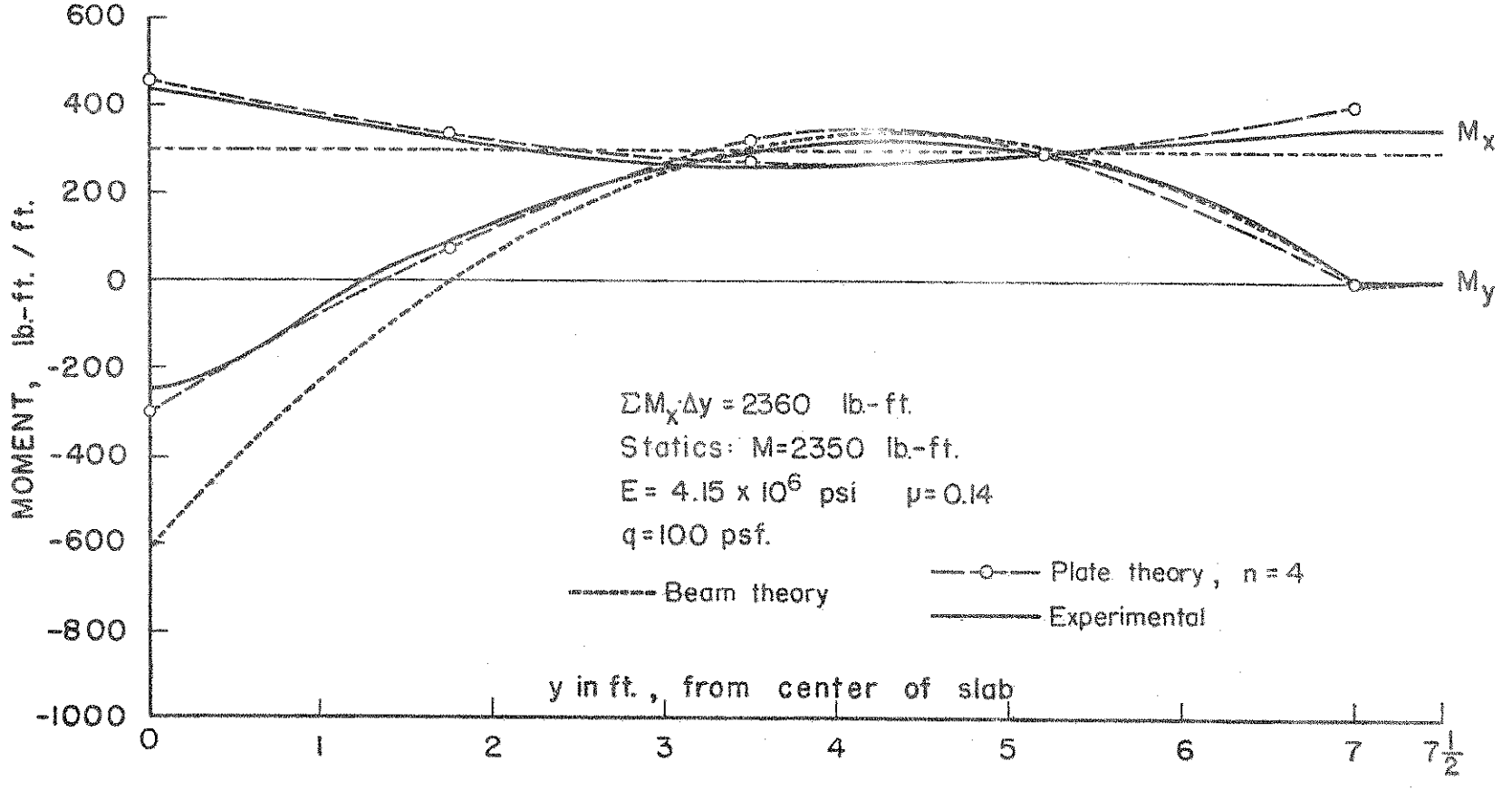

FIGURE 41. UNIFORM LOAD MOMENTS at x = 5.25 ft.

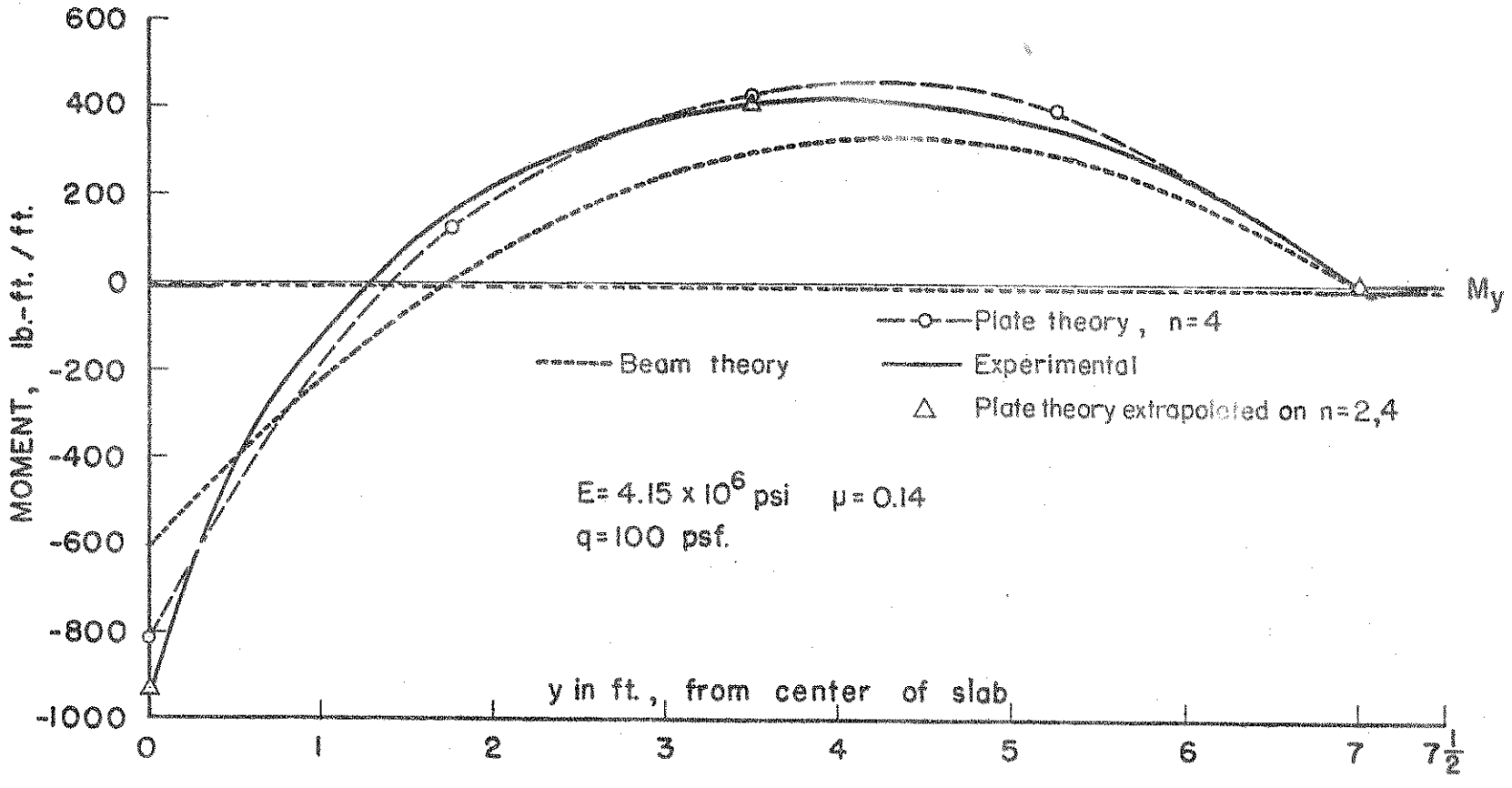

FIGURE 42. UNIFORM LOAD MOMENTS at x = 7.0 ft.

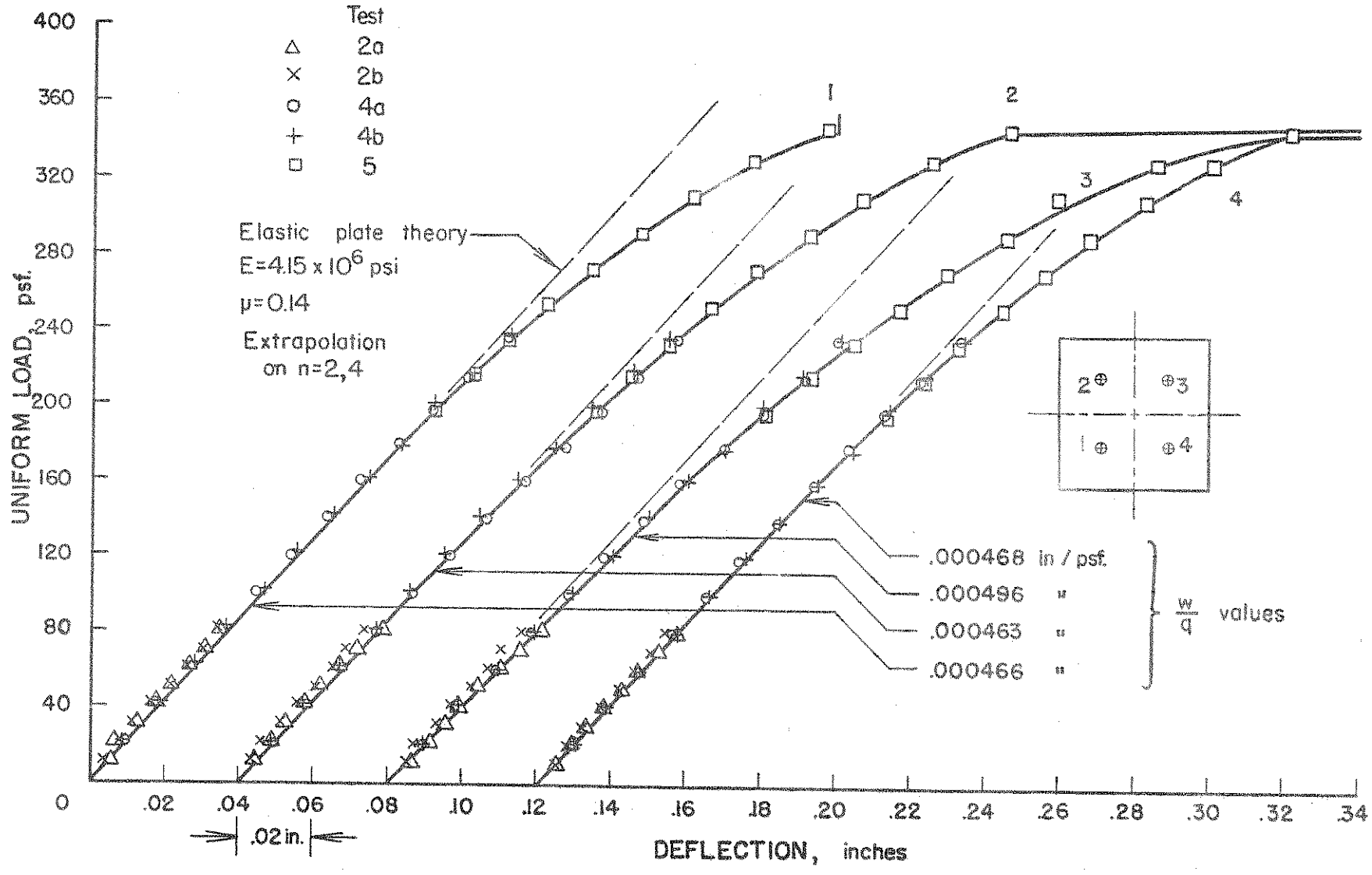

FIGURE 43. UNIFORM LOAD-DEFLECTION CURVES for PANEL CENTERS

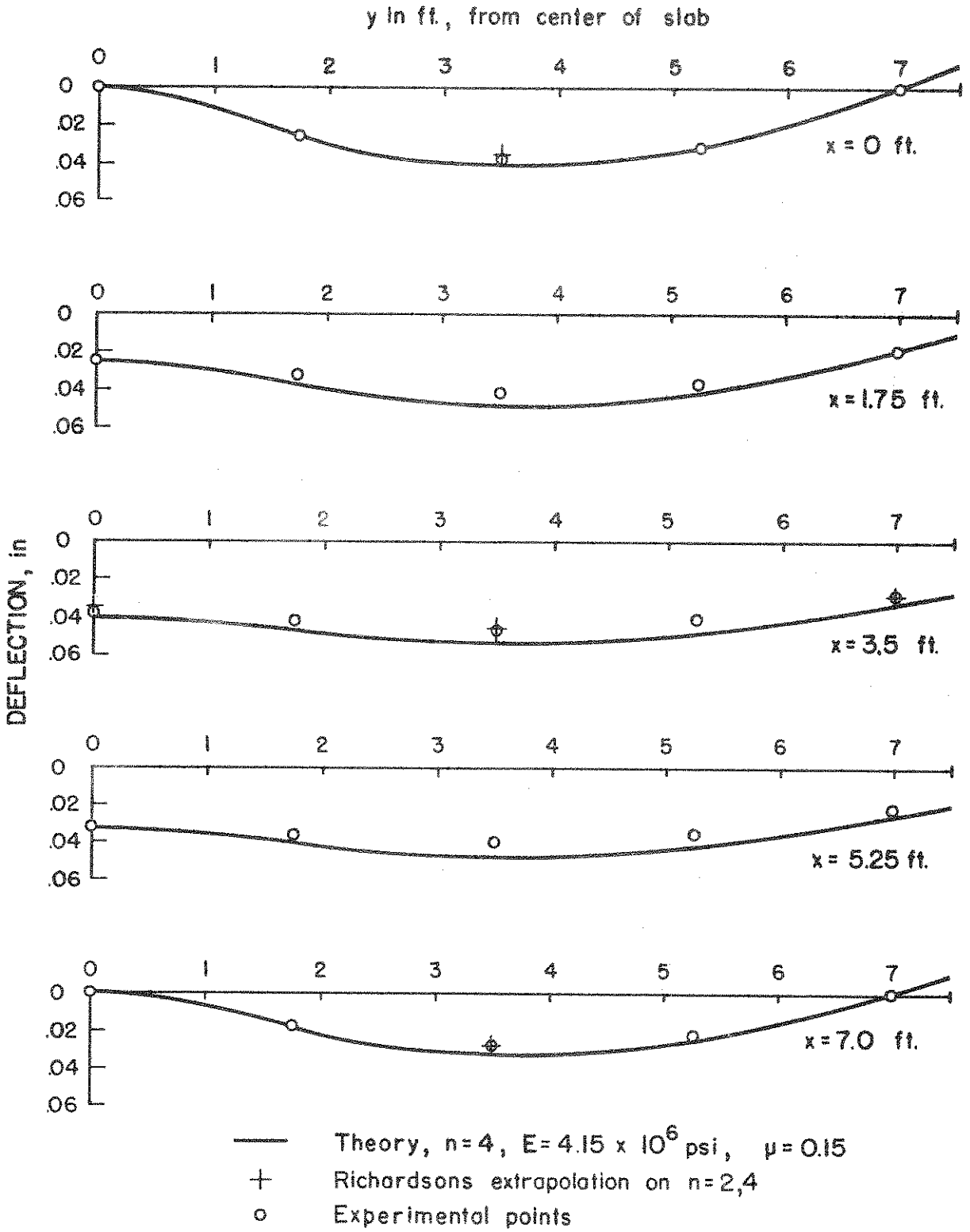

FIGURE 44. DEFLECTED SHAPES for UNIFORM LOAD of 100 psf.

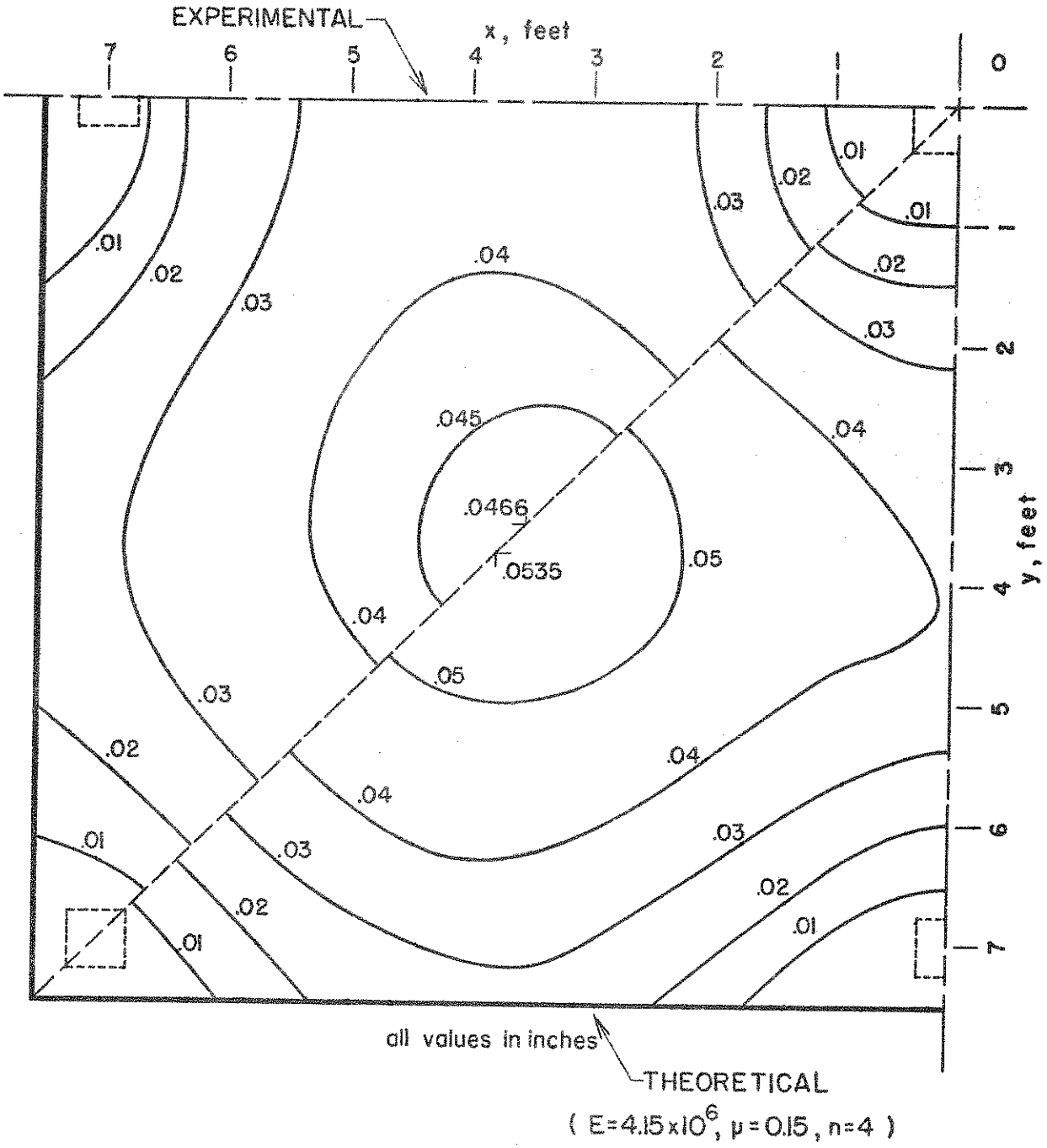

FIGURE 45. THEORETICAL and EXPERIMENTAL DEFLECTIONS for a UNIFORM LOAD of q=100 psf.

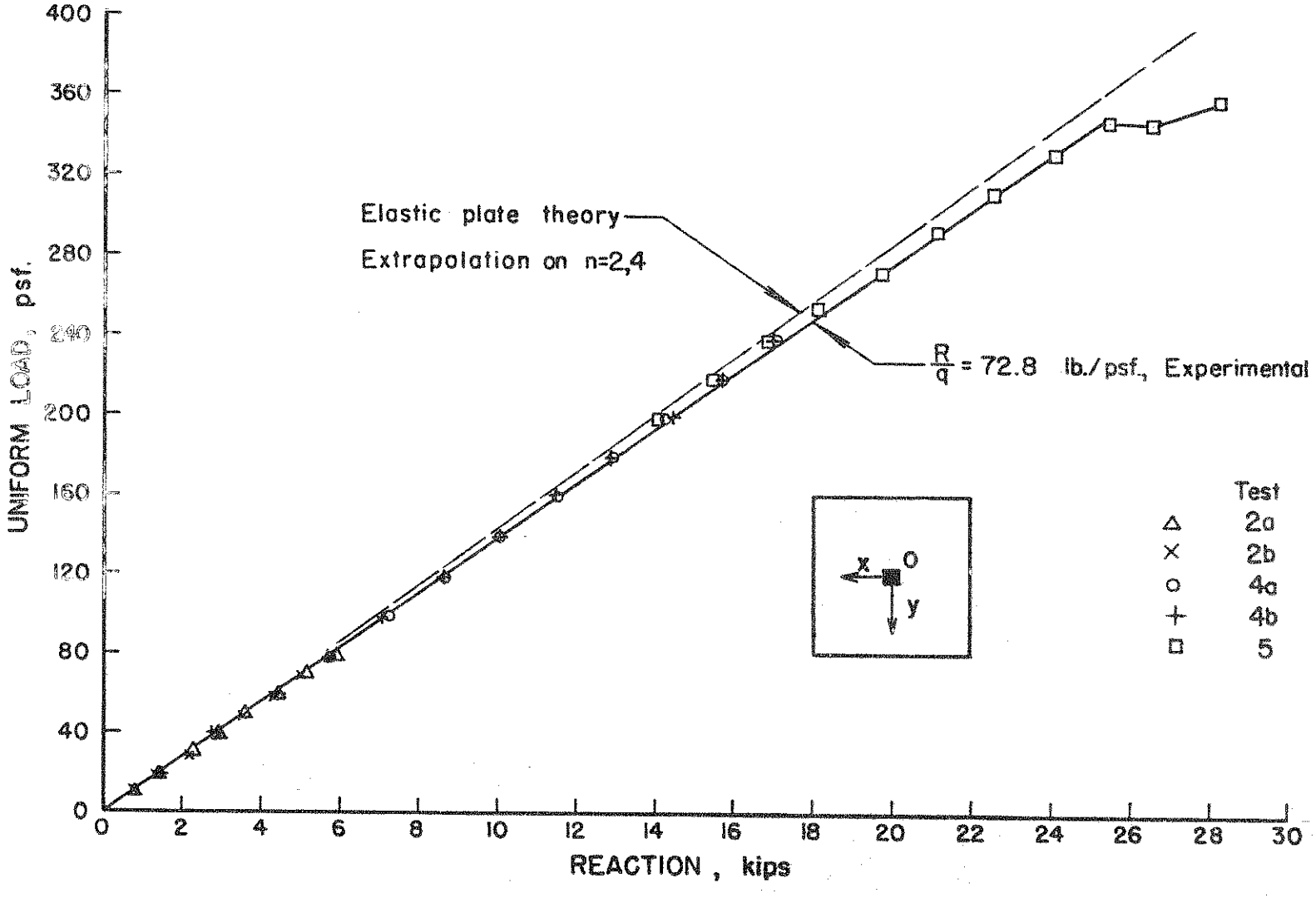

FIGURE 46. UNIFORM LOAD-REACTION CURVE for CENTER SUPPORT

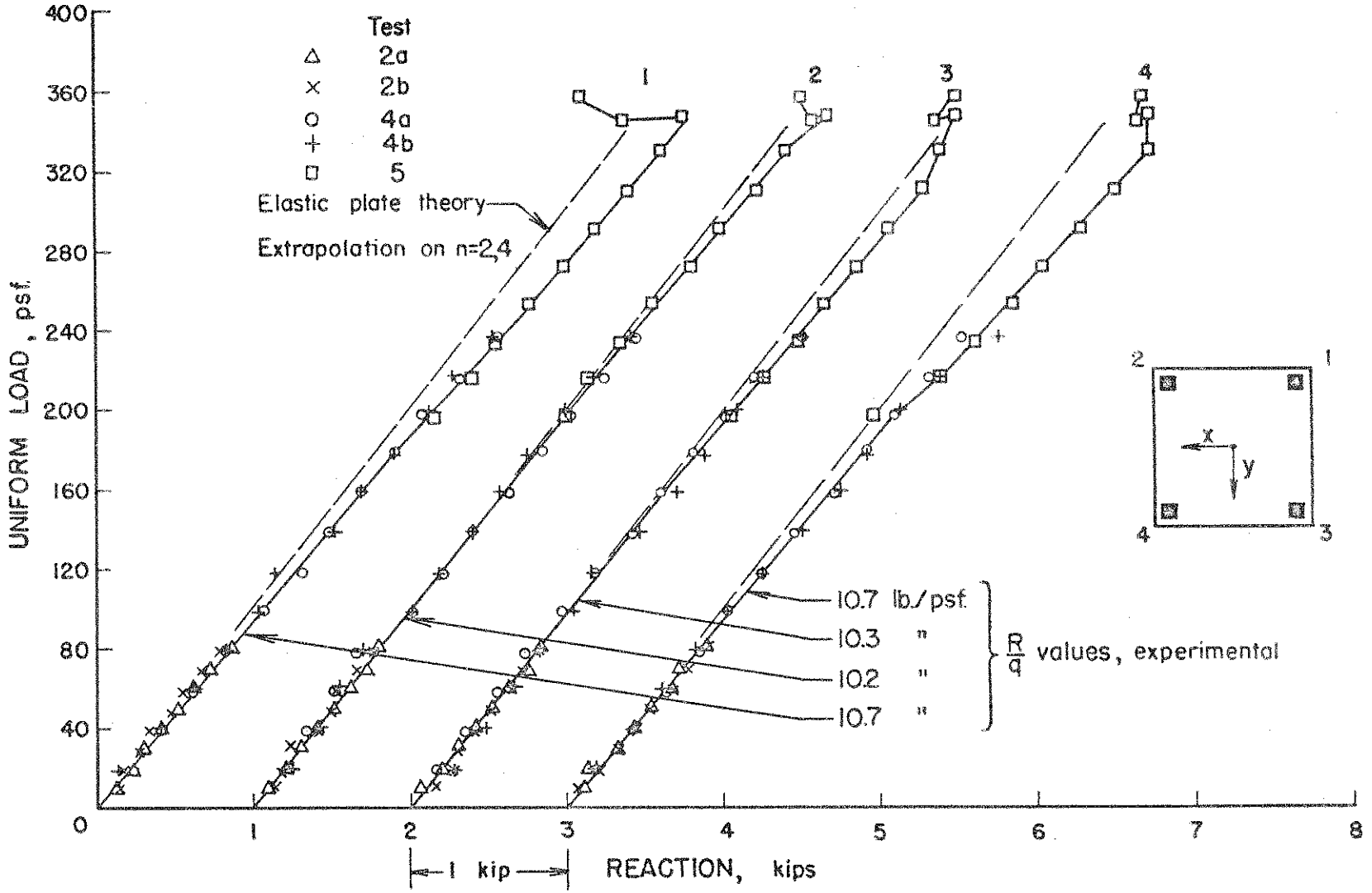

FIGURE 47. UNIFORM LOAD-REACTION CURVES for CORNER SUPPORTS

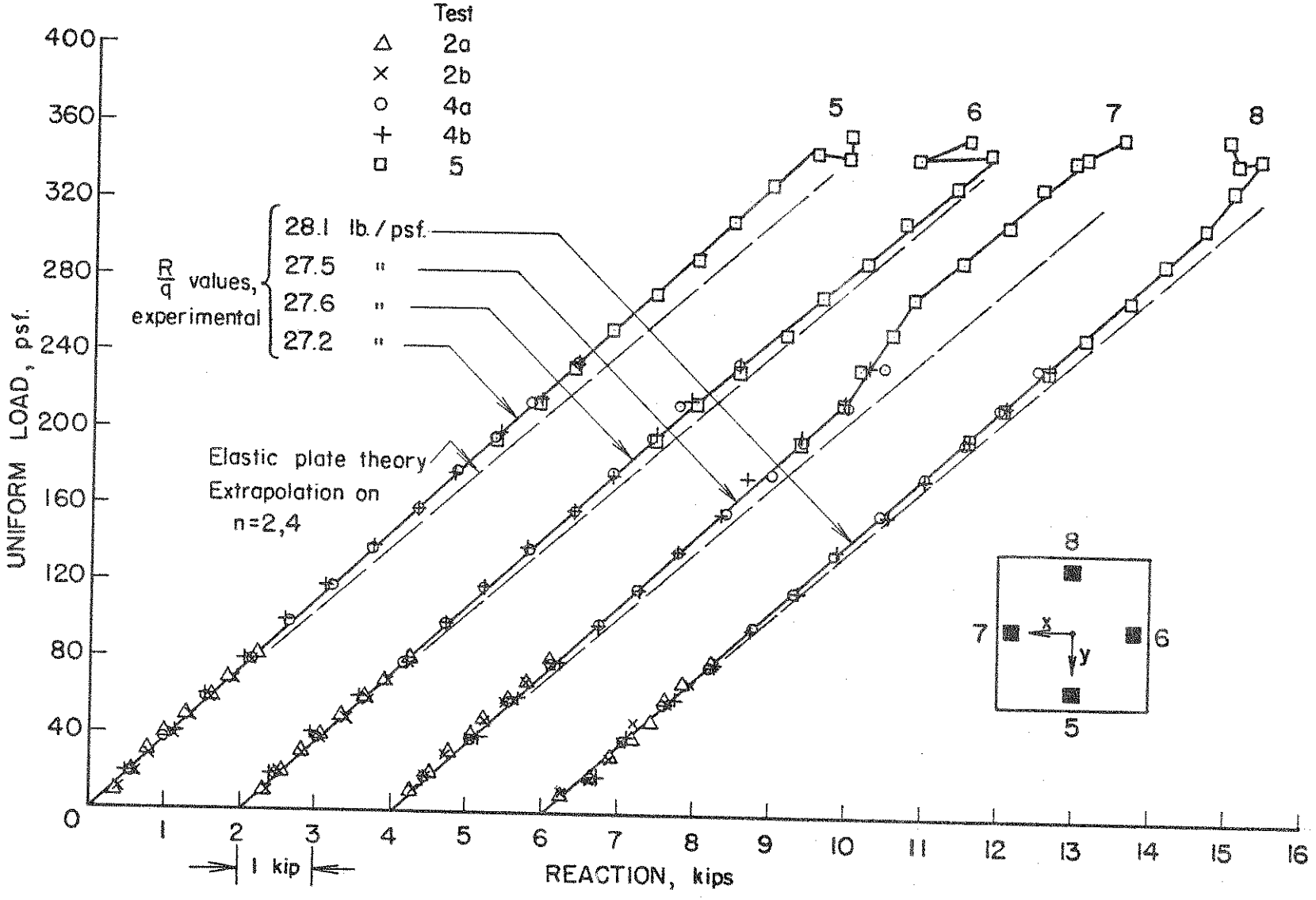

FIGURE 48. UNIFORM LOAD-REACTION CURVES for INTERMEDIATE SUPPORTS

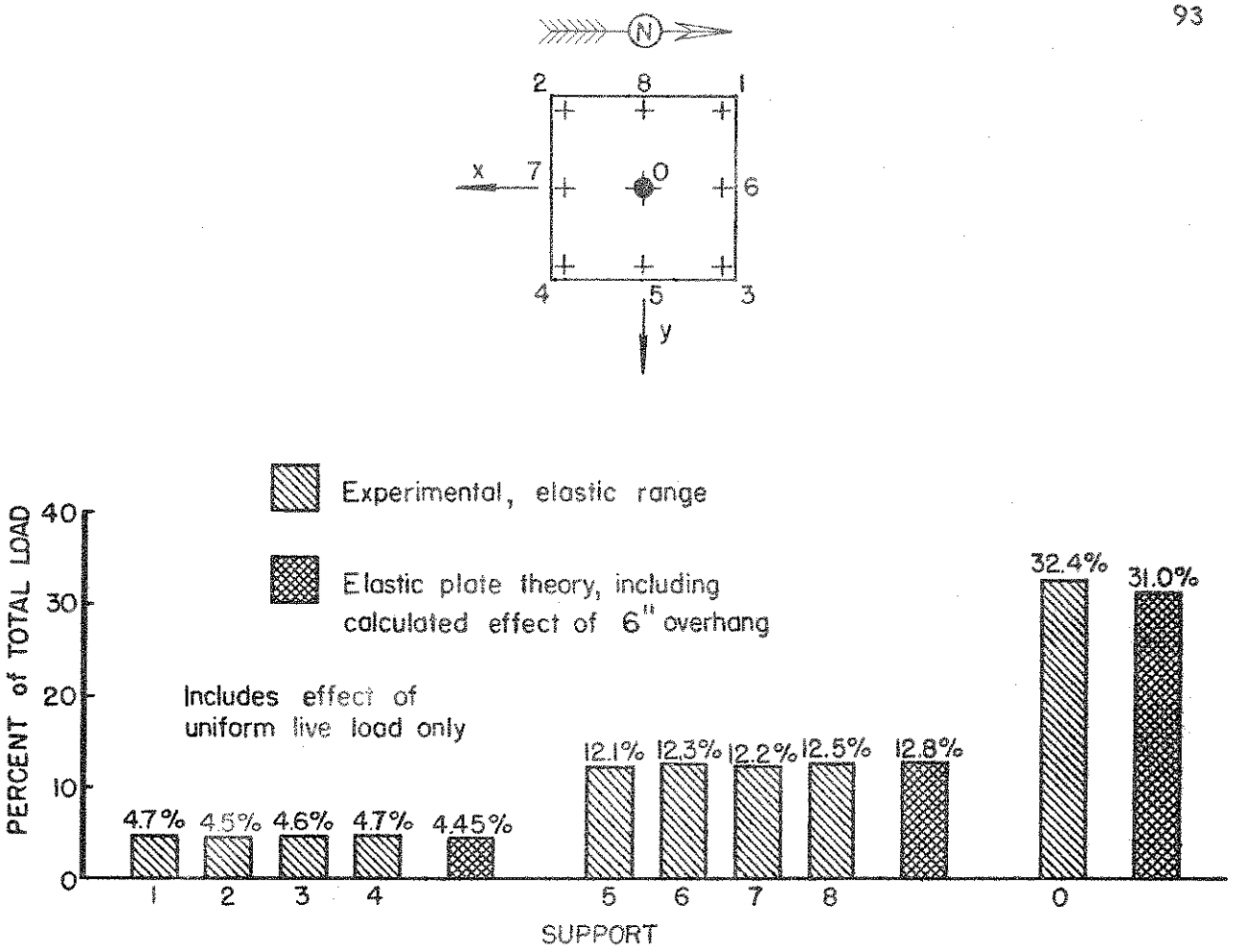

FIGURE 49. DISTRIBUTION of LIVE LOAD to SUPPORTS for UNIFORM LOAD on ENTIRE SLAB, ELASTIC RANGE

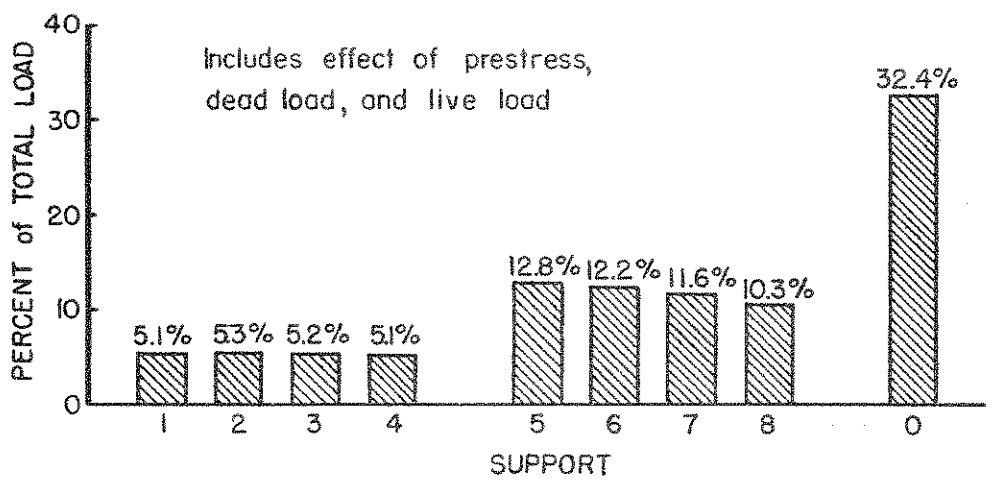

FIGURE 50. DISTRIBUTION of TOTAL LOAD to SUPPORTS for UNIFORM LOAD on ENTIRE SLAB at ULTIMATE (q_{LL} = 356 psf) (EXPERIMENTAL VALUES ONLY)

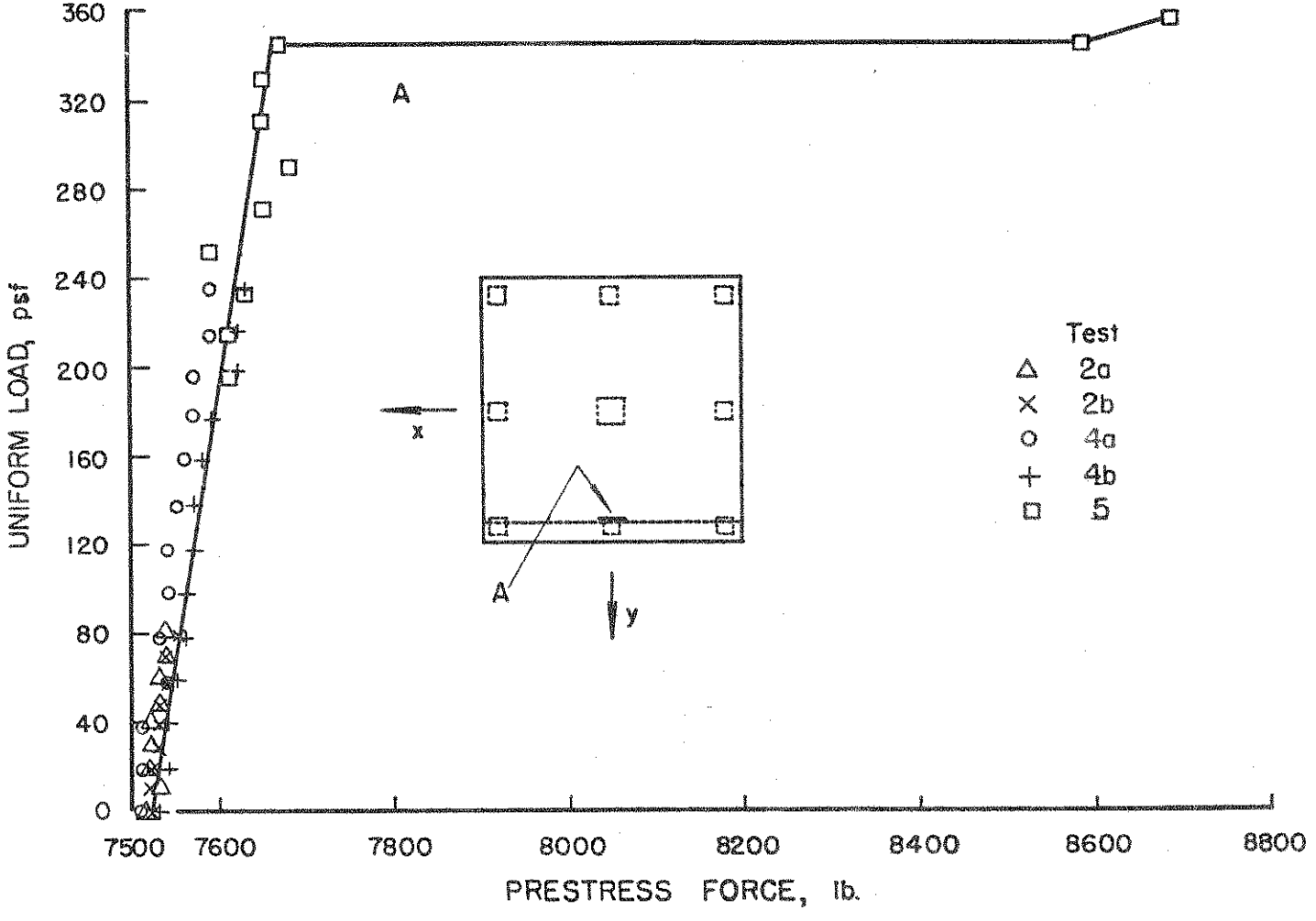

FIGURE 51. TYPICAL BEHAVIOR of PRESTRESSING STEEL UNDER UNIFORM LOAD

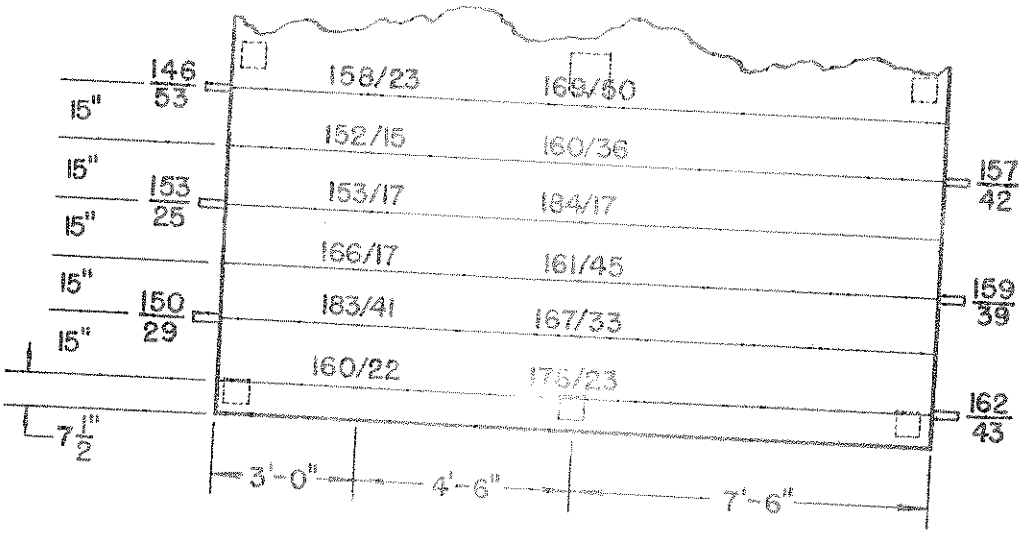

TOTAL STRESS in CABLE at q_{LL} = 356 psf, in ksi
INCREASE in CABLE STRESS from q_{LL} = 0 psf to q_{LL} = 356 psf, in ksi

FIGURE 52. CABLE STRESSES at ULTIMATE (q_{LL} = 356 psf)
(EXPERIMENTAL VALUES ONLY)

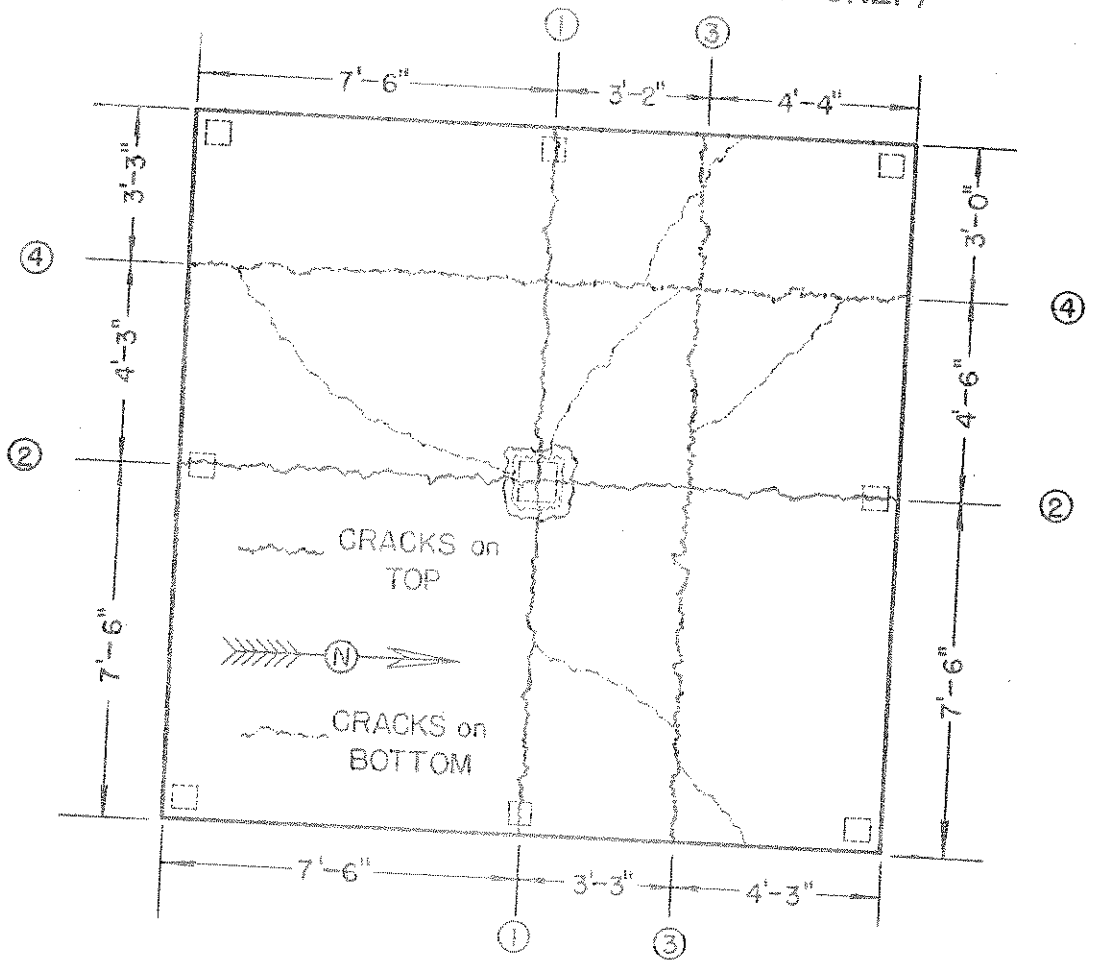

FIGURE 53. CRACK PATTERN at FAILURE (q_{LL} = 362 psf)
for UNIFORM LOAD on ENTIRE SLAB